COLLABORATION BASED SPECTRUM SHARING ALGORITHMS IN COGNITIVE RADIO NETWORKS

By

Chowdhury Sayeed Hyder

A DISSERTATION

Submitted to
Michigan State University
in partial fulfillment of the requirements
for the degree of

Computer Science - Doctor of Philosophy

2017

ABSTRACT

COLLABORATION BASED SPECTRUM SHARING ALGORITHMS
IN COGNITIVE RADIO NETWORKS

By

Chowdhury Sayeed Hyder

Radio spectrum assignment to wireless providers using traditional fixed allocation policy will no longer be a viable technique to meet the growing spectrum demand of emerging wireless applications. This is because while the available pool of unassigned radio spectrum is low, the spectrum already assigned to existing applications is also often underutilized in time, frequency, and location. With features like transmission flexibility and adaptability cognitive radio (CR) provides a useful means of spectrum sharing among growing users as an alternative to the current fixed policy. The cognitive radio network (CRN), based on the functionality of CR, consists of two types of users — primary users (PU) and secondary users (SU). Primary users are licensed users who have exclusive access rights of a fixed spectrum range. Secondary users are unlicensed users who opportunistically exploit the spectrum holes or negotiate with primary users to earn transmission access rights.

The CRN based efficient spectrum sharing algorithms work on different forms of collaboration between the PUs and the SUs (inter-user collaboration) and among the SUs themselves (intra-user collaboration). In the sensing based collaboration model, the SUs sense licensed spectrum and collaboratively decide about its availability based on the sensing results without any involvements from the PUs. In the relay based collaboration model, the SUs coordinate with the PUs directly, relay primary packets in exchange for transmission opportunities, and thus build a win-win cooperative framework to attain mutual benefits. In the auction based collaboration model, the SUs bid for temporary or permanent usage rights of unused licensed spectrum bands that are put into auction

for sale by the PUs. Each of these collaboration models faces different sets of challenges towards achieving high spectrum utilization. In this dissertation, we address some of these challenges and present a set of efficient spectrum sharing algorithms based on these collaboration models.

The first work in this dissertation addresses the spectrum sensing data falsification (SSDF) attack in IEEE 802.22 wireless regional area network (WRAN) under the sensing based collaboration model. We discuss different strategies of manipulating sensing reports by one or more malicious users and how these manipulation strategies may affect the spectrum utilization. To defend against such malicious attacks, we present an adaptive reputation based clustering algorithm. The algorithm combines the clustering technique with feedback based reputation adjustment to prevent independent and collaborative SSDF attacks and quarantines the attackers from the decision making process.

Our next set of work in this dissertation falls under the relay based collaboration model. We investigate the feasibility of this collaboration model in the case of real-time applications. We quantify the impact of packet deadlines and cooperation overhead on the system performance. We discuss the impact of interference that may cause from secondary transmissions. Based on the analysis, we develop an interference aware reliable cooperative framework which improves the packet reception rate of both users with low overhead. We extend our investigation of this relay based collaboration model from single hop to multiple hops in the form of cooperative routing. We formulate the routing problem as an overlapping coalition formation game where each coalition represents a routing path between primary source and destination consisting of multiple SUs as intermediate relays. The proposed model allows SUs to participate in more than one coalitions and creates more transmission opportunities for them while achieving stable routing paths for PUs.

Our final set of work in this dissertation deals with the challenges in the auction based collaboration model. We consider an online setting of spectrum auctions where participation and valuation of both bidders and sellers are stochastic. We analyze the behavior of bidders and sellers in such settings and develop truthful auction mechanisms with respect to bid and time, improving spectrum reuse, auction efficiency, and revenue. The findings from our research will help to understand the underlying challenges in future networks, build a better spectrum ecosystem, and encourage new spectrum sharing models in wireless broadband communications.

To my parents.

ACKNOWLEDGMENTS

All praises are due to Allah, the most benevolent and merciful. I would like to thank Dr. Xiao for giving me an opportunity to work as one of her PhD students. From the beginning, she instructed me to investigate research problems on my own which helped me to understand the challenges in the field of my research. She taught me how to present ideas into writing, how to review a paper, how to address the comments of the reviewer, and so on. This knowledge definitely helped me to find my limitations, realize my weaknesses, and I am grateful to her for that valuable insight. I would also like to thank my other PhD committee members - Dr. Mutka, Dr. Esfahanian, Dr. Jeitschko, and Dr. Mandrekar for their flexibility with the schedule, patience to sit through hours of my presentation, and their input to make it better.

I have been working with Dr. Jeitschko for the last couple of years. His profound knowledge in auction theory made the interdisciplinary research so much easy, fun, and interesting. He became my mentor, guide, and a friend. I will remain ever grateful to him for his support and encouragement during the darkest times of my life. In this regard, I also want to show my gratitude to those people who have not dismissed my conditions like others and generously extended their help through counseling and guidance. Had I not received that support, it could have been entirely a different story.

I also want to thank all of my coauthors who have collaborated with me in different projects and contributed with their valuable inputs and corrections. I want to specially thank Dr. Alim al Islam (Razi) whose mental support, domain knowledge, and unyielding attitude led to some good finished projects. I want to thank Dr. Torng for his valuable suggestion and important contribution to the joint research work. Apart from that, I want to specially thank him for his support as the graduate director of the department. He along with Dr. Mckinley were the two teachers who showed how to make a graduate class fun and interesting. Despite their different teaching styles, I enjoyed both of their classes and will not hesitate to follow their styles (if I ever pursue an academic career).

I am also grateful to the local Bangladeshi Community (Jewel vai & vabi, Kabir vai & vabi, Toufiq vai & vabi, Jamal vai & vabi, Aftab vai & vabi, Lincon vai & vabi, Soma apa and Zibi) who embraced us as one of their own and East Lansing became my home away from home. I also want to thank the MSU Bangladeshi Students Association (ABSS) and its members for organizing colorful events to remind us our beautiful culture every year.

I was fortunate enough to get the opportunity to study in the topmost engineering university, Bangladesh University of Engineering and Technology (BUET) in Bangladesh at almost no cost. I am grateful to the hard working taxpaying common people of Bangladesh whose contribution to the national economy made this possible for thousands like me.

In this occasion, I also remember my teachers and colleagues from my undergraduate institution - Dr. Masroor Ali, Dr. Sohel Rahman, Dr. Ashikur Rahman, Dr. Masud Hasan, Dr. Humayun Kabir, Dr. Yusuf Sarwar, Dr. Atif, Dr. Rifat, Dr. Enamul, and Arup. All of them has made a positive change in my life. Perhaps I would not be here if I had not the opportunity to meet my two uncles at a very early stage of my life. My 'Boro mama' was a high school math teacher who taught me math in my high schools. My 'choto mama', an electrical engineer by profession, was my source of inspiration to problem solving and that early childhood experience led me to pursue my studies in computer science. I remember their contribution in my academic life with respect and humility. I am also grateful to my two friends - Saidul and Masud who always kept me focused in the big picture through difficult times.

Finally, it is because of my parents, my brother, and my family I keep going against all odds. My parent's upbringing taught me to enjoy success with humility, and embrace failure with stronger determination. My medical doctor brother demonstrated in his daily life how to become a compassionate human being. I am who I am because of their love, sacrifice, guidance, and practice. My wife Tamanna has been a true friend throughout my PhD years and always believed in me when I myself was doubtful. My little angel Priyota always brought smile to my face even at the lowest point of my life. I thank the Almighty for this whole roller coaster experience and for strengthening my belief on this saying "all the hardships and negativity in life is short-lived and the beauty and blessings in life is eternal."

TABLE OF CONTENTS

LIST OF TABLES

LIST OF FIGURES

KEY TO SYMBOLS

n	number of secondary users
n_a	number of malicious secondary users
n_h	number of honest secondary users
m	number of primary users
$\mathcal{P}$	set of primary users
$\mathcal{S}$	set of secondary users
p	primary user
s	secondary user
P_{fa}	probability of false alarm in individual channel sensing
P_{md}	probability of misdetection in terms of channel sen
P_I	probability that a channel is idle
P_B	probability that a channel is busy
P_{detect}^{h}	PU detection probability of an honest secondary user
P_{detect}^{a}	PU detection probability of an attacker
P_{HH}^{diff}	probability that two honest users differ
P_{AH}^{diff}	probability that an honest user and an attacker differ
P_{ma}	attacking probability
$\Lambda_{KL}(x\|\|y)$	KLD measures between distribution x and y
d_{xy}	distance between x and y
Q_E	error rate
Q_D	false detection rate
Q_F	false positive rate

ρ_i	reputation of user i
δ	weight factor $0 \leq \delta \leq 1$
$\mathbb{V}_i$	decision of a virtual cluster about channel status
$\mathbb{V}$	decision of the BS about channel status
Δ	number of dimension of sensing reports per user maintained by BS
Q_{goal}	target set by an attacker
E_p	primary transmission power
E_s	secondary transmission power
H_i	hypothesis i
L	queue length
P_x	probability of event x
h_i	channel gain
Σ	set of states
$\mathcal{A}$	set of actions
ϕ	transmission policy
σ	system state
Γ	discount factor
$a(t)$	action at time t
$U_a(x, y)$	utility of a user after action a and moving from state x to y
t	time period
$D_a(x, y)$	packet drop probability due to queue overflow
$V_a(x, y)$	successful delivery probability of a packet
$W_a(x, y)$	successful delivery probability of queued packets

$P(x, y)$	transition probability from state x to y
R	data rate
C_i	coalition i
$\mathcal{CS}$	coalition structure
r_i	resource of user i
T	total time
λ	traffic rate
B	bandwidth
δ_d	convergence parameter
G_t	transmitter gain
G_r	receiver gain
$R_i(C_i)$	data rate profit of coalition i
$D_i(C_i)$	delay profit of coalition i
ψ_j	seller j's payment
v_i	valuation of bidder i
b_i	bid of a secondary user i
$b_{(h)}$	h-th highest bid in the set
a_i	ask of a primary user i
$a_{(h)}$	h-th lowest ask in the set
o_i	arrival time of user i
d_i	deadline of user i
g_i	location of user i
$\mathbb{E}[\pi_\tau(v_i)]$	expected payoff of a bidder of value v_i with τ more periods to live

$\beta_\tau(v_i)$	priority of a bidder i with valuation v_i and τ periods to live
$L_\tau(v_i)$	losing probability of a bidder i with valuation v_i and τ periods to live
ϕ_j^p	sales/bid request
$C_i(i)$	coalition join request of user i
V_j	set of user in the neighborhood of user j
F_k	cumulative distribution function of users' lifetime
F_n	cumulative distribution function of arriving bidders
F_m	cumulative distribution function of supplies

Chapter 1

Introduction

1.1 Present Status and Core problem

The communication world has witnessed a tremendous advancement in wireless technology over the last few decades. A diverse range of wireless services has been offered starting from health-care applications to vehicular networks, from real-time system monitoring to Internet of Things (IoT) applications. A new set of wireless communication devices like smartphones, tablets, wearable devices have been introduced with useful and interesting features. As a result, the usage of wireless devices has skyrocketed, wireless communication has become an integral part of our daily lives, and wireless traffic has grown at an exponential rate. According to Cisco study [25], mobile data traffic has grown 4000-fold over the last 10 years with 74% growth in the last year only, and this trend will continue to increase in future. In the same study, it is expected that monthly mobile data traffic will be 30.6 exabytes (EB) by 2020. This huge traffic has to be carried over a fixed range of radio spectrum whose usage and access are regulated by Federal Communications Commission (FCC) in the US.

Traditionally the FCC approves different service providers an exclusive license of a fixed spectrum band. In the face of growing traffic demand, such fixed allocation cannot meet future demand with the unassigned spectrum bands only. The service providers with already licensed spectrum are not utilizing their share very efficiently as well. For example, Shared Spectrum Company (SSC) conducted a citywide experiment in Vienna, VA on the usage of spectrum between 30MHz and 3GHz [108]. The study showed that a significant number of spectrum bands were "highly underutilized" or "almost never used." Similar spectrum occupancy studies have been performed in different cities, and the results are consistent throughout all these studies [116] [89] [11] [17]. Therefore, the current allocation system is proved to be inadequate, and its reformation is a necessity to develop an efficient spectrum sharing platform.

1.2 Solution with Cognitive Radio Network

Federal Communications Commission (FCC), the spectrum regulation committee in the US has taken significant steps (see Sec. 2.1.2) to accommodate new users and satisfy their requirements. Similar steps have been taken by other spectrum regulation committees in Europe and Asia [91]. The concept of cognitive radio (CR) is introduced as a viable solution to both the spectrum scarcity problem and underutilization problem by dynamically sharing spectrum to end users according to their quality of service requirements.

By definition, cognitive radio can change its transmission parameters based on interaction with the environment. There are two features that make cognitive radio unique in the networking world [3]: (1) its cognitive capability to capture the information from the radio environment and (2) its reconfigurability to work on diverse frequencies in different transmission access technologies.

Based on the usage rights, cognitive radio network (CRN) consists of two types of users — primary users (PU) and secondary users (SU). Primary users are basically the license holders, and they have exclusive access rights to use a fixed spectrum band. On the other hand, secondary users either opportunistically exploit free spectrum or negotiate with primary users to transmit their own data. Cognitive radio network has thus become a prominent research field to address the spectrum allocation and sharing problem. Various spectrum sharing algorithms have been proposed and developed based on the collaboration between PUs and SUs in CRN. In this dissertation, we have explored several of these collaboration models. We have discussed the unique challenges associated with each model, and developed efficient spectrum sharing algorithms addressing some of these challenges.

1.3 Collaboration based Spectrum Sharing

Initial focus of the CRN research was to find unused spectrum without interfering primary users' transmission. Spectrum sensing techniques became the center of research to identify primary users' activity, detect unused spectrum, and opportunistically utilize that spectrum for transmission of secondary packets. Over the years different sensing techniques were developed by the researchers (for a comprehensive summary of sensing techniques, readers are referred to Sec. 2.1.3). While the sensing techniques offer an immediate opportunity to utilize unused spectrum without any major change in the existing primary user architecture it also faces several challenges. For example, determining sensing duration and sensing frequency while maintaining a high sensing accuracy were a major concern. Further research shows that cooperative sensing can reduce the sensing error and provide better detection and spectrum utilization than independent sensing. Consequently, an IEEE standard [110] is developed around collaborative sensing to design a regional area network.

The strict requirement of spectrum sharing is later relaxed, and secondary users are allowed to transmit as long as the interference caused from their transmission do not exceed a predefined threshold. In this model, collaboration between primary-secondary pairs is established on the basis of cooperative diversity and mutual needs. These collaboration models of spectrum sharing, their implementation challenges, and future prospects were discussed in the 2009 NSF workshop [109].

In parallel to these techniques, there is a continuous effort to ensure efficient spectrum sharing

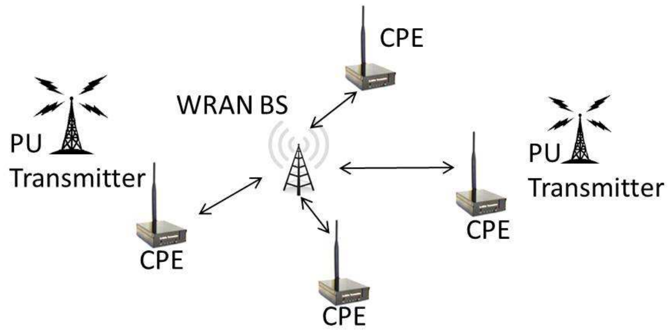

Figure 1.1: Sensing based collaboration model

by improving the existing spectrum regulation system. A well regulation system should motivate the primary users to share their unused spectrum to secondary users in exchange for additional revenue. This effort from the researchers and policymakers leads to design of various innovative auction mechanisms with dynamic network settings. These ongoing efforts have been recognized in the 2013 NSF workshop on wireless networking [13] and well adapted by FCC in designing future spectrum trading. We summarize these spectrum sharing techniques into the following three categories based on the collaboration between the primary and secondary users as follows [6].

1.3.1 Sensing based Collaboration Model

The first spectrum sharing model involves collaboration among the secondary users only. The primary users are unaware of the existence of the secondary users, and therefore secondary transmission must not interfere their transmission. To avoid interference with primary transmissions, the secondary users apply spectrum sensing techniques, and together, they decide the presence or absence of PU activity. When their collaborative decision implies the absence of PUs, the secondary users can share the unused spectrum for their own transmission.

An industry standard [110] IEEE 802.22 is being developed for Wireless Regional Area Network (WRAN) based on this sensing based collaboration model. Fig. 1.1 shows a WRAN consist-

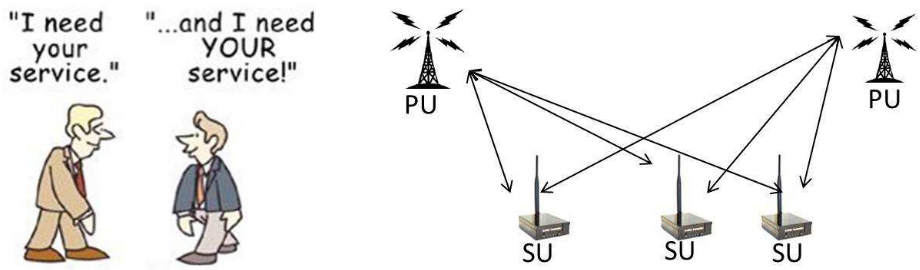

Figure 1.2: Relay based collaboration model[1]

ing of one base station (BS) and multiple secondary users as consumer premise equipments (CPE). In this standard, a base station instructs the CPEs to sense spectrum, and the secondary users send back their reports to the base station. The base station then makes a decision based on the sensing reports. However, this collaboration among secondary users also gives a malicious user an opportunity to manipulate the system [15]. An individual secondary user may send an incorrect sensing result, lead the base station to a wrong decision, and use the spectrum for its own benefits. This form of manipulation is referred to as 'spectrum sensing data falsification' or SSDF attack in IEEE 802.22 networks. In our research work, we address this problem and develop a decision making algorithm that prevents SSDF attack and isolates the manipulators from the decision making.

1.3.2 Relay based Collaboration Model

This spectrum sharing model involves mutual need based collaboration between primary and secondary users (see Fig. 1.2). Secondary users intend to access primary spectrum for their own transmission in exchange for relay services to primary users. This relay based communication reduces the impact of path attenuation, multi-path propagation, shadowing by obstacles and thus helps to strengthen the primary signal at the destination. PUs and SUs exchange their cooperation information and build a collaborative spectrum sharing model. This model is also known as

[1] the picture is partially taken from http://famousbloggers.net/quickhaggle.html

cooperative cognitive radio network (CCRN).

In this CCRN model, the PUs share their licensed spectrum in temporal, spectral, and spatial domain if the SUs offer relaying services to PU traffic. The PUs and SUs coordinate and schedule their cooperative transmissions for achieving mutual benefits by applying different relaying strategies (see Sec. 2.1.5). Since video will be the dominant part of the future traffic, we investigate whether mutual cooperation helps to support real-time traffic. We present a detailed analysis of the collaboration model between PUs and SUs addressing the impact of cooperation overhead and interference constraints. We develop a distributed interference aware reliable cooperation algorithm that helps a user to make cooperation decision and transmits its data.

Next we take our investigation from single hop to multi-hop cooperative communication in relay based collaboration model. We consider multi-hop cooperative relaying to establish a routing path through the SUs in exchange of their transmission opportunities. We apply the concept of an overlapping coalition game to define the reward of an individual user for participating in a cooperation. The simulation results show that it increases transmission opportunities of the secondary users while improving the reward of the primary users in terms of data rate and transmission delay.

1.3.3 Auction based Collaboration Model

In the auction based collaboration model, the primary and secondary users collaborate via a third party e.g., FCC [39]. The PUs auction their unused spectrum for extra revenue whereas the SUs bid in the auction to acquire necessary usage rights. Usually a trusted authority (e.g., FCC) holds the auction, administers spectrum allocation, and manages the payment transaction. Fig. 1.3 illustrates different components of a spectrum auction. Recent initiatives from the FCC strongly indicate that spectrum auctions will play a significant role in revolutionizing future spectrum distribution in general as well as in military use.

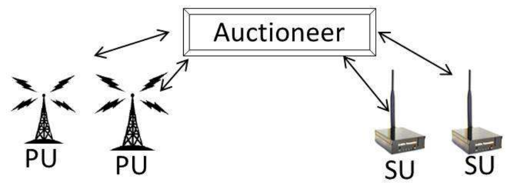

Figure 1.3: Auction based collaboration model

The major challenge in this model is to accommodate diversity in bidders and sellers while ensuring integrity and reliability of the auction. The licensed users may auction their spectrum in temporal and spatial domain with different values. Similarly, the secondary users place their bids according to their transmission requirements which also vary from users to users. In presence of such diversity, an auction mechanism must ensure truthfulness that cannot be achieved with well-known VCG mechanism (see Sec. 2.1.6). Additionally, spectrum auctions must ensure reusability which is different from traditional auctions. In traditional auctions, a single unit of product is sold to a single bidder whereas in spectrum auctions, the same spectrum can be allocated to more than one users as long as they are not interfering with each other. These unique differences make the traditional auction algorithms inapplicable to spectrum auctions.

In this context, we focus on online auctions in particular where the number of bidders and spectrum units are not known a priori and the auctioneer needs to make decision online. This setting is inline with the PU activity and spectrum demand from the opportunistic users. We also consider the diversity in bidders' transmission requirements. For example, a delay tolerant user can offload data at later time whereas an interactive user wants immediate spectrum access. We consider diverse features of bidders and sellers and design strategyproof auction algorithms which are then evaluated in terms of efficiency and revenue.

1.4 Contribution

With the arrival of new applications offering different services, the future network requires to accommodate the spectrum demand of their users. In this dissertation, we address some of the challenges towards accomplishing that requirement. The highlights of our contribution are as follows:

(i) IEEE 802.22 [110] is the wireless standard for rural broadband access. SSDF attack is a major problem in IEEE 802.22 networks. Our solution of this problem presented in Chapter 3 will be helpful to develop a secure collaborative sensing platform in IEEE 802.22.

(ii) Since the video traffic will dominate in near future, the network should be able to support reliable video transmission with low infrastructure cost. Our results from the relay based collaboration model will be useful to develop a reliable network based on mutual cooperation benefits between the PUs and SUs. The results are further extended from a single hop model to multi-hop collaboration model.

(iii) The ubiquitousness of wireless services will increase the number of consumers who will want to access networks anytime anywhere. The diversity in the requirements of these users and supplies need to be addressed online to build better spectrum sharing models around it. Our proposed auction mechanisms presented in this dissertation ensure online spectrum allocation and determine price considering diversities of both the buyers and sellers.

1.5 Organization

This dissertation is organized into several chapters. In Chapter 2, we first provide some background information related to our research, then present an extensive summary of related work on different collaboration models. Each of the following chapters addresses a specific problem based on user requirements and collaboration models. Chapter 3 addresses the SSDF attack in IEEE 802.22 networks under sensing based collaboration model and presents an adaptive clustering algorithm to prevent such attacks. Chapter 4 focuses on the challenges with real-time traffic and presents an interference aware reliable cooperation algorithm in relay based collaboration model. Chapter 5 explores the multi-hop relay based collaboration model to establish stable routing paths for the PUs while ensuring SU transmission opportunities. In Chapter 6, we analyze the diversity of bidders and sellers under auction based collaboration model. We develop online single and double auction algorithms that ensure truthfulness, individual rationality, budget balance, and improve efficiency and revenue. Finally, Chapter 7 concludes our work and discusses our future research directions.

Chapter 2

Background and Related Work

To better understand the research problems and the proposed solution, we provide some background information about some relevant topics. We also present a comprehensive summary of existing research work on three collaboration models.

2.1 Background

2.1.1 Spectrum Licensing

In each country, spectrum licensing is handled by a government authorized entity that regulates spectrum allocation, usage and distribution among the interested providers. In the US, Federal Communication Commission (FCC) is responsible for managing and licensing radio spectrum throughout the country to a diverse range of commercial and non-commercial users including public safety and emergency response services [36]. Since its formation in 1934, the FCC works with specific goals of advocating innovation and investment in broadband services, offering highest and best spectrum allocation techniques, and ensuring efficient and reliable access to allocated spectrum. Currently, the FCC controls the allocation of spectrum between 9KHz and 275GHz. Basically there are two ways the FCC makes spectrum available to wireless services - licensed and unlicensed. The licensed spectrum assignment is usually done through spectrum auctions. Note that different radio frequencies hold different propagation characteristics and are suitable for different services. The FCC holds auction for a specific frequency band and selects the highest bidder as winner among the interested service providers. The FCC then grants the winner permission to use that spectrum band for a specific or entire geographical location. For example, cellular service is in the range of 824-849MHz and 869-894MHz [107]. In the unlicensed spectrum, users operate without any license, however, must comply with the technical requirements guided by the FCC. The FCC also grants exclusive access to specific spectrum range to public safety agencies and first responders.

2.1.2 FCC Reformation Initiatives

It is evident from the present statistics and the Cisco traffic forecast [25] that it is not possible to satisfy the growing demand using traditional spectrum licensing techniques. The FCC advocates an innovative approach of spectrum sharing between legacy networks and new users via dynamic spectrum access (DSA). Based on early statistics, the FCC opens the TV broadcast channels for unlicensed access with an imposed interference constraint [38] [37]. It has been proposed to create a database with spectrum information. In 2010, the FCC presented the National Broadband Plan (NBP) which recommends several steps to reform the spectrum policy to address the spectrum situation [90]. The recommendations include taking initiative to make 500MHz of spectrum available for broadband access, offering incentives and mechanisms to repurpose spectrum, and expanding opportunities for innovative spectrum access models. Subsequently, the FCC has started an incentive auction, first of its kind, in the month of March of 2016 [58]. Recently, the FCC is planning to share the 3.5GHz spectrum which is currently used by the government radars and fixed satellites [26]. A three layer access policy has been proposed. In this proposal, the legacy network has the highest priority and operates on the first layer, the second layer provides access based on an incentive auction, and the third layer is open to users for unlicensed access.

2.1.3 Spectrum Sensing

A number of different sensing algorithms are presented in literature [101] [42] [9]. The most common sensing technique is energy based detection due to its low computational cost and implementational complexities. The received signal is compared with a preset threshold value to detect the presence of PU. The challenge of this technique includes the appropriate threshold selection and its differentiation between PU signal and noise under low signal-to-noise (SNR) values. In the wavelet-based sensing, known pattern is used to detect PU signal that ensures higher reliability and faster convergence than the energy detection method. Another sensing method is to exploit cyclostationary features of the received signals. Cyclostationary features can even be used to distinguish among different types of transmissions and primary users. With the knowledge of the technology used in PU transmission, several features can be extracted from the received signal and various classification model can be applied to detect the PU signal. Besides these sensing methods, few other methods are presented in literature [133]. However, detection performance of an individual secondary user often suffer from multipath fading, shadowing, receiver uncertainty issues [4]. Collaborative spectrum sensing is found to be an effective solution to overcome these limitations [133].

2.1.4 IEEE 802.22 WRAN Standard

The IEEE 802.22 standard has been started being developed in 2004 [1] [29]. It is targeted to provide low population density rural areas with broadband access. IEEE 802.22 defines a centralized, single hop, point to multi-point communication standard for wireless regional area network (WRAN). The base station is connected to the Internet through a backhaul while the customer premise equipments (CPE) are connected to the base station through vacant TV channels. The users apply cognitive radio techniques to avoid interference to broadcast users. The spectrum sensing is controlled and coordinated by the base station. The base station also has an interface to access the spectrum database. The network operates over 54-862MHz and uses OFDMA technology [1]. A complete proposal draft and its amendments can be found here [122].

2.1.5 Relaying Strategies

In relay based collaboration model, the primary source node sends packet to an intermediate secondary node, and then intermediate secondary node forwards it to the destination. There are generally two strategies used in relaying packets from source to destination. They are as follows:

(a) Amplify and Forward (AF) [28]: The relay node receives the signal at first, then amplifies it, and finally relays it to the destination.

(b) Decode and Forward (DF) [28]: The relay node tries to decode the signal after it received it from the source and extract the intended message. It then re-encodes the message and transmits it to the destination.

The AF strategy is preferred when the relay node is closer to the destination, and the relay does not need to use much power. Since the relay amplifies the noisy received signal, the noise is also amplified and its effect becomes more severe when the relay is far from away from the destination. On the other hand, the DF strategy works better if the relay node is closer to the source. It is then more probable that the relay node decodes the message without any error. Both these relaying strategies are studied in relay based collaboration model [86] [50] [23] to explore the cooperation benefits of transmitting primary packets through secondary users in cognitive radio networks under inter-user collaboration model. There is another less known relaying strategy called compress and forward (CF) [28]. In this strategy, the relay node quantizes the received signal, encodes the samples into a new message, and then forwards the message to the destination.

2.1.6 VCG Auctions

In general, an auction mechanism should have the following properties such as truthfulness, individual rationality, and budget balance. The truthfulness property ensures that a bidder cannot increase its profit by manipulating any of its information. Individual rationality means that any participant in the auction must achieve nonnegative profit. An auction is budget balanced if the total amount paid to the sellers is no greater than the total amount paid by the bidders.

The design of second price auction by Vickrey ensures truthful bidding of bidders. According to this auction [72], bidders place their sealed bids. The highest bidder wins but pays equal to the second highest bid. This concept is further generalized by Vickrey, Clarke, and Groves [138]. In their proposed sealed bid multi-unit auction (referred to as 'VCG auction'), bidders bid their valuations for the desired item without knowing the bid information of competing bidders. The auctioneer assigns items in a socially optimal manner. Each winner is charged the amount equal to the bid of the losing bidder who could win if the winner were not present. This mechanism is a generalization of the second price auction and is proved to be incentive compatible and individual rational. The mechanism is attractive since it guarantees truthful reporting as the best strategy of a bidder and a bidder cannot increase its profit by manipulating its bid. However, this mechanism does not guarantee truthfulness when the bidders have flexible deadlines and their arrival is dynamic.

2.1.7 McAfee Auction

McAfee in his seminal paper [88] designed a dominant strategy for both buyers and sellers in a static double auction. This strategy is used to design a truthful mechanism for spectrum double auctions [20, 143]. According to this strategy, bidders in the set **T** are sorted into non-increasing order of bid $b_1 \geq b_2 \geq \ldots \geq b_{n'}$ where n' denotes the number of bidders in the auction, i.e., $|\mathbf{T}| = n'$. The sellers in set $\mathbf{S}'$ are sorted into non-decreasing order of ask $a_1 \leq a_2 \leq \ldots \leq a_{m'}$ where m' denotes the number of sellers in the auction, i.e., $|\mathbf{S}'| = m'$. The minimum bid of the bidders $b_{(n'+1)}$ and the maximum ask of the sellers $a_{(m'+1)}$ are set to $-\infty$ and ∞ respectively. Then, h pairs are selected such that $\forall\ i \leq h$, $b_i \geq a_i$ and $b_{(h+1)} < a_{(h+1)}$. So, there are $h - 1$ trades in the auction, and the $h - 1$ highest bid buyers and the $h - 1$ lowest ask sellers are selected as winners. If $h = 1$, no winner is selected. This implies that there must be at least two pairs of bidders and sellers to have one successful trade. Each winning bidder $i \in \mathbf{T}$ pays the amount equal to $b_{(h)}$, and each winning seller $j \in \mathbf{S}'$ is paid the amount equal to $a_{(h)}$. The auctioneer's utility is equal to $(h - 1) \times (b_{(h)} - a_{(h)})$. While this mechanism works for static setting, it fails to ensure truthfulness in online setting consisting of bidders with transmission deadlines.

2.2 Related Work

We discuss the existing research work based on the collaboration models between the primary and secondary users in the network.

2.2.1 Related Work on Sensing based Collaboration Model

Early research on cognitive radio network mostly addresses the independent effort of secondary users to find spectrum holes without primary users [77] [83] [100] [56] [8]. Further research showed that collaborative sensing improves the sensing accuracy and increases secondary transmission opportunities in comparison to independent sensing [133] [4] [42].

While cooperative sensing improves the accuracy of primary user detection, it brings different form of challenges such as SSDF attack. We divide the existing solutions to combat against SSDF attack into three categories — reputation-based, data mining based, and artificial intelligence approaches. Wang et al. [120] proposed an onion peeling approach based on Bayesian statistics to assign suspicion levels to all nodes in the network. They test their heuristic based approach for false alarm attacks, miss detection attacks, and combinations thereof. However, they assume that base station has prior knowledge about the activities of attackers, which is not very common. Also, Qin et al. [93] proposed a trust based model and use a weighted sensing result aggregation method to remove malicious nodes from the decision making process. Chen et al. [18] presented a hybrid method called the weighted sequential probability ratio test (WSPRT) that combines a node's reputation and the use of a sequential probability ratio test to identify malicious or faulty units. WSPRT is only tested against attackers utilizing an always-false or always-free response which are unsophisticated attack strategies not likely to reflect real scenarios. Rawat et al. in [7] explored independent and collaborative SSDF attacks and proposed a simple reputation-based method to identify attackers. They determined optimal attacking strategies for collaborating attackers where the BS cannot possibly discriminate between honest and attacking CRs. A mathematical analysis of detection performance was carried out using the Kullback-Leibler divergence (KLD). According to their results, in presence of 50% independent attackers, BS cannot differentiate between the honest users and the attackers. However, for collaborative attack, this ratio reduces to 35%.

A new approach based on K-neighborhood distance algorithm is presented in [78] to detect independent malicious users. This approach does not need any prior knowledge of attacker distribution and exposes attackers across multiple sensing rounds. However, when attackers collaborate, they can successfully evade detection. Further work has been done by [65] in establishing a more robust decision algorithm corroborating information regarding PU positioning and path loss to the secondary user. The proposed method dramatically increases misdetections when using incorrect static thresholds.

Clancy et al. [27] addressed a series of steps to combat the sensitive areas in CR by assuming a noisy environment, implementing levels of common sense, and programmatically resetting learned values to avoid extended corruption from attackers. They offer up the use of swarm behavior in determining a global decision on whether a sensed signal was actually generated by a primary user, along with a trust-based method. However the proposals on how these CRs should operate in the field are presented without details for verification. They also do not address how to incorporate this new information into the current IEEE 802.22 networks. Besides these approaches, Yu et al. in [132] considered data falsification attacks in ad hoc cognitive networks and used a consensus based algorithm inspired from animal life to detect independent attackers only.

Few more research studies have addressed the spectrum sensing data falsification attacks by using support vector machine [35], suspicion level [84], incentive based approaches [105], radio propagation characteristics [85], cross layer information and statistical analysis [106]. However, none of these studies have considered to be effective in the case of collaborative attackers.

2.2.2 Related Work on Relay based Collaboration Model

Over the years researchers have shown great interest in developing cooperation frameworks between the primary and secondary users using game theory approaches like Stackelberg game [136] [131], [103], [48], noncooperative games [81], back-pressure algorithm [67, 127] and so on. Also, initial research work in this category mainly focuses on single hop communication [53, 61, 62, 64, 67, 76, 131, 136]. The single hop cooperation is considered in time domain or frequency domain or in both.

Zhang et al. [136] modeled the cooperation as a Stackelberg game and analytically found the Nash equilibrium. In this cooperation model, a primary user uses a secondary user as a relay to improve its throughput while the secondary user can access a fraction of the channel as payment for relaying the primary traffic. The same model is also considered in [115], [131], and [103]. According to this model, time slots are divided into subslots. The primary user broadcasts its packet to a chosen set of secondary users in the first subslot. In the next subslot, all the secondary users relay primary traffic while the primary user transmits the packet directly. In the last subslot, secondary users transmit their traffic. However, this model is designed for one primary transmitter and one primary receiver. They assume that the primary transmitter uses a predefined fixed traffic rate. The focus here is on maximizing primary user utility while secondary user utility is ignored. Also, in [103], cooperation between primary and secondary users is investigated using Stackelberg game. Cooperation model based on packet retransmissions only is analyzed in [74].

Yi et al. [131] [130] also study the cooperation framework among users where the primary access point (AP) and secondary AP sequentially decide the strategy for cooperative relay selection, slot allocation among multiple users, and spectrum leasing price. The sequential process is again formulated as a Stackelberg game, and a unique Nash equilibrium is found using backward induction analysis. However, this work also considers a fixed traffic rate for the primary users and no minimum requirement for the secondary users. Since, we consider cooperation, secondary users' performance cannot be ignored. Authors in [111] consider a slightly different model where the primary users give up a part of their bandwidth for the secondary users exclusively to transmit their traffic and propose an optimized allocation mechanism to maximize primary users' power saving and secondary users' transmission rate.

The study in [69] considers cooperation between primary and secondary users in a primary multicast network. In this context, primary users leverage secondary users as relays in return for part of their transmission time which is distributed among all secondary users in TDMA fashion. The authors formulate an optimization problem to find the time allocation between primary and secondary users to improve utility of both networks. An approximation algorithm based on linear programming is proposed to solve the problem. Khalil et al. [67] added immediate reward and long term reward for secondary users in the cooperative model. In the case of immediate reward, the primary user shares the same time slot with the secondary user while in the case of long term reward, the secondary user is guaranteed to get a share of the spectrum in the long term. However, like previous approaches, it schedules only one pair of primary and secondary users and assumes both types of users have backlogged traffic. Additionally, the algorithm sacrifices the primary users' transmission to support the long term transmission opportunity for the secondary users. This framework may not be suitable for packets with deadline constraints.

Besides game theory approaches, one of the common tools used to formulate and analyze the cooperation framework is a Markov decision process (MDP). For example, authors in [87] consider a network consisting of a single primary user with infinite buffer and multiple secondary users and formulate a constrained MDP problem with the aim of maximizing secondary transmission opportunities while guaranteeing stability of the queue of the primary user. The authors in [117] derived a stable throughput region considering a single primary-secondary user pair where a secondary user's sequential decision to cooperate or not is formulated as a MDP problem focusing on the tradeoff between gain and cost of cooperation. A few papers address the delay issue in different settings. For example, Shafie et al. in [98] considered delay sensitive primary users, Ashour et al. in [10] analyzed the tradeoff between throughput and delay, Elmahdy et al. in [34] studied finite relaying buffers, and Hyder et al. in [53] presented an analytical framework for delay optimization in cognitive radio networks.

The research paradigm is recently shifted from single hop to multi-hop cooperative communication. Intermediate relays in a cooperative transmission try to achieve the same goal as does the primary source. For example, the authors in [2, 57, 68] exploited the routing information for different channel models to minimize the overall energy consumption. In the context of CCRN, the intermediate relays are secondary users who may have different and contrasting goals. A cross-layer optimal scheduling algorithm was proposed in [127] for cooperative multi-hop CRNs. In this network, the secondary users cooperate with primary users to transmit in a multi-hop fashion, and the secondary users earn transmission opportunity in return. The analysis was developed to achieve optimal throughput for the primary users where the upper bound was derived. However, the analysis considers a fixed routing path between a pair of primary source and destination nodes. Li et al. [79] considers multi-hop cooperation among primary and secondary users in both time and frequency domain and investigates the cooperation opportunity for finding a stable routing path. Accordingly, the routing path construction problem is formulated as a network formation game, and utility and payoff functions are defined accordingly. Primary users sequentially construct routing paths through one or more secondary users. However, members of two separate routing path are mutually exclusive i.e. no secondary user can participate in more than one routing path, which limits the opportunity of secondary users to improve its winning probability. Therefore, it is important to study the cooperation behavior considering the strategic independence of primary and secondary users.

2.2.3 Related Work on Auction based Collaboration Model

Spectrum auctions can be categorized in single (single-sided) and double (double-sided) auctions or static (offline) and real-time (online) auctions. In single auctions, one or more sellers have one or multiple number of spectrum units for sale but they have not set minimum price per unit. However, the bidders make different bids for one or multiple units of spectrum. In double auctions, sellers also set different selling prices for their units. In static auctions, the number of bidders and the number of sellers are fixed and the auctioneer is aware of the entire set. In online auctions, the auctioneer does not know the number of future participants and take decision on-the-fly about the allocation and pricing.

VERITAS [142] presents a framework so that the auctioneer can apply different allocation algorithms according to its objective function where the objective can be ensuring fairness or maximizing revenue. The proposed auction mechanism is proved to be truthful and efficient. Sengupta et al. in [96, 97] presents an auction mechanism where wireless service providers (WSP) bid to acquire spectrum. The allocation problem is mapped to a knapsack problem and winner selection and pricing are optimized under both first price and second price bidding strategies. Sun et al. in [113] proved the existence of Nash equilibrium in an auction where users are bidding for wireless fading channel with budget constraint. Kong et al. in [71] uses a variation of the VCG algorithm to allocate resources in a non-cooperative OFDM network and ensures truthfulness of the mechanism. Wu et al. in [123] proposed an auction algorithm focusing on waiting time instead of auction revenue. Their analysis proves the existence of a unique Nash equilibrium and the simulation results show that the proposed auction improves the winning probabilities of secondary users.

Later work captures the diversity in sellers' valuations in double auction settings. TRUST [143] is the first double auction mechanism that ensures spectrum reusability and satisfies auction properties such as truthfulness. Later work ([21, 22, 31, 40]) on double auctions considers similar static models and improves certain auction outcomes such as revenue and fairness.

All of these above research consider static models and present offline auction mechanisms. Recent research focuses on online spectrum auction models [30, 41, 63, 125, 126]. Considering the online arrival of users, the authors in [30] proposed an efficient online spectrum auction mechanism with preemption which prevents both bid-based and time-based cheating. However, it does not provide a performance bound on revenue with respect to the optimal solution. Under the same online auction model, Xu et al. [125] proposed TOFU, another online semi-truthful spectrum auction mechanism with channel preemption. In contrast to previous solutions, TOFU achieves only semi-truthfulness where users may underbid to gain. TORA [63], on the other hand, considers a reverse auction where number of bidders is fixed throughout the auction. LOTUS [20] proposed a location and distribution aware online double auction mechanism where dynamic requests from bidders are satisfied from a fixed set of spectrum units. However, it cannot ensure truthfulness in the presence of dynamic availability of spectrum and bidders with transmission deadlines.

Chapter 3

ARC: an Adaptive Reputation based Clustering Algorithm against SSDF Attack in IEEE 802.22 Networks

As the research on cognitive radio matured, it was realized that cooperative sensing based collaboration model[1] among secondary users may detect the PU presence more quickly and accurately than independent sensing [4]. This realization was reflected on the design of the first cognitive radio based network standard, IEEE 802.22 for wireless broadband access (see Sec. 2.1.4). This standard defines the implementation of opportunistic spectrum sharing (OSS) by outlining how/when wireless devices are able to utilize temporarily idle bands in licensed radio spectrums. The proposal also defines the cellular like communication interface between a base station (BS), and secondary users called consumer premise equipments (CPE). The BS is responsible for controlling the spectrum usage and channel assignment to CPEs. All CPEs in a cell periodically monitor primary user signals and the BS leverages the distributed sensing power of CPEs through continual spectrum

[1] The work presented in this chapter has been published in two research articles:

(i) Chowdhury Sayeed Hyder, Brendan Grebur, Li Xiao, "Defense Against Spectrum Sensing Falsification Attacks in Cognitive Radio Networks", International Conference on Security and Privacy in Communication Networks (Securecomm), pp 154, London, UK, Sept 7-9, 2011.

(ii) Chowdhury Sayeed Hyder, Brendan Grebur, Li Xiao, Max Ellison, "ARC: an Adaptive Reputation based Clustering against Spectrum Sensing Data Falsification Attacks", IEEE Transaction on Mobile Computing, 13(8), pp 1707-1719, August 2014.

reports obtained from them.

To coordinate the process, a centralized BS collects sensing information from the secondary users attached to the cell. Each user submits a hypothesis regarding whether or not they suspect the primary user is transmitting. As radio waves are affected by physical barriers or environmental conditions, the detection accuracy of any node within sensing range of the PU's signal varies from time to time. Malfunctions associated with the sensing equipment may also influence the node's observed measurements. From the hypotheses supplied by the secondary users, the BS must decide on the actual state of the associated spectrum. Once a decision is made, the base station informs SUs and revokes permission of the users currently transmitting on that spectrum.

Due to its unique characteristics, CRNs face new security threats in addition to the common existing security challenges in wireless network. One typical type of attack is the Spectrum Sensing Data Falsification (SSDF) attack or Byzantine attack. During such an assault, the malicious user compromises one or more of the secondary users and may begin sending modified sensing reports to the BS. In this way, an attacker tries to influence the BS into producing a wrong decision about the channel status. Compromised nodes may work independently, or may collaborate to reduce spectrum utilization and degrade overall performance of the network.

Constructing a decision-making strategy that mitigates the impact of both independent and collaborative SSDF attackers will be invaluable to the advancement of CRN. By strengthening the base station against malicious or malfunctioning users, the interference produced from CRNs will be minimized, potentially expediting the implementation of such network alternatives. Ultimately, both users and businesses can reap the benefits of efficient radio spectrum usage through CRNs.

Existing research studies like [78], [120], [121] mainly consider independent malicious attack. However, these approaches either require prior information of attackers (e.g. number of attackers [121], attackers' distribution, attacking strategy [120] etc.) or depend on careful threshold selection

[78]. To the best of our knowledge, only one work [7] handles both independent and collaborative attacks using a reputation based method and limits the error rate in deciding channel status and in identifying attackers. Although the identification rate of attackers of this approach is high, it also misdetects a large number of honest users as attackers. Additionally, this approach fails completely when only a few users collaborate in SSDF attack, and error rate (i.e. number of incorrect decisions) increases almost linearly with number of attackers.

In this regard, we propose an adaptive reputation based clustering algorithm to defend against both independent and collaborative SSDF attacks that does not require prior information about the number of attackers or attacking strategies [55] [54]. The whole process goes through a sequence of phases to make a decision. First, the nodes are clustered based on the sensing history and initial reputation of nodes. The channel status is decided through intra-cluster and inter-cluster voting. The final decision is propagated back to the clusters and then to the individual nodes for adjusting the reputation of the nodes. We compare the performance of our algorithm with that of the algorithm proposed in [7] under different attacking scenarios. Our algorithm handles SSDF attacks significantly better than the one in [7] and minimizes the error in deciding channel status. Our algorithm also identifies most of the attackers while keeping a much lower misdetection rate.

3.1 System Model

In this section, we explain the topology of the CR network. We also consider both independent and collaborative attacking models and explain the decision mechanism of the BS.

3.1.1 Network Model

We consider an IEEE 802.22 WRAN network where the BS is the central coordinator and acts as the fusion center that regulates the medium access of all n secondary nodes attached to it. Among the n secondary nodes, n_a nodes are attackers and n_h are honest users ($n_a \leq n_h$). Honest users are completely unaware of the presence of the attackers. We do not consider the number of attackers more than 50% because it is not productive to study a network where a majority of nodes are attackers.

The BS performs distributed sensing through secondary users to decide on the channel status. At the start of each time period, SUs periodically sense a channel and report it back to the BS. The BS takes the final decision based on the reports and if the channel is free, it allocates the channel among the users. We assume that SUs use the threshold based energy detection technique [133] for spectrum sensing and the threshold for primary user detection is defined by the BS.

All secondary nodes decide about the PU presence independently based on the detection technique and send their reports to the BS. According to the IEEE 802.22 standards [99], the required sensing time of a node is 2 sec and the probability of a false alarm should be kept to 0.1 at maximum. However, due to the sensing time constraints and limitation of detection techniques, it is not possible for SUs to detect PU presence with 100% accuracy. We also assume that neither secondary users nor the base station have any knowledge about the actual channel status.

In each time slot, honest SUs sense the channel, compare the sensed energy with the threshold, and decide independently about the channel status. Finally, they report their findings to the BS without any alteration. On the other hand, the dishonest users can be selfish or malicious based on their intention; both are commonly referred to as 'attackers'. From a selfish attacker's point of view, the goal is to make the base station take a wrong decision about the channel status so that it may exploit the spectrum opportunity to transmit its own data. On the contrary, a malicious attacker's goal is not only to minimize the spectrum utilization, but also to degrade the network performance. The latter one is more harmful than the former since it also increases the interference with primary users.

3.1.2 The Decision Rules

The BS performs a binary hypothesis test to decide on the actual channel status that can be defined as follows.

$$
\begin{aligned}
H_0 &: \text{ Primary user is absent (channel is free)} \\
H_1 &: \text{ Primary user is present (channel is busy)}
\end{aligned}
$$

When there is no attack prevention mechanism, the BS generally follows a 'n_0 out of n' rule to decide on the channel status where n denotes the total number of secondary users. Accordingly, if each secondary user i sends its own individual hypothesis ($\mathbb{D}_i \in \{0, 1\}$) to the base station, the final decision $\mathbb{D}$ can be defined as follows [32].

$$
\mathbb{D} = \begin{cases} H_1 & \text{if } \sum_{i=1}^{n} \mathbb{D}_i \geq n_0 \\ H_0 & \text{otherwise} \end{cases}
$$

The special case (when $n_0 = 1$) is referred to as OR rule (if any of the nodes sense the channel busy, BS decides a busy channel). This approach is very conservative in the sense that one single attacker or even a malfunctioning honest node can reduce the spectrum utilization. The alternative approach is to decide depending on majority voting (e.g. $n_0 = \frac{n}{2}$). This resolves the spectrum underutilization problem but significantly increases the misdetection rate. As a result, it becomes vulnerable when attackers collaboratively decide their attacking strategy as well.

3.1.3 Honest User Model

We assume that even an honest user cannot detect PU presence with 100% accuracy. We define *false alarm rate* as the probability of sensing the presence of a PU when it is actually not transmitting, and we define *misdetection rate* as the probability of not sensing a PU when it is actually operating. Let us assume that the probability of false alarm and misdetection rate of a user are P_{fa} and P_{md} respectively.

$$P_{fa} = \Pr(y_i = 1|H_0),\ P_{md} = \Pr(y_i = 0|H_1)$$

where y_i represents the sensed result by user i.

As explained, honest users do not change their sensing results. Let us assume that x_i represents the report sent to the BS by user i.

$$\Pr(x_i = 1|y_i = 1) = 1, \Pr(x_i = 0|y_i = 1) = 0, \Pr(x_i = 0|y_i = 0) = 1, \Pr(x_i = 1|y_i = 0) = 0$$

Accordingly, we can calculate the detection probability of an honest user, P^h_{detect} using Eqn. 3.1.

$$\begin{aligned} P^h_{detect} &= \Pr(x_i = 0|H_0)\Pr(H_0) + \Pr(x_i = 1|H_1)\Pr(H_1) \\ &= (1 - P_{fa})P_I + (1 - P_{md})P_B \end{aligned} \tag{3.1}$$

Here, P_I and P_B denote the actual idle and busy rate of the channel respectively.

3.1.4 Attack Model

We consider that attackers devise their plan independently or collaboratively. Based on their attacking strategy, each attacker node may alter its sensing result from busy to idle and from idle to busy with different probability. We also assume that both of the probabilities are the same. However, our results can be easily extended for different probability. Accordingly, we consider one independent and three collaborative attacking techniques. We selected the attacking techniques considering the ease of implementation, impact of the attack, frequency of attack and so on. The first collaborative technique "n_l out of n_a" was already shown to be effective in [7]. The second technique is considered here due to ease of implementation and it follows an intuitive attacking model. The third technique is considered to exploit the proposed decision mechanism used.

3.1.4.1 Independent Attack

Each independent attacker changes its sensing result with probability P_{mal}. The detection probability of an individual attacker, P^a_{detect} while working independently can be expressed using Eqn. 3.2.

$$\begin{aligned} P^a_{detect} &= \Pr(x^a_i = 0|H_0)\Pr(H_0) + \Pr(x^a_i = 1|H_1)\Pr(H_1) \\ &= [(1 - P_{mal})(1 - P_{fa}) + P_{mal}P_{fa}]P_I + [(1 - P_{mal})(1 - P_{md}) + P_{mal}P_{md}]P_B \end{aligned} \tag{3.2}$$

Similarly, we can find the false alarm probability of an attacker (P^a_{fa}).

3.1.4.2 Collaborative Attack

In the case of a collaborative SSDF attack, attackers exchange their sensing information and decide their response collaboratively. First, we consider the collaboration strategy 'n_l out of n_a' attack.

It is shown in [7] that only 35% of attackers using this approach can blind the decision mechanism of the BS. Let us assume that P^{a1}_{detect} and P^{a1}_{fa} denote the common detection probability and false alarm probability of attackers. In this case, P^{a1}_{detect} and P^{a1}_{fa} will be,

$$P^{a1}_{detect} = \sum_{i=n_l}^{n_a} \Psi(n_a, i, P^a_{detect}), \quad P^{a1}_{fa} = \sum_{i=n_l}^{n_a} \Psi(n_a, i, P^a_{fa}) \tag{3.3}$$
$$\text{where, } \Psi(n_a, i, k) = \binom{n_a}{i}(k)^i(1-k)^{n_a-i}.$$

Here, n_l is defined in [7]

$$n_l = \min\left(n_a, \left\lceil \frac{n_a}{1+\zeta} \right\rceil\right) \text{ where, } \zeta = \frac{\ln \frac{P_{fa}}{P^h_{detect}}}{\ln \frac{1-P^h_{detect}}{1-P_{fa}}}$$

The second collaboration technique is inspired from the fact that if a majority of the nodes alter their sensing reports, the BS will take a wrong decision. Accordingly, we consider the *Going Against MAjority (GAMA)* attack to analyze the impact of collaboration in which all attackers share their true sensing results and then decide to send to the BS the opposite to the majority sensing result with a certain probability. For example, if two attackers sense the channel idle and one attacker senses the channel busy, all three attackers report to the BS that the channel is busy. In this case, the common detection probability of attackers will be

$$P^{a2}_{detect} = \sum_{i=l}^{n_a} \Psi(n_a, i, 1 - P^h_{detect}), P^{a2}_{fa} = \sum_{i=l}^{n_a} \Psi(n_a, i, 1 - P_{fa}) \tag{3.4}$$

where $l = n_a/2 + 1$.

The third collaboration technique we consider is the *SubGroup (SG)* attack. The reason we select this approach is to investigate whether it is possible for attackers to successfully attack and avoid being detected simultaneously if they attack in subgroups. Consequently, attackers form small groups, and each group changes their sensing result according to the first approach. Finally, one group is chosen randomly, and all the attackers in that group report the same sensing result.

We did not consider that attackers can overhear the honest users and devise their plan accordingly since it is not easy to overhear the sensing reports from all users. Even if an attacker can report its sensing report based on that, its response will incur a significant latency to reach to the BS which can be exploited to discard it from the decision mechanism. Also, this type of attack will be more effective if the BS follows an OR rule instead of majority rule [32].

3.2 Algorithm Design - Attackers vs BS

In this section, we show the impact of attackers in the decision mechanism and explain the defense mechanism that the BS uses to defend against different attacking strategies in detail.

3.2.1 Attackers' Impact

In this section, we analyze the impact of attackers, both independent and collaborative, in the decision mechanism of the BS.

Let us assume that the base station decides based on a majority voting. Let X and Y denote the number of honest users and malicious users that detect the channel status correctly. Since all the honest users are independent, X follows a binomial distribution with parameter n_h and P^h_{detect}. Similarly, in the case of independent malicious attack, Y also follows a binomial distribution with parameter n_a and P^a_{detect}. So, P_S, the overall detection probability of the system, can be calculated using the joint distribution of detection probability of independent honest users and independent

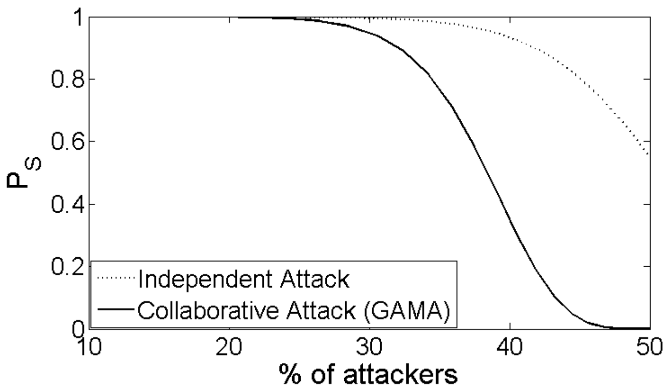

Figure 3.1: System detection accuracy with varying attackers

attackers. Let, $k = (n_a + n_h)/2$.

$$P_S \quad = \quad \Pr(X + Y > k) = \sum_{i=1}^{n_h} \Psi(n_h, i, P^h_{detect}) \sum_{j=k-i}^{n_a} \Psi(n_a, j, 1 - P^a_{detect})$$

In the case of collaborative attack, the detection probability degrades according to their collaboration strategy. Here, we only demonstrate the impact of a GAMA attack as a representative of collaborative attack. Similarly, other variations of collaborative attacks can be explored.

Let us consider the GAMA attack when all the attackers change their decision against the majority sensing result with probability α i.e. $P_{mal} = \alpha$. So, either all attackers send correct channel status or none of them sends correct report. For simplicity, let us assume that probability of attack α is 1. So, attackers always send the opposite of the majority sensing results.

Let P_Y denote the probability that all the attackers will send correct sensing report in GAMA attack. This is equivalent to the case when majority attackers fail to sense the correct channel condition.

$$P_Y \quad = \quad \Pr(Y < \frac{n_a}{2}) = \sum_{j=1}^{n_a/2-1} \Psi(n_a, j, P^h_{detect}) = P^{a2}_{detect}$$

The overall detection accuracy of the system depends on the joint distribution of attackers and honest users' detection probability. Eqn. 3.5 represents the correct detection probability in presence of collaborative GAMA attackers.

$$\begin{aligned} P_S &= P_Y \Pr(X \geq k - n_a) + (1 - P_Y) \Pr(X \geq k) \\ &= P^{a2}_{detect} \sum_{i=k-n_a}^{n_h} \Psi(n_h, i, P^h_{detect}) + (1 - P^{a2}_{detect}) \sum_{i=k}^{n_h} \Psi(n_h, i, P^h_{detect}) \end{aligned} \tag{3.5}$$

The impact of both independent and collaborative attackers in the decision making process is shown in Fig. 3.1. We calculate the detection accuracy of independent attackers according to Eqn. 3.5. and of collaborative attackers according to Eqn. 3.5. We achieved similar results for other type of collaborative attacks. The parameters we consider here are as follows: P_I = 0.9, P_B = 0.1, P_{fa} = P_{md} = 0.2.

3.2.2 Design of the Algorithm

The decision mechanism should be robust and capable of defending against any attacking strategy adopted by any number of malicious users. However, the BS does not have any information about the attacking strategies or number of attackers. The only information available to the BS is the sensing reports sent by users attached to it. So, the defense mechanism should be able to nullify (or at least reduce) the impact of collaboration of attackers, identify them and quarantine them from the process.

Accordingly, we design an adaptive reputation based clustering (ARC) algorithm to defend against both independent and collaborative SSDF attacks. The algorithm works against the intention and motivation of malicious users and tries to nullify their influence on the final decision.

To reduce the impact of attackers, we create clusters so that nodes with similar sensing history

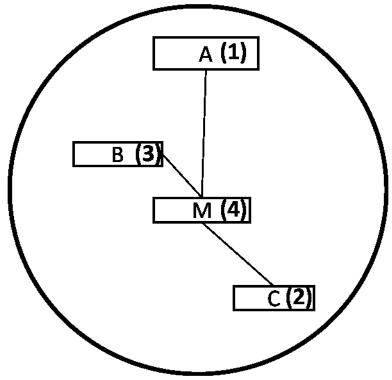

Figure 3.2: Reputation distribution

will be in the same cluster. Then, each cluster has only one vote to cast and the channel status is decided based on majority voting of the clusters. The idea behind this is that if the attackers attack frequently, attackers and honest nodes will be in separate clusters due to their different sensing reports. Also, the collaboration of attackers will not help to increase the error rate since each cluster has only one vote.

The key to attackers' success is to avoid being in the same cluster and to take control of the majority of the clusters. To handle these issues, we introduce distance weighted voting in a cluster and a feedback component in each node's reputation. Each node's voting weight in the cluster is inversely proportional to its distance from the median of that cluster. Similarly, each node gets reputation, which is inversely proportional to its distance from the median of that cluster. By distributing the reputation based on distance from the median, nodes are only impacted relative to their "confidence" of that group.

The reputation assignment to each node in a sample cluster is demonstrated in Fig. 3.2 where the reputation of each node is shown inside the parenthesis of each node. As explained, the closer is the node to the median (M), the higher is the reputation of the node. Accordingly, the median node (M) has the highest reputation (4) while the node farthest from the median (A) has the lowest reputation.

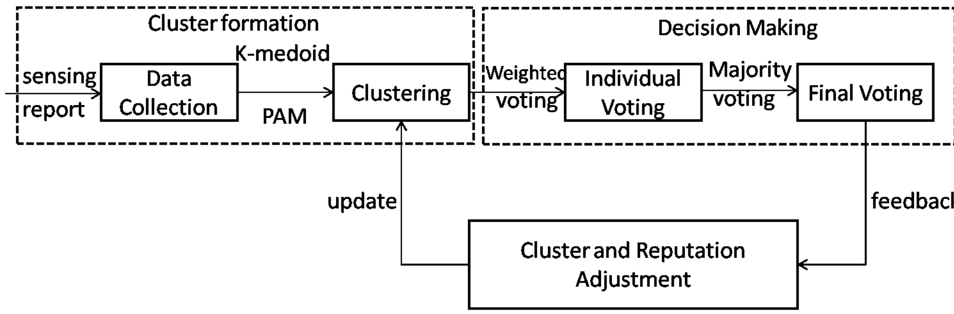

Figure 3.3: Block diagram of different phases of the algorithm

Furthermore, from the next round, nodes' modified reputation is also used for clustering in addition to sensing history. In this way, even if an attacker and an honest user incorrectly fall in the same cluster, attackers cannot establish their decision. Furthermore, as time goes on, the distance between an honest user and an attacker will be amplified due to the joint consideration of reputation and sensing history in cluster formation.

3.3 Adaptive Reputation based Clustering (ARC) Algorithm

The proposed adaptive reputation based clustering (ARC) algorithm executes a sequence of phases to reach the final decision (Fig. 3.3). In the $collection$ phase, the BS collects the sensing reports from all the nodes in its cell. In the $clustering$ phase, the modified version of the partitioning around medoids (PAM) algorithm is applied to create k equal sized virtual clusters. In the $voting$ phase, final decision is made based on intra-clustering and inter-clustering voting. This is followed by an $update$ phase where the number of clusters are adjusted and the reputation of all nodes are reevaluated. Next, the major components of our algorithm are explained.

3.3.1 Cluster Formation (Clustering Phase)

Clustering techniques are often used in anomaly identification or outlier detection. Two of the prominent clustering techniques are K-means and K-medoid [66]. K-means defines a cluster in terms of a centroid, which is usually the mean of the group of points. It clusters the objects in a way to minimize the sum of squared Euclidean distance. On the other hand, K-medoid defines a cluster in terms of a medoid, which is the most representative object for a group of objects and can be applied to a wide range of data. The K-medoid algorithm requires only a proximity measure for a pair of objects and tries to minimize the total error. We prefer K-medoid to K-means algorithm for clustering since the former is more robust to noise and outliers than the latter and minimizes a sum of pairwise dissimilarities instead of a sum of squared Euclidean distances.

Several algorithms have been proposed to implement K-medoid clustering. We use the Partitioning Around Medoid (PAM) algorithm [66] to cluster nodes based on their sensing reports. A medoid is the node of the cluster whose average dissimilarity to all other nodes in the same cluster is minimal. Given the number of clusters and sensing reports from all the nodes as input, PAM sequentially finds the same number of nodes as medoids around which all other nodes are clustered in a way so that the objective function is minimized. We modify PAM so that each cluster has equal number of nodes.

The BS maintains a $\Delta + 1$ dimensional vector (X_i = [$\rho_i, x_{1,i}, \ldots x_{\Delta,i}$]) to store information for each node i. The first entry in the vector represents the reputation and the remaining ones represent latest Δ sensing reports. The most recent $\Delta - 1$ sensing reports of each node i (from $x_{2,i}, \ldots x_{\Delta,i}$) are directly considered in calculation while the prior history is also maintained in one entry $x_{1,i}$ as weighted average of previous sensing reports. So, the effect of past sensing reports decrease with time. We do not consider large dimension of vector for two reasons. First, the algorithm may

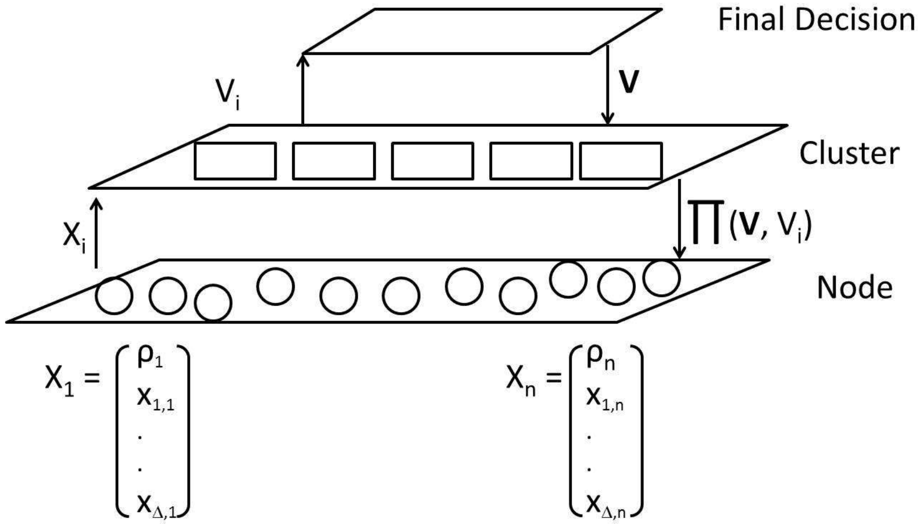

Figure 3.4: Information propagation

suffer as the dimension increases since the data points become more uniform in high dimensions. This is popularly known as *curse of dimensionality*. Second, higher dimensions of data increase computational cost that makes the algorithm undesirable.

3.3.2 Decision Making (Voting Phase)

One of the key features in our algorithm is how we reach the final decision and use that decision recursively to update the clustering. The flow chart of information propagation in each time step is illustrated in Fig. 3.4. As stated earlier, the BS considers the most recent Δ sensing reports of each node in addition to their reputation during cluster formation. The reputation score is always between 0 and 1. We assume that the BS is unaware of the location of nodes attached to it. All nodes are assigned 0.5 as the initial reputation score. The decision process goes through two substeps: intra-cluster voting and inter-cluster voting.

3.3.2.1 Intra-Cluster Voting

Each cluster finalizes its decision about channel status in a unique way. Only the last round sensing report of each node in the cluster is considered. However, each response is weighted with an impact factor that is inversely proportional to the distance between the node and the median of that cluster. The impact factor of a node j denoted by $\mathbb{I}_j$ is defined as

$$\mathbb{I}_j = \frac{1}{d(j, m_i)}$$

where m_i is the median of the cluster i and $d(j, m_i)$ denotes the distance between node j and median m_i of the same cluster. Nodes closer to the median have higher influence in decision making process than the far ones. Accordingly, the voting $\mathbb{V}_i$ of cluster i is determined by Eqn. 3.6.

$$\mathbb{V}_i = \frac{\sum_{j=1}^{n_h/k} \mathbb{I}_j \times x_{\Delta,j}}{\sum_{j=1}^{n_h/k} \mathbb{I}_j} \tag{3.6}$$

Here, k is the number of clusters and $x_{\Delta,j}$ is the latest sensing report from node j that takes value from $\{0, 1\}$.

3.3.2.2 Inter-Cluster Voting (Final Decision)

After each cluster finalizes its decision, the BS checks the validity of each cluster and makes the final decision $\mathbb{V}$ on the basis of majority voting among the valid clusters. If the average reputation of all member nodes of a cluster is below a threshold, the cluster is invalid; then the members in that cluster cannot vote and are marked as attackers. The cluster validation process is performed periodically. Assuming k' valid clusters, $\mathbb{V}$ = $\lceil 2 \times \sum_{i=1}^{k'} \mathbb{V}_i / k' \rceil$.

3.3.3 Reputation Adjustment (Update Phase)

At the end of every time step, the BS updates the reputation of all the nodes according to the algorithm and if needed, increases the number of clusters.

The final result is propagated back to the clusters, and then to the individual nodes. If the final decision matches with a cluster decision, that cluster gets a positive feedback; otherwise, it gets negative feedback. Similarly, if a node's decision matches with its cluster decision, it gets positive feedback while it receives negative feedback for a mismatch. Each node's reputation is then adjusted according to Eqn. 3.7.

$$\rho_j = \rho_j + \Pi\left(\mathbb{V}_i, \mathbb{V}\right) \times \frac{\sum_{j=1}^{n_h/k} \Pi(\mathbb{V}_i, x_{\Delta,j}) \times \mathbb{I}_j}{\sum_{j=1}^{n_h/k} \mathbb{I}_j} \tag{3.7}$$

where r_j denotes the reputation of node j and $\Pi(a, b)$ is an indicator function that returns 1 if a equals b, and it returns -1 otherwise.

The final result is also used to adjust the number of clusters. Initially, we start with 5 clusters with 5 random medoids. After each validation period, if all clusters pass the validation (i.e. average reputation score exceeds threshold, $\epsilon = 0.5$), we increment the number of clusters and continue the same process. Otherwise, we remove all the nodes in the cluster that fails the test. After few periods, we go back to initial state removing "attacker" tag and start the algorithm from the beginning.

3.4 Analysis of Attack Models

In this section, we explain the significance of the users' sending reports in decision making. We then analyze how the attackers exploit the mechanism to their own benefits and how our proposed algorithm works against the attacking strategies.

To begin with, the BS performs a binary hypothesis test based on the sensing reports sent by the secondary nodes. The test can be expressed as $\Pr(H_j|x_1, x_2, \ldots x_n)\ \forall j \in \{0,1\}$. According to the Bayesian theory, the hypothesis test can be further simplified as

$$\begin{aligned}\Pr(H_j|x_1 = j, x_2 = j, \ldots, x_n = j) &= \frac{\Pr(x_1 = j, x_2 = j, ..., x_n = j|H_j)\Pr(H_j)}{\Pr(x_1 = j, x_2 = j, ..., x_n = j)} \\ &= \frac{\Pr(x_1 = j|H_j)\Pr(x_2 = j|H_j)\ldots\Pr(x_n = j|H_j)\Pr(H_j)}{\Pr(x_1 = j, x_2 = j, \ldots, x_n = j)}.\end{aligned}$$

Since the BS does not know the actual channel statistics, the test result depends on the probabilities of sensing reports of individual nodes. Accordingly, for any user i, we calculate the conditional probabilities $\Pr(x_i = j|H_j)$ and $\Pr(x_i = \bar{j}|H_j)\ \forall j \in \{0,1\}$ and these probability distributions determine the accuracy of the decision mechanism. Therefore, we need to determine the closeness between these probability distributions.

We employ the Kullback-Leibler divergence (KLD) to analyze the difference in the probability distribution. The KLD is being used in different detection scenarios including Byzantine attacks in cognitive radio networks [7]. Technically, KLD is a statistical measure that quantifies in bits how close a probability distribution a = a_i is to a model (or candidate) distribution q = q_i [102].

$$\Lambda_{KL}(a||q) = \sum_i a_i \log_2 \frac{a_i}{q_i} \tag{3.8}$$

Similarly, we can express the KLD between the distributions $\Pr(x_i|H_0)$ and $\Pr(x_i|H_1)$ as

$$\Lambda(\Pr(x_i|H_1)||\Pr(x_i|H_0)) = \sum_{j\in\{0,1\}} \Pr(x_i|H_1)\log_2 \frac{\Pr(x_i|H_1)}{\Pr(x_i|H_0)}. \tag{3.9}$$

For an honest user i, the distributions $\Pr(x_i|H_1)$ and $\Pr(x_i|H_0)$ depend on the node's sensing accuracy.

$$\Lambda(\Pr(x_i|H_1)||\Pr(x_i|H_0) = P_{md}\log_2\frac{P_{md}}{1-P_{fa}} + (1-P_{md})\log_2\frac{1-P_{md}}{P_{fa}}$$

When there is no attacker, the false alarm (P_{fa}) and misdetection (P_{md}) probabilities are significantly small. Therefore, the KLD value is large and the BS mostly takes the right decision about channel status.

However, in the presence of attackers, the probabilities are different. Let us assume that δ denotes the fraction of nodes acting as attackers and each attacker independently changes its sensing report with probability P_{mal}. Accordingly, the collective probability distribution can be expressed as

$$\Pr(x|H_j) = \delta\Pr(x_i^a|H_j) + (1-\delta)\Pr(x_i|H_j)\ \forall j \in \{0,1\}. \tag{3.10}$$

Using results from Eqn. 3.8, independent attackers can disrupt the decision mechanism if $\Lambda(\Pr(x|H_1)||\Pr(x|H_0) = 0$ which implies the following condition

$$\Pr(x|H_1) = \Pr(x|H_0). \tag{3.11}$$

Solving the above equation leads us to find the necessary condition for attackers to be successful. The condition can be stated as follows

$$\delta P_{mal} = \frac{1}{2}\ \text{where}\ 0 \leq \delta, P_{mal} \leq 1. \tag{3.12}$$

According to the condition, if half of the nodes independently always change (i.e. with probability 1) their sensing report, attackers take complete control of the decision mechanism of the base station. As attacking probability of individual node decreases, it needs more and more nodes to act as attackers to blind the base station. In a similar analysis in [7], it is shown that if $\delta = 35\%$, collaborative attackers can disrupt the decision mechanism completely.

Next, we explain how ARC prevents both independent and collaborative attackers from disrupting the decision mechanism. ARC separates attackers from honest users based on sensing reports using an adaptive clustering technique. As a result, if two users follow the same probability distribution, they end up in the same cluster. Therefore, in addition to the conditional probabilities, attackers must make sure that their sensing reports are not too different from those of honest users to avoid being detected by ARC. Otherwise, attackers will be separated into the same cluster and thus, will be detected and eliminated.

Let P_{HH}^{diff} denote the probability that two honest users differ in their sensing report at any time.

$$P_{HH}^{diff} = 2[P_I P_{fa}(1 - P_{fa}) + P_B P_{md}(1 - P_{md})] \tag{3.13}$$

Similarly, let P_{AH}^{diff} denote the probability that an attacker and an honest user differ in their sensing reports at any time.

$$\begin{aligned} P_{AH}^{diff} &= 2P_I(1 - P_{mal})P_{fa}(1 - P_{fa}) + P_I P_{mal}\left[(1 - P_{fa})^2 + P_{fa}^2\right] \\ &+ 2P_B P_{md}(1 - P_{md})(1 - P_{mal}) + P_B P_{mal}\left[P_{md}^2 + (1 - P_{md})^2\right] \end{aligned} \tag{3.14}$$

Accordingly, if the attackers want to be successful, the KLD value of these two probabilities should

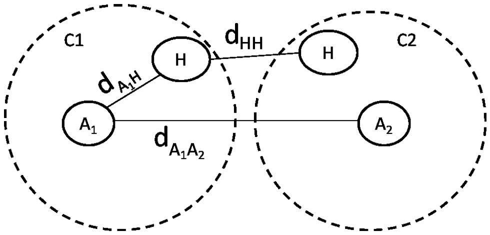

(a) case 1: $d_{A_1H} > d_{A_1A_2}$ and $d_{A_1H} > d_{HH}$

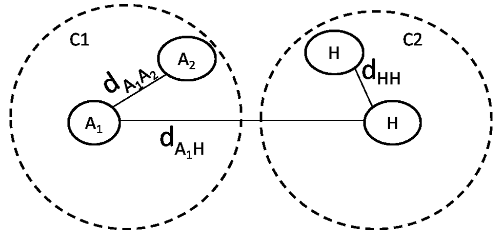

(b) case 2: $d_{A_1A_2} > d_{A_1H}$ and $d_{HH} > d_{A_1H}$

Figure 3.5: Relationships among attackers and honest users

be equal to zero.

$$\Lambda(P_{HH}^{diff}||P_{AH}^{diff}) = P_{HH}^{diff}\log_2\frac{P_{HH}^{diff}}{P_{AH}^{diff}} = 0 \tag{3.15}$$

On the other hand, we can estimate the distance between an honest user and an attacker and between two honest users according to the strong law of large numbers from the clustering point of view. Accordingly, the normalized distance between any two honest users d_{HH} converges to P_{HH}^{diff} with time. Similarly, the normalized distance between an honest user and an attacker d_{AH} converges to P_{AH}^{diff} with time.

It follows that if these two probabilities are equal, then distance between an honest user and an attacker and between two honest users are approximately equal. Hence, attackers and honest users will end up in the same or different clusters with equal probability and cannot be separated by ARC. With similar analysis in [78], it can be shown that malicious users can avoid the detection by setting proper P_{mal} if the false alarm and misdetection probabilities are greater than or equal to 0.4. However, as the standard false alarm and misdetection probability are 0.1, we can conclude that independent attackers cannot defeat the ARC in normal conditions.

The alternative approach to deceive ARC is to take control of the majority of the clusters which we explored in SubGroup attack. It is easily obtainable if attackers outnumber the honest users.

Otherwise, the possible way to manipulate the decision mechanism is to spread out into different clusters and dominate in decision making of every cluster (or, majority of the clusters) consistently. Accordingly, each attacker group works with a different attacking probability, and all members in a group report the same sensing result to influence the cluster decision in their favor.

Let us assume that the attacking probability of the attacker group A_i is α_i, and the probability that the attacker group A_i and the honest user differ in their sensing reports at any time is $P^{diff}_{A_iH}$. Similarly, $P^{diff}_{A_iA_j}$ denotes the probability that any attacker group A_i and attacker group A_j differ in their sensing reports at any time.

$$\begin{aligned} P^{diff}_{A_i,A_j} &= [\alpha_i P_{fa} + (1-\alpha_i)(1-P_{fa})] \times [\alpha_j(1-P_{fa}) + (1-\alpha_j)P_{fa}] \\ &+ [\alpha_i(1-P_{fa}) + (1-\alpha_i)P_{fa}] \times [\alpha_j P_{fa} + (1-\alpha_j)(1-P_{fa})] \end{aligned} \tag{3.16}$$

Here for simplicity, we assume $P_{fa} = P_{md}$. According to the strong law of large numbers, the normalized distance $d_{A_iA_j}$ between any two independent attacker groups A_i and A_j converges to $P^{diff}_{A_iA_j}$ with time. Similarly, the normalized distance between honest users and between any attacker group and honest user can be estimated and are represented as d_{HH} and d_{A_iH} respectively which are equivalent to P^{diff}_{HH} and P^{diff}_{AH}. So, the clusters are formed based on the relative distance between honest users and different attacker groups.

Now, we need to answer the following question from attackers' perspective: *What should be the relationship among d_{HH}, d_{A_iH}, and $d_{A_iA_j}$ to manipulate the cluster formation and deceive ARC completely?* In order to achieve that, different groups of attackers should not be in the same cluster and also attackers must prevent cluster formation with honest users only. Fig. 3.5 illustrates the cluster characteristics for different cases. Case 1 shows the expected cluster formation for any detection algorithm where attackers and honest users are in different clusters. Case 2 shows the expected formation for attackers where each cluster is formed with combination of attackers and honest users.

The attackers will try to maximize the error in decision making while satisfying the conditions of case 2 in Fig. 3.5. For example, consider the case of 3 clusters. The attackers will be successful if at least two of the groups attack and if the probability of difference in sensing result between any group of attacker and honest users must be less than minimum of the difference between two groups of attackers and between any two honest users. Furthermore, attackers must be dominating in the majority of clusters to take control of the decision mechanism that depends on initial seed selection and number of iterations used for cluster formation. Hence, the maximization function for attackers can be stated as follows.

$$\max_{\alpha_1,\alpha_2,\alpha_3}\left[\sum_{i,j,k}\alpha_i\alpha_j(1-\alpha_k)+\prod_i \alpha_i\right]$$
$$\text{such that } \forall_{i,j}\ P^{diff}_{A_iH} < \min\left(P^{diff}_{HH}, P^{diff}_{A_iA_j}\right) \text{ and } \ \alpha_1,\alpha_2,\alpha_3 > 0$$

Since the nodes do not know the actual channel status, it is unlikely that the attackers can calculate the exact value of P^{diff}_{HH}. Even if they can estimate P^{diff}_{HH} (it will be significantly small), finding the attacking probability for different groups of attackers while satisfying the necessary condition cannot be possible in a normal condition.

From the above probabilistic analysis, we can conclude that ARC can withstand all kinds of nonadaptive independent and collaborative attack under normal conditions.

3.5 Performance Evaluation

In this section, we discuss the performance results of our proposed method by specifically comparing its effectiveness against a previously proposed method in [7]. From this point, we will refer to this algorithm as "Rawat method" or 'R', by the name of the first author of the work [7]. We compare these two algorithms across both independent and collaborative attacks as well as various probabilities of attack under a range of sensing conditions.

3.5.1 Performance Metrics

In order to evaluate the performance of our algorithm, we use three performance metrics. First one is the probability of error or **error rate**, denoted as Q_E. It denotes how many times the base station makes an incorrect decision. The lower is the error rate, the better is the algorithm. The second metric is called true detection rate or **recall** and is denoted as Q_D. It is widely used in data mining applications to evaluate the successful detection of members of a class that are considered more significant than the detection of members of other classes. Algorithms with higher value of recall are desirable. In our work, identifying attackers is more significant than identifying honest users. The third metric is **false positive rate** and is denoted as Q_F. This metric represents how many nodes are misidentified as attackers. In this case, the lower the false positive rate, the better the algorithm is.

$$Q_E = \frac{\text{\# of incorrect decision}}{T} \tag{3.17}$$

$$Q_D = \frac{\text{\# of attackers truly identified}}{\text{\# of actual attackers}} \tag{3.18}$$

$$Q_F = \frac{\text{\# of honest users misidentified}}{\text{\# of nodes identified as attackers}} \tag{3.19}$$

3.5.2 Simulation Parameters

We consider that a channel's idle time follows a Bernoulli distribution with parameter 0.6. In other words, primary users transmit over the channel with probability 0.4. At each time step, the channel status is randomly drawn from the probability distribution function. For each test, the methods are run for 80 time steps. For each time step, the methods must produce a final hypothesis, which is compared against actual transmission state of the primary user to determine the method's error rate (Q_E). Rates for the correct detection of attacking nodes (Q_D) and the incorrect detection of honest users as attackers (Q_F) are also reported at the end of the test. Each test is then repeated 30 times with an average of the values displayed in the graphs. A test consists of randomly generated reports for each secondary user, adhering to labeled probability distributions. For a validation test, we consider $\epsilon = 0.5$.

For each type of attack, we test the performance of the algorithm with three variations. They are as follows.

- varying number of attackers
- varying attacking probability
- varying detection probability

3.5.3 Independent Attack

In the next step, we compare the performance of our algorithm with reputation based method in [7] for independent SSDF attacks. In this attack, attackers do not collaborate to exchange their reports. Each attacker works independently to maximize its goal. Fig. 3.6 shows the error rate of two algorithms with varying number of attackers. We keep the attacking probability $P_{mal} = 1$.

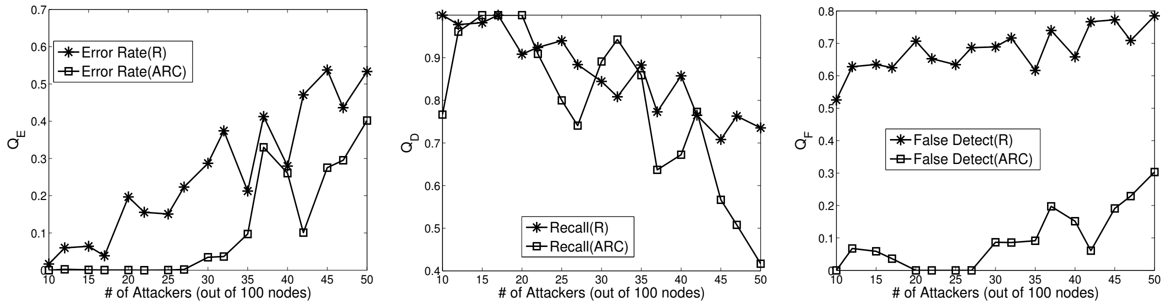

(a) Error rate Q_E (b) Recall Q_D (c) False Positive rate Q_F

Figure 3.6: Independent attack with varying number of attackers

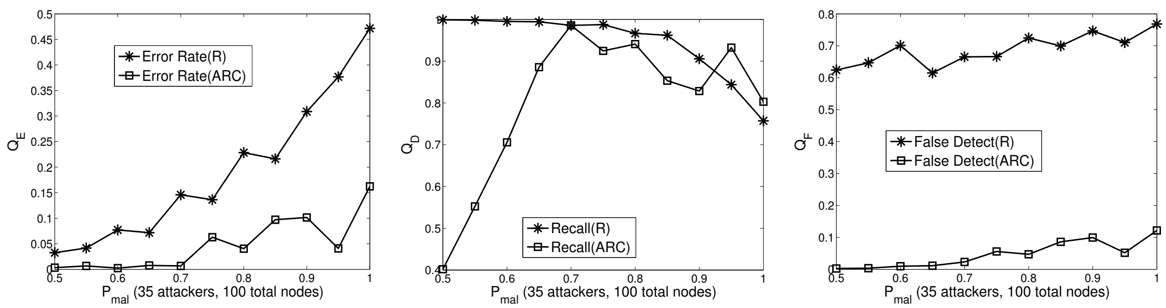

(a) Error rate Q_E (b) Recall Q_D (c) False Positive rate Q_F

Figure 3.7: Independent attack with varying attacking probability

Also, probabilities for true and false detection of a signal are set to P^h_{detect} = 0.9 and P_{fa} = 0.1. Although our algorithm performs better than Rawat algorithm, the error rate increases with the number of attackers. On the other hand, our algorithm performs moderately to detect malicious attackers while their algorithm consistently identifies attackers with high precision. However, their algorithm eliminates a large number of honest users incorrectly. Fig. 3.6 shows that about 40% honest users are misidentified as attacker. On the other hand, false detection rate of our algorithm is almost negligible. Although the reputation based algorithm performs better in detecting attackers than our algorithm, they misidentified a large number of honest users as attackers, which makes their algorithm less effective.

Similarly, we run the simulation for independent SSDF attacks with varying attacking probability. We vary the attacking probability from 0.5 to 1 and plot Q_E, Q_D, and Q_F in Fig. 3.7

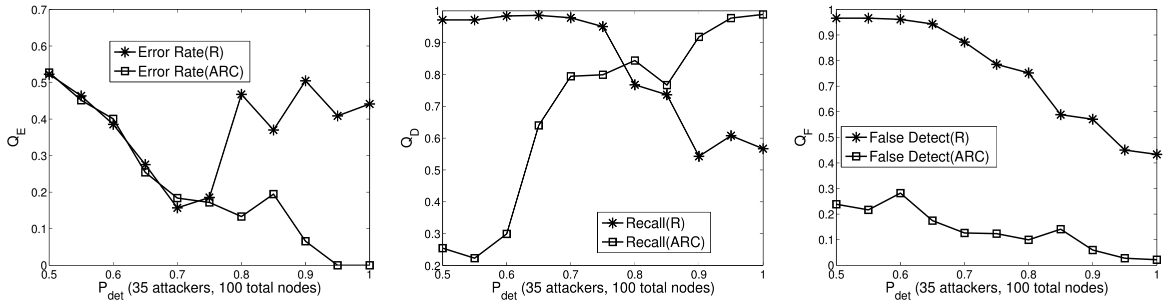

(a) Error rate Q_E (b) Recall Q_D (c) False Positive rate Q_F

Figure 3.8: Independent attack with varying detection probability

for our algorithm and reputation based algorithm proposed in [7]. Again, our algorithm performs better in decision making (Fig. 3.7). Error rate of our algorithm is almost negligible while their error rate of their algorithm increases almost linearly with attacking probability. The true attacker detection rate is almost the same for both algorithms when the attacking probability exceeds 0.65. However, their algorithm constantly eliminates 60% of honest nodes as attackers for any attacking probability ranging between 0.5 and 1.0. On the other hand, our algorithm performs significantly better and keeps a false detection rate close to zero.

Next, we vary the detection probability of nodes from 0.5 to 1.0 and plot Q_E, Q_D and Q_F in Fig. 3.8 for our algorithm and reputation based algorithm proposed in [7]. As usual, the error rate of our algorithm outperforms their algorithm. Also, our algorithm performs better in terms of misidentification of attackers. However, their algorithm identifies almost all attackers irrespective of the detection probability. On the other hand, our algorithm gradually increases the true detection rate with the increase of detection probability.

3.5.4 Collaborative Attack

We tested both methods (Rawat method [7] and ARC) against each of the collaborative byzantine attacks discussed in Section 3.1.4.2. The first set of simulation (Fig. 3.9) presents the result for

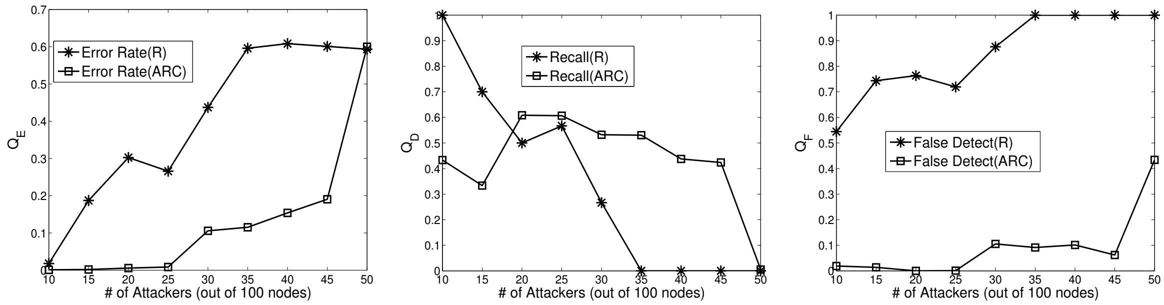

(a) Error rate Q_E (b) Recall Q_D (c) False Positive rate Q_F

Figure 3.9: Collaborative attack with varying number of attackers

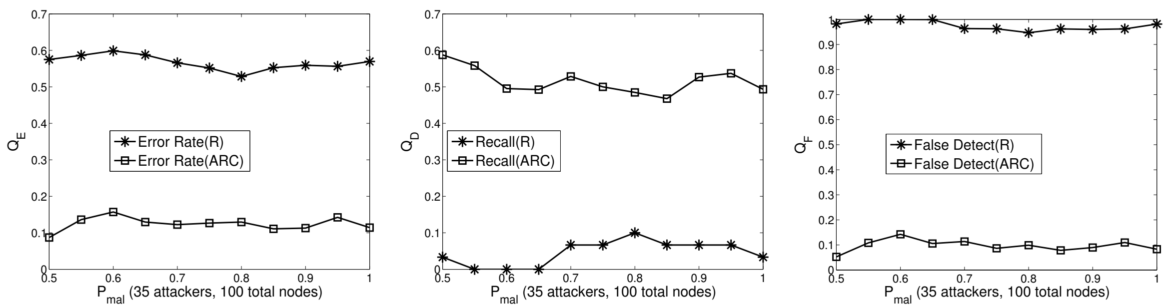

(a) Error rate Q_E (b) Recall Q_D (c) False Positive rate Q_F

Figure 3.10: Collaborative attack with varying attacking probability

the collaborative attack defined in [7]. The number of malicious users range from 10 to 50 out of 100 total secondary users. The attacking probability (P_{mal}) is set to 1. Sensing probabilities for correctly detecting a signal and falsely detecting a signal were set to (P^h_{detect}) = 0.9 and (P_{fa}) = 0.1 respectively.

ARC outperforms consistently with respect to (Q_E) showing a markedly decreased error rate until roughly 50% of the population becomes attackers. Once the population contains a majority of malicious users, it is impossible for any sensing strategy to sustain an error rate under 50%. The Rawat method shows a high Q_D initially but quickly diminishes after 20% of nodes are attackers and becomes completely ineffective when $1/3$ of the population are attackers. At approximately the same attacker concentration, our method exceeds and maintains a marked increase in identifying attackers. Conversely, the Rawat method begins with a significant false detection rate (Q_F)

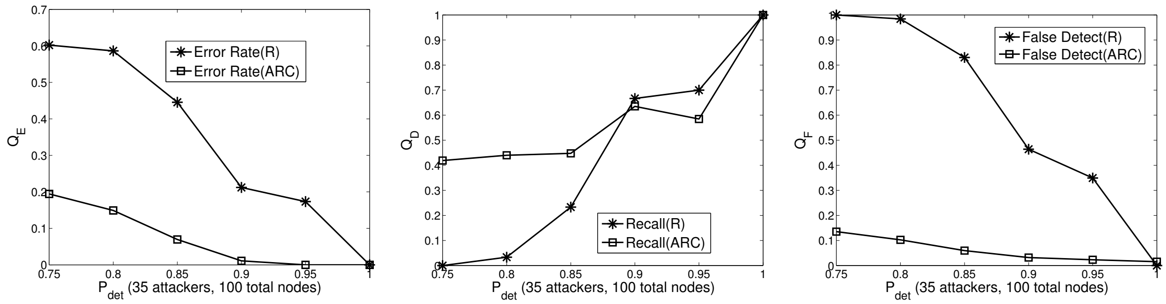

(a) Error rate Q_E (b) Recall Q_D (c) False Positive rate Q_F

Figure 3.11: Collaborative attack with varying detection probability

while our method minimizes this rate across the entire range of attackers. Maintaining a low misdetection rate allows our method to maximize honest user reports and mitigate the impact of attackers even under heavy attacks.

A second set of measurements observed the impact of collaborating malicious users when varying their probability of attack. Malicious users can utilize this technique to escape detection from high dimensional clustering methods. In Fig. 3.10, attackers produce on average less than 20% error rates while the Rawat method sustains significant errors. Regardless of attacking rate, our method consistently identifies 50% of the attackers. The Rawat method exhibits an unusually high attacker misdetection rate, which is likely to lead to the high error rate.

The next test looks at consequences of variable sensor accuracy (Fig. 3.11). Here, 35 collaborating malicious users attack during each sensing step. Both methods begin with relatively high error rates, as the sensing reports of honest users resemble that of attackers due to the inaccurate sensor readings. Once sensing errors fall below 65%, our proposed method shows a linear decrease in the Hypothesis error rate. The Rawat method takes significantly higher detection rates (approximately 80%) before error rates begin to decline.

We also test our algorithm in the case of subgroup collaborative attacks (Fig. 3.12). We assume that attackers know the number of clusters and create equal number of groups of attackers. At-

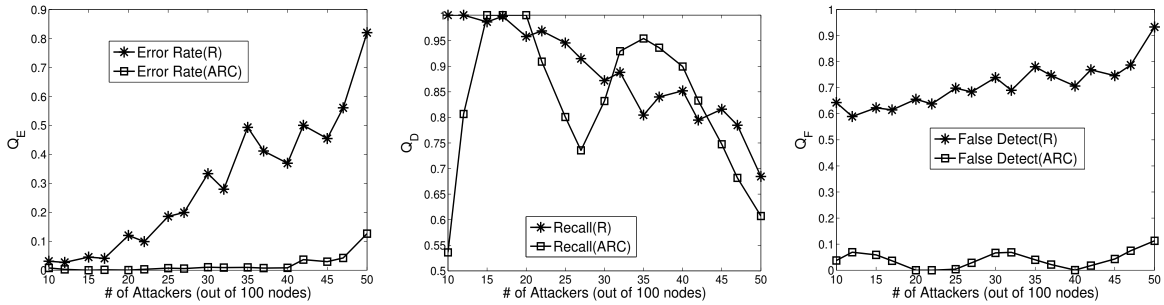

(a) Error rate Q_E (b) Recall Q_D (c) False Positive rate Q_F

Figure 3.12: Collaborative SubGroup attack with varying number of attackers

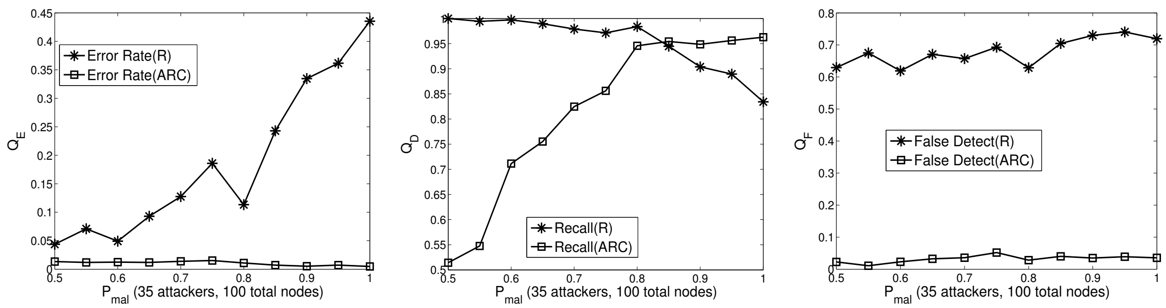

(a) Error rate Q_E (b) Recall Q_D (c) False Positive rate Q_F

Figure 3.13: Collaborative SubGroup attack with varying attacking probability

tackers are equally distributed in all subgroups. As the number of attacker increases, Q_E increases slightly in our algorithm while Q_E reaches almost 40% in the reputation method. As expected, both their true detection and false detection rate is high. On the other hand, Q_D is about 65% and Q_F is almost negligible in our algorithm. Similarly, our algorithm outperforms Rawat algorithm in terms of error rate, recall and false detect with varying attacking probability (Fig. 3.13) and with varying detection probability (Fig. 3.14).

We find interesting results for attackers with GAMA strategy. In the case of our algorithm, Q_E is 0 and only increases when the number of attackers exceeds 37. On the other hand, Q_E increases almost linearly with the number of attackers in the reputation based method. We get similar results in true and false detection rate. The results are plotted in Fig. 3.15. Similarly, our algorithm outperforms Rawat algorithm with varying attacking probability and with varying

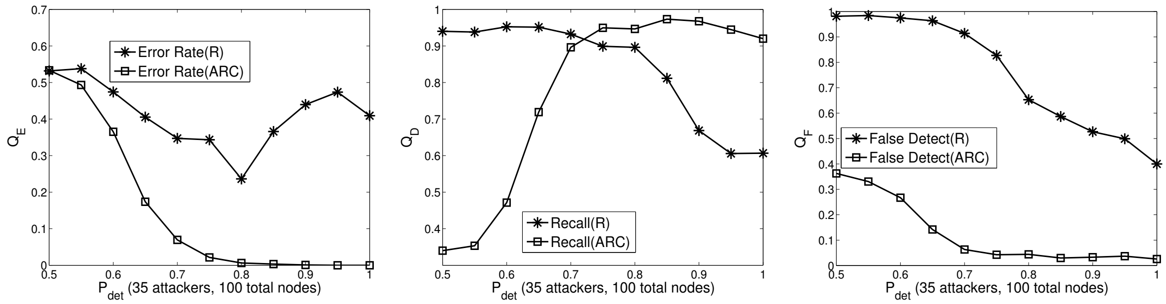

(a) Error rate Q_E (b) Recall Q_D (c) False Positive rate Q_F

Figure 3.14: Collaborative SubGroup attack with varying detection probability

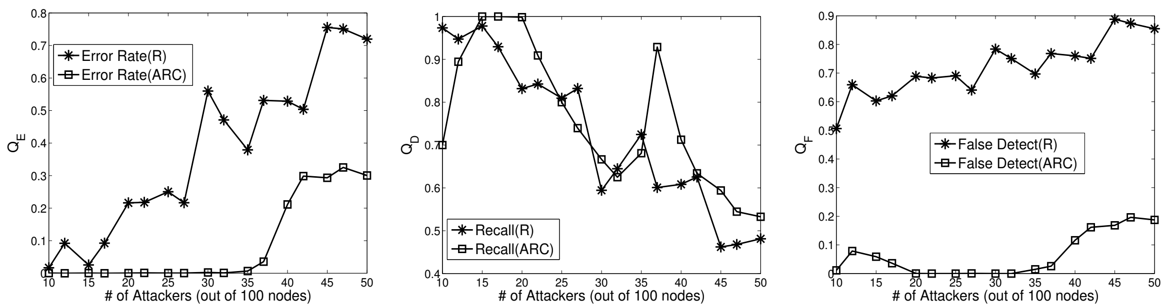

(a) Error rate Q_E (b) Recall Q_D (c) False Positive rate Q_F

Figure 3.15: Collaborative GAMA attack with varying number of attackers

detection probability. The results are not shown due to page limitation.

Interestingly, Rawat algorithm shows higher error rate with higher detection probability in all cases (see Fig. 3.8a, 3.14a). This is because the attackers contribute to the correct decision making by altering the sensing results in the case of low detection probability. As detection probability increases, altering the sensing result helps attackers increasing error rate. The true detection rate also decreases with higher detection probability for the same reason.

We also examined the clusters' convergence time. The clusters become stable after 8 to 10 time steps on average. However, if the starting dimension Δ of each node goes below 20, the cluster performance degrades significantly. Therefore, to start with, we maintain the latest 20 sensing reports of all nodes in our simulation. We also simulated an alternative approach where instead of removing attacker nodes from the decision mechanism completely, we reset their identity and start

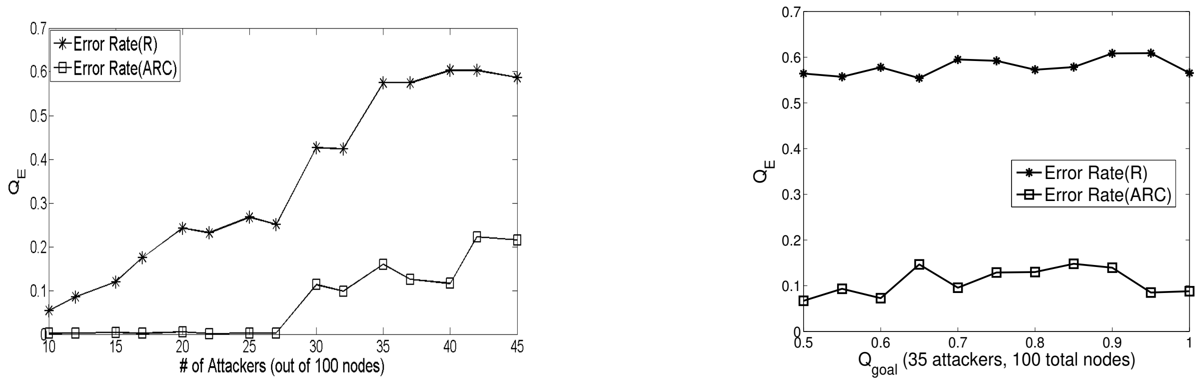

(a) with varying number of attackers

(b) with varying attacking goal

Figure 3.16: Adaptive collaborative Subgroup attack

the algorithm again. The reset timer is set after the convergence of the clusters (e.g. after 10 time steps). As a result, the performance results do not change significantly.

3.5.5 Adaptive Attack

So far, we have only considered non-adaptive attack. In this section, we consider an adaptive variation of both independent and collaborative attacks where attackers adaptively changes their strategies to reach certain goal in terms of attack. In the independent adaptive attacking approach, each attacker starts with a random attack rate, periodically compares its success rate with its set goal, and adjusts its attack rate accordingly. We find that independent attackers cannot significantly impact the decision mechanism of the BS in both approaches (the error rate never goes above 10%).

In the case of adaptive collaborative attack, we only consider the variation of SubGroup attack. Similar to independent adaptive attack, attackers set a common goal (Q_{goal}) of achieving success in terms of attack. Each subgroup of attackers starts with random attacking probability P_{mal}, periodically checks their present success rate (Q_E) with the set goal and linearly increases (or, decreases) their attacking rates (P_{mal}) to reach their target success rate. In the first simulation set, we set $Q_{goal} = 0.8$ and vary the number of attackers. The simulation result in Fig. 3.16a shows that our algorithm performs significantly better than Rawat algorithm in terms of error rate. The number of attackers are varied up to 45 since both the algorithm shows random behavior in the presence of 50% attackers. In the second simulation, the number of attackers are set to 35 and number of subgroups created are 5. The simulation results are presented in Fig. 3.16b with varying attacking goal for both the algorithms, and it shows that our algorithm outperforms Rawat algorithm with significant margin.

3.6 Summary

In this chapter, we discuss one of the major security problems afflicting CRNs and propose a reputation based clustering algorithm to defend against these attacks. We use reputation of nodes in addition to their sensing history to form clusters and then adjust reputation based on the cluster output. This recursive approach is tested in the presence of independent and collaborative spectrum sensing data falsification attacks. With respect to current approaches, our algorithm significantly reduces the error rate in the final decision making process, thus increasing spectrum utilization. The false detection rate by our algorithm is almost negligible while true attacker detection rate performs reasonably well. However, the initial number of clusters plays an important role in overall performance of the algorithm.

Chapter 4

Interference Aware Reliable CCRNs for Real-time Applications

With growing real-time traffic and limited spectrum resources, the communication system must adopt reliable and efficient spectrum sharing techniques for providing improved services to end users. Relay based collaboration model between the primary and secondary users will play an important role in reshaping and restructuring the spectrum allocation mechanism. In the work presented in this chapter[1], we propose a new method for constructing reliable real-time network systems such as real-time industrial automation mesh networks [46] and time-critical sensor networks [24]. Such a real-time network requires packets to be delivered within a deadline. Accordingly, we measure the reliability of these real-time networks using packet reception rate. When a user in such networks transmits a packet, a receiver may fail to decode the packet in time because of a temporarily unstable link due to random noise, fading, and shadowing or collision with other ongoing transmissions. Waiting until such a link is usable again is not acceptable in real-time sys-

[1]The work presented in this chapter has been published in three research articles:

(i) Chowdhury Sayeed Hyder, ABM Alim al Islam, Li Xiao, and Eric Torng. ”Interference aware Reliable Cooperative Cognitive Networks with for Real-time Applications”, in IEEE Transactions on Cognitive Communications and Networks (TCCN), 2(1), pp 53-67, May 2016.

(ii) Chowdhury Sayeed Hyder, ABM Alim Al Islam, Li Xiao, ”Enhancing Reliability of Real-time Traffic via Cooperative Scheduling in Cognitive Radio Networks”, at 23rd International Symposium on Quality of Service (IWQoS), pp 249-254, Portland, Oregon, USA, June 15-16, 2015.

(iii) Chowdhury Sayeed Hyder, Li Xiao, and Max Ellison, ”Exploiting Cooperation for Delay Optimization in Cognitive Networks”, at 9th International Conference on Mobile Adhoc and Sensor Systems (MASS), pp 362-370, Las Vegas, Nevada, USA, October 8-11, 2012.

tems if link downtime can exceed packet deadlines. Even if the link becomes stable, traditional retransmission of dropped packets may not deliver the packet in time at the receiver.

We propose to use relay based collaboration model as part of the solution for developing reliable real-time network systems leveraging the flexibility and diversity of CRN to overcome transient packet transmission issues. For example, cooperative communication can mitigate channel fading by exploiting spatial diversity which leads to new transmission paths [52, 57, 136]. Based on the transmission model in CRN, secondary users are granted channel access by primary users in return for their service in relaying primary packets.

4.1 Relay based Collaboration Model

Relay based collaboration model is also referred to as cooperative cognitive radio network. To design a transmission model in CCRN, we need to define three components. The first component of the model is to select the cooperative transmission strategy (i.e. how to cooperate). We use the two phase power division approach proposed in Han et al. [47] to schedule cooperative transmissions (explained in Section 4.2.4). The second component of the design is to determine the condition for cooperation (i.e. when to cooperate). The final component of the design is to select matching cooperation pairs and schedule their transmissions considering mutual interference between users. Throughout this chapter, we discuss the challenges we face in developing each component of the cooperative transmission model, and how we address these issues into our proposed model focusing on unique features of real-time traffic.

4.1.1 Limitations of Prior Work

While there has been extensive research in CCRN where the goal is to optimize specific network traits such as maximizing throughput [70] or minimizing delay [53] or exploring the tradeoff between them [10], this research is not applicable to real-time systems because of the following reasons. First, existing research does not include packet deadlines into the cooperation model and thus ignores the effect of each transmission decision on the success probability of remaining packets in the queue, and future packets that have not yet arrived. Second, this research does not discuss the overhead associated with cooperative transmission. For example, before a cooperative transmission takes place, users need to exchange cooperation information (e.g. transmission time) and select cooperation pairs which introduces significant overhead [124]. Ignoring this overhead may increase packet loss rate. Finally, most of the existing research focuses on a single cooperating pair of primary and secondary users which may not extend to a multi-user environment. For example, allowing a secondary user to transmit as part of cooperation agreement may change the interference relationship between existing users, and if not properly administered, it may interfere with other ongoing transmissions causing packet loss. Furthermore, most existing work assumes infinite queues whereas real systems have only finite queues.

4.1.2 Proposed Approach

In this chapter, we propose a new method for constructing reliable real-time network systems based upon CCRN that overcomes the limitations of prior work. Our approach is to formulate the multi-user real-time communication system with finite queues as a Markov decision process (MDP) where we model the impact of transmission deadlines and cooperation overhead in the reward functions of the MDP and control mutual interference by regulating transmission power of secondary users. The model decides between direct and relay based cooperative transmission and chooses the transmission power of secondary users considering the tradeoff between the successful reception probability of the current packet and the impact of cooperation overhead on later packets. For example, while cooperative transmission may increase the success probability of the current packet, the associated overhead may reduce the success of remaining packets in the queue. Thus, the MDP reward functions represent the deadline constraints and help a user make effective transmission decisions.

We further study and analyze the MDP of a single pair of primary and secondary users to understand the dynamics of cooperation. Based on this analysis, we develop a distributed cooperation algorithm for use in practical settings to help users make cooperation decisions and schedule their transmissions. We evaluate the performance of the proposed algorithm in comparison with an existing cooperation algorithm [117].

4.1.3 Key Design Challenges

To build a successful system, we must address three design challenges.

(i) cooperation overhead vs. transmission deadlines: The process of relay selection and channel estimation requires exchange of control information among users which causes significant overhead and impacts the performance of cooperative relaying [124]. This overhead issue becomes even more critical in the case of real-time systems because of transmission deadlines. Therefore, we need to quantify the overhead of relay selection and incorporate it into transmission decisions. For example, a cooperative transmission may increase the probability of successful delivery of the current packet at the cost of decreasing probability of successful delivery of packets in the queue. So, instead of deciding to transmit solely based

Figure 4.1: Impact of secondary interference in cooperative communication

on the current packet, we must also consider queued packets. We define the reward functions of the MDP where each transmission decision is evaluated considering its impact on both the current packet and queued packets.

(ii) cooperation duration: Another design issue is to determine the optimum cooperation duration for a pair of users. Cooperation duration refers to the amount of time two users engage in cooperative transmission according to their agreement. Whereas frequent cooperation negotiation may give better estimates of channels and more up-to-date cooperation opportunities, it also increases overhead. On the other hand, a longer cooperation period reduces the overhead but may extend cooperative transmission longer than needed. We address this issue by introducing a low overhead protocol where the cooperating users assess their status and extend the cooperation period if appropriate.

(iii) secondary interference: The third design issue is to control the interference caused by secondary users' transmissions. For example, consider the simple scenario depicted in Fig. 4.1 where two pairs of primary transmitter and receiver (A, A') and (B, B') are communicating over channel 1 out of the interference range of each other. If the primary transmitter A cooperates with a secondary user (SU) and relays its packet through SU, SU's transmission over channel 1 may interfere with B'. A successful model must consider the impact of secondary interference while scheduling cooperative transmission. We regulate the transmission power of secondary users based on the interference relationship between users and present a handshaking protocol to ensure interference free data transmission.

4.1.4 Our Contributions

To summarize, we make the following key contributions in the work in this chapter.

- We identify the challenges associated with designing a relay based collaboration model in CCRN for real-time systems. We formulate the transmission model as an MDP. We convert the essence of transmission deadlines and cooperation overhead into reward functions. We define the action sets of MDP by imposing power constraints on secondary transmission to control mutual interference between users in the network.

- We present an extensive analysis of the collaboration model of a single pair of primary and secondary users and compare its performance with an existing model [117]. The analysis shows that the latter model leads to poor reception rate due to ignoring cooperation overhead and transmission deadlines in their formulation while our proposed model provides higher packet reception rate and low waiting time. The analysis also reveals the impact of various network parameters on system performance.

- We propose a distributed cooperation algorithm where primary users negotiate with secondary users about cooperation duration and transmission power. A user makes transmission decision based on cooperation gain that is calculated in terms of transmission opportunity, transmission power, and queue size. We also present a handshaking protocol for cooperating users to schedule data transmission avoiding mutual interference.

- Finally, we consider different primary real-time traffic models to evaluate the performance of the proposed cooperation model in comparison to an existing cooperative transmission model [117]. The simulation results show that the proposed relay based collaboration model achieves higher packet reception rate than the prior model under different network settings. We also provide an overhead analysis in terms of frequency of cooperation negotiation and cost benefit analysis in terms of energy consumption in relaying.

4.2 System Model and Problem Formulation

In this section, we describe network setup, explain the power division cooperative transmission approach, and formulate the relay based collaboration model.

4.2.1 Preliminaries

We consider a CRN consisting of a set of m primary transmitters $\mathcal{P} = \{p_1, \ldots, p_m\}$, their corresponding m primary receivers $\mathcal{P}' = \{p'_1 \ldots p'_m\}$, and a set of n secondary transmitters $\mathcal{S} = \{s_1, \ldots, s_n\}$, and their corresponding n secondary receivers $\mathcal{S}' = \{s'_1 \ldots s'_n\}$. Each (primary or secondary) user has a single transceiver radio and cannot transmit and receive simultaneously. Since the cooperation decision is taken among the transmitters only, we use primary transmitter and primary user, and secondary transmitter and secondary user interchangeably.

We assume that the primary network has an exclusive license of a fixed bandwidth spectrum. Each primary user is assigned a fraction of this bandwidth which is referred to as a 'channel'. Channels may be overlapping (similar to 802.11) or completely disjoint based on the allocation algorithm. Since our focus is to analyze the cooperation model, we will not discuss the channel allocation algorithm (please see [95] for a list of channel selection algorithms). Secondary transmitters, on the other hand, depend on the primary users for their transmission opportunity to their respective secondary destinations.

We assume that a primary user contends for channels with other primary users in the same network. Let us denote that a primary user is assigned a channel by the controller with probability q. In other words, a primary user cannot transmit or engage in any transmission activities (cooperative or non-cooperative) with probability $1 - q$ independent of its queue status. Finally, we assume a primary user may either choose to transmit directly or agree to cooperative transmission.

Each primary and secondary transmitter has a finite priority queue $Q(\cdot)$ of length L to store packets. Each packet has a deadline Δt; the packet must be delivered within Δt time units from the time of its generation. If the queue is full, the next packet generated is dropped. Otherwise, the packet is added at the end of the queue. Users in the system do not retransmit packets. Once a packet is transmitted, it is removed from the queue even if is not successfully received at the destination.

4.2.2 PU Traffic Model

Various traffic models are studied to accurately represent PU activity in cognitive radio networks [19] [94]. Markov modulated process is the most common model among them. In Sec. 4.3, we assume that the primary traffic follows a Bernoulli distribution to keep our analysis simple. However, this analysis can be extended to a Markov modulated process as mentioned in [117]. Later in Sec. 4.5, we use a three state Markov chain to represent the PU traffic model [49] and evaluate the proposed cooperation model with simulation. We also consider Poisson distribution to represent the PU traffic model [134] [80] to demonstrate the performance of the proposed cooperation model with a different traffic model.

4.2.3 Channel Model

We consider that channels experience Rayleigh flat fading which implies that the channel gain remains constant within a time slot where it changes from one slot to another [104], [33]. Channel gain h_i is expressed as a Gaussian random variable with mean 0 and variance $d_i^{-\nu}$ where d_i is the normalized distance between sender and receiver and ν is the path loss exponent. Channel experiences additive white Gaussian noise at the receiver with mean 0 and variance η^2. Since channel gain h_i follows a Rayleigh distribution, it can be shown that $\gamma_i = |h_i|^2$ follows an exponential distribution with mean d_i^{ν} i.e. $\gamma_i \sim exp(d_i^{\nu})$ [47].

4.2.4 Cooperative Transmission

For cooperative transmission, we prefer the power division approach to the time division approach [34, 98] because the former approach provides flexibility to control the secondary transmission power and the primary user does not incur additional overhead for secondary transmission. In this model, a primary user may establish a relay transmission path via a secondary user by adopting the power division transmission approach proposed in [47] where cooperative transmission is scheduled in two phases. In the first phase, a primary user transmits its packet to its destination which is also received by the participating secondary transmitter. In the second phase, the cooperating secondary transmitter regenerates the primary signal and superimposes it with its own transmission. The transmission power of the secondary transmitter is proportionally allocated to the primary signal and secondary signal, and the combined signal is then transmitted by the secondary transmitter. The primary receiver decodes the packet from these two signals received from direct and relayed transmission.

The joint transmission decision between a primary transmitter $p_i \in \mathcal{P}$ and a secondary transmitter $s_j \in \mathcal{S}$ can thus be characterized with α ($0 \leq \alpha \leq 1$), the transmission power distribution ratio. Primary user p_i first transmits the packet to its destination, and it is also received by the secondary user s_j. The secondary user s_j assigns transmission power αE to the primary signal and $(1-\alpha)E$ to the secondary signal and transmits the combined signal. Additionally, the user p_i may opt for direct transmission without any cooperation, and the user s_j may transmit only when the queue of the p_i is empty. This transmission decision is represented with $\alpha = \emptyset$.

We make the following assumptions regarding the cooperation model. First, users exchange cooperation information over a common control channel and cannot transmit while negotiating cooperation terms. Second, a primary user may participate in a cooperative transmission with at most one secondary user at any time. There may be multiple cooperating pairs based on the number of users and availability of resources (channels). Third, a primary (or secondary) user already involved in a cooperative transmission does not initiate or accept another cooperation request until the present cooperation agreement ends (i.e. ongoing transmission phase finishes). Forth, all packets have the same length, and decoding and regenerating a primary packet at the secondary user takes constant time. Finally, the primary packet received by a secondary user is immediately relayed to its destination; the relayed packet does not experience significant waiting time in the queue of the secondary user.

4.2.5 Packet Loss

Packet loss may occur for the following reasons. First, if a queue is full, an incoming packet to that queue is dropped. Second, if the waiting time of a packet exceeds its deadline, the packet is removed from the queue. Finally, if a receiver fails to decode a packet by its deadline due to interference, the packet is lost and is counted as an unsuccessful transmission. Our goal is to develop a cooperative transmission model that reduces packet losses.

4.2.6 MDP Formulation

We model the joint transmission decision of the primary and secondary users as a Markov Decision Process (MDP). In an MDP, each state is associated with a set of actions and corresponding rewards. Thus, the cooperation model is represented with an MDP (Σ, $\mathcal{A}$, $P_{\cdot}(\cdot, \cdot)$, $U_{\cdot}(\cdot, \cdot)$, Γ) where

- Σ is a finite set of states. Each state denotes the present number of packets waiting in the queue of all the users in the network. Thus a state $\sigma \in \Sigma$ can be represented as $\sigma = (i_1^p, \ldots i_m^p, j_1^s, \ldots j_n^s)$. Here i_m^p and j_n^s denote the number of packets waiting in the queue of a primary user p_m and a secondary user s_n. The number of different states of the system is $|\Sigma| = (L+1)^{m+n}$ where L denotes the queue size.

- $\mathcal{A}$ is a set of all possible actions where each action represents a joint transmission decision of a primary and a secondary user. We express an action as $\alpha(p_i, s_j)$ which denotes the distribution of power allocation between the signals of the primary user (p_i) and the secondary user (s_j). Since α can be any value between 0 and 1, the number of possible actions is theoretically infinite. We use $\alpha = \emptyset$ to express the direct transmission approach. The action set can thus be represented as $\mathcal{A} = \{\alpha(p_i, s_j) = \emptyset \vee \alpha(p_i, s_j) \in [0, 1], p_i \in \mathcal{P}, s_j \in \mathcal{S}\}$. We drop the index in $\alpha(p_i, s_j)$ when we discuss on transmission power in general. At time t, a subset of actions $a(t) \subset \mathcal{A}$ is chosen as the transmission decisions of primary and secondary users in the network such that no two actions of the set involve the same primary user or the same secondary user or both.

- $P_{a(t)}(\sigma, \sigma') = Pr(\sigma_{t+1} = \sigma' | \sigma_t = \sigma, a(t) = \{\alpha(\cdot, \cdot)\} \subset \mathcal{A})$ denotes the transition probability from state σ to state σ' if the action set $a(t) \subset A$ is taken at time t.

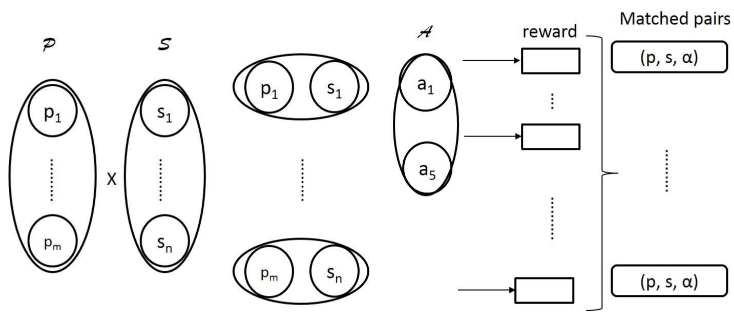

Figure 4.2: Matching pair and action selection

- $U_{a(t)}(\sigma, \sigma')$ denotes the reward of transferring from state σ to σ' due to the action set $a(t)$ at time t. The reward function is calculated in terms of immediate reward discounted by the future opportunity cost. The reward function also includes the impact of the change in the status of the queue.

- $\Gamma \in [0, 1]$ is a discount factor that balances the importance of immediate rewards versus long term rewards.

Our goal is to determine the optimum policy φ that maximizes the expected reward of the cooperating users over a long period T. Assuming empty queues of all users as the initial system state σ_0, we express the objective function as follows

$$\max_{\varphi} \lim_{T\to\infty} \frac{1}{T} \mathbb{E}_{\varphi} \left(\sum_{t=0}^{T} \Gamma^t U_{a(t)}(\sigma, \sigma') | \sigma_0 = (0, \ldots, 0) \right). \tag{4.1}$$

where $a(t)$ represents the actions taken in state σ at time t according to the policy φ and $\mathbb{E}_{\varphi}(\cdot)$ is the expectation taken under policy φ.

The objective function investigates the impact of different actions $a \in \mathcal{A}$ on all pairs of primary and secondary users ($\mathcal{P} \times \mathcal{S}$) to determine the optimal policy that recommends optimum action at different system state (see Fig. 4.2). If the pairs are mutually independent in terms of the chosen action and their impacts, we can separately calculate the reward component for all such pair

$(p_i, s_j) \subseteq \mathcal{P} \times \mathcal{S}$. We use the Bellman equation or dynamic programming to solve the problem for a pair of primary and secondary user and determine optimum action in their different states. We repeat the same procedure to calculate the reward component for all possible pairs in their different states for different actions. Finally, we can use weighted bipartite matching to determine the optimum action and optimum matching pairs from the set at any given time t that maximizes reward. To better understand the procedure, we analyze the MDP cooperation model of a single pair of primary and secondary users in Sec. 4.3. However, in practice, an action of a pair of users affects the reward of another pair due to mutual interference and the reward dependency between pairs make it intractable to find a deterministic solution at time t. We therefore develop a distributed multi-user cooperation algorithm (Sec. 4.4) addressing the mutual interference between users with simultaneous transmission.

4.3 Analysis of a Cooperative Transmission Model

To understand the dynamics of system parameters on our multiuser cooperation model, we first take a closer look at the cooperation model for the case of a single pair of primary and secondary users. The single pair analysis will help us identify the impact of different system parameters; these results will be used to develop the distributed algorithm in Sec. 4.4.

We depict the network consisting of a primary transmitter p, a primary destination p', a secondary transmitter s, and a secondary destination s' in Fig. 4.3. We denote the channel gain between p and p', p and s, p and s', s and p', and s and s' as h_1, h_2, h_3, h_4, and h_5 respectively. Both users have a finite queue of length L. We denote the transmission power of the cooperating primary user p and secondary user s as E_p and E_s, respectively. Primary and secondary packets' arrival follow a Bernoulli distribution with mean λ_p and λ_s respectively. The same distribution

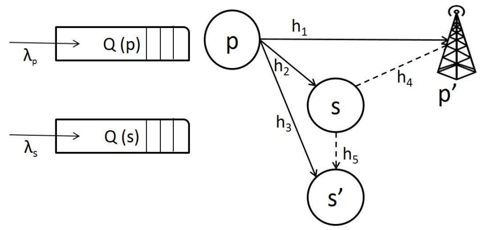

Figure 4.3: Cooperation between a primary and a secondary user

is used to model primary user activity in [12] [94]. We can extend this analysis from a Bernoulli distribution to a Markov modulated process [117].

This two user MDP model has a total $(L+1)^2$ states. Each state $\sigma \in \Sigma$ is represented with $\sigma = (\sigma_p, \sigma_s)$ where σ_p and σ_s denote the number of packets in primary and secondary queue respectively, and $0 \leq \sigma_p, \sigma_s \leq L$. We assume that system parameters remain unchanged while a user completes an action; changes occur only at state transitions.

At the beginning of each state, a user takes a transmission decision for the first packet of the queue. A user's default transmission decision in the model is to take the single action available in a non-cooperative system i.e. direct transmission where p transmits directly to p' and s transmits to s' only when the primary queue is empty ($\sigma_p = 0$). The successful delivery of the first packet and waiting time of the queued packets depends on the direct data rate, traffic rate, and channel availability. When the users in the network intend to explore cooperative transmission opportunities, they need to go through a negotiation period. While this cooperative transmission may improve the successful delivery of the first packet, the negotiation period contributes to additional waiting time to queued packets that may affect their successful delivery at later time.

4.3.1 Action Set

The transmission decisions are represented as actions $\alpha(p, s) \in \mathcal{A}$ in MDP. Since we are considering a single pair of primary and secondary users, to simplify notation, we refer to $\alpha(p, s)$ as α.

In summary, the actions are as follows

- $\alpha = \emptyset$: This represents the default non-cooperative transmission approach where p transmits directly to p' and s transmits only when the queue of p is empty. Users execute this action with no additional cost of cooperation negotiation.

- $\alpha = 0$: This represents the cooperative transmission decision where p defers its transmission and lets s transmit with full transmission power. This action is preceded by cooperation negotiation.

- $\alpha = 1$: This represents the cooperative transmission decision where s relays the primary packet with its full transmission power and does not combine s's own transmission. This action is also preceded by cooperation negotiation.

- $0 < \alpha < 1$: This represents the case where s allocates αE_s power to the primary signal and $(1 - \alpha)E_s$ power to its own signal, combines both signals, and then transmits. This action is also preceded by cooperation negotiation.

At any time t, p and s take a joint transmission decision $a(t) = \alpha$, which moves the system from a state σ to a state σ' with a probability of $P_{a(t)}(\sigma, \sigma')$ and achieves reward $U_{a(t)}(\sigma, \sigma')$. Note that, theoretically the cooperating users can select any value between 0 and 1 for transmission power. However, based on the relative distance between transmitters and receivers, small changes in transmission power may not affect the signal strength significantly and thus it can be narrowed down to a finite number of values. For analysis, we use $\alpha = 0.65$ to represent the average power division with extreme values of $\alpha = 0$ and 1.

No.	next state	transition probability	conditions
(1)	(i-1, j-1)	$q(1-\lambda_p)(1-\lambda_s)$	$1 \leq i, j \leq L$
(2)	(i-1,j)	$q(1-\lambda_p)\lambda_s$	$1 \leq i, j \leq L$
(3)	(i,j-1)	$q\lambda_p(1-\lambda_s)$	$1 \leq i, j \leq L$
(4)	(i+1,j+1)	$(1-q)\lambda_p\lambda_s$	$0 \leq i, j \leq L-1$
(5)	(L, 1)	$(1-q)\lambda_s + q\lambda_p\lambda_s$	$i = L, j = 0$
(6)	(0, j+1)	$(1-\lambda_p)\lambda_s$	$i = 0$

Table 4.1: State transition probabilities

4.3.2 Transition Probability Matrix

The transition probability matrix represents the transition probabilities from one state to another state depending on the action taken by the users. Due to page restrictions and to improve readability, we avoid listing the entire matrix. Instead, we present a list of transition probabilities at state $\sigma(\sigma_p, \sigma_s)$ when an action α ($0 < \alpha < 1$) is taken followed by a short description (see Table 4.1) where q represents the channel access probability of user p. The following state transition occurs

(i) when both p and s decide to transmit cooperatively and no new packets arrive at the queue at that time.

(ii) when both p and s cooperatively transmit and only a new secondary packet arrives.

(iii) when both p and s cooperatively transmit and only a new primary packet arrives.

(iv) when p does not get channel access and both primary and secondary packets arrive.

(v) when the primary queue is full and the secondary queue is empty and only a new secondary packet arrives.

(vi) when the primary queue is empty and only a new secondary packet arrives.

Similarly, we can list state transition probabilities for all other cases.

4.3.3 Reward Function

The reward function $U_{a(t)}(\sigma, \sigma')$ denotes the total reward achieved by the cooperating primary and secondary user for action $a(t)$ where we weight the relative importance of the two users with parameter δ. If successful delivery of primary packets is more (less) preferred to that of secondary packets in the system, the value of δ is set higher (smaller) than 0.5. Later in simulation, we set $\delta = 0.5$ considering both reward components with equal importance. We omit the index ('p' or 's') from the reward component when it applies for both users.

$$U_{a(t)}(\sigma, \sigma') = \delta U^{p}_{a(t)}(\sigma, \sigma') + (1 - \delta) U^{s}_{a(t)}(\sigma, \sigma') \tag{4.2}$$

The key challenge in modeling the MDP is to select an appropriate reward function that accurately measures the impact of the chosen action on the system performance in terms of packet loss. As mentioned earlier, while a cooperative transmission decision at a state may increase the probability of successful delivery of the first packet of the queue it also adds waiting time to later packets. This may decrease the successful delivery of later packets. Likewise, a decision to defer packet transmission may increase the dropping probability of an incoming packet. Therefore, given a pair of primary and secondary user and the system state σ, the reward function $U_{a(t)}(\sigma, \sigma')$ should answer the following two questions

- How does the action $a(t)$ at state σ change (increase / decrease) the drop probability of incoming packets due to queue overflow?
- How does the action $a(t)$ at state σ change (increase / decrease) the success probability of the packets waiting in the queue?

To answer these questions, we consider an example of a pair of a primary and a secondary user with queue length 10. We consider that the success probability of a primary packet with $\alpha = \emptyset$, and $\alpha = 1$ is 0.65, and 0.9 respectively. Assume that if the transmission decision reduces the number of waiting packets in the queue by 1, the drop probability of an incoming packet is reduced by 0.2. Any cooperative action adds waiting time and reduces the success probability of a primary packet with direct transmission by 0.05. We evaluate the impact of direct and cooperative action from the perspective of a primary user when the system moves from a state with 3 waiting packets to a state with 2 waiting packets. The total impact of direct transmission can thus be quantified as summation of 0.2 (change in dropping probability) and 0.65 (success probability of the first packet). Let us consider a cooperative action with $\alpha = 1$. In this case, the impact of the cooperative action is 0.2 from the change in dropping probability and 0.9 from the success probability of the first packet. Furthermore, the remaining 2 packets in the queue experience additional waiting time which reduces the probability of successful delivery by $0.05 \times 2 = 0.1$. So, the total impact is 0.2 + $0.9 - 0.1 = 1.0$. The net reward of using action $\alpha = 1$ over $\alpha = \emptyset$ is $1.0 - 0.85 = 0.15$.

Based on the above example, we define the reward function $U_{a(t)}(\sigma, \sigma')$ for each action that includes its impact on 1) the packet at the head of the queue, 2) the remaining packets in the queue, and 3) incoming packets not yet in the queue. Both the reward functions $U^p_{a(t)}(\sigma, \sigma')$ and $U^s_{a(t)}(\sigma, \sigma')$ have three components (see Eqn. 4.3) that are measured in comparison with direct transmission.

- The first component measures the change in the drop probability of an incoming packet because of queue overflow if action $a(t)$ is applied instead of direct transmission. This component depends on both the chosen action $a(t)$, current state σ, and the next state σ'. We denote this reward component as $D_{a(t)}(\sigma, \sigma') - D_{\emptyset}(\sigma, \sigma')$.

- The second component measures the probability of successful delivery of the packet at the head of the queue if action $a(t)$ is applied instead of direct transmission. The second component depends only on the action $a(t)$, and current state σ. We denote the second component as $V_{a(t)}(\sigma) - V_{\emptyset}(\sigma)$.

- The third component measures the net change in probability of successful delivery of the queued packets if action $a(t)$ is applied at present state σ instead of direct transmission. We denote the third component as $W_{a(t)}(\sigma) - W_{\emptyset}(\sigma)$. The users in the current state do not know which actions (except the default action) will be available at future states. Therefore, the impact of current action on later packets is evaluated on the basis of direct (default) transmission decision. For a secondary user, the success probability of default transmission decision does not change as long as the primary queue is not empty. Therefore, the third component does not contribute to the reward function of a secondary user s.

In summary, we express the reward of an action at any given state as the difference between the impact of that action and default action.

$$U^p_{a(t)}(\sigma,\sigma') = D^p_{a(t)}(\sigma,\sigma') - D^p_{\emptyset}(\sigma,\sigma') + V^p_{a(t)}(\sigma) - V^p_{\emptyset}(\sigma) + W^p_{a(t)}(\sigma) - W^p_{\emptyset}(\sigma) \quad (4.3)$$

$$U^s_{a(t)}(\sigma,\sigma') = D^s_{a(t)}(\sigma,\sigma') - D^s_{\emptyset}(\sigma,\sigma') + V^s_{a(t)}(\sigma) - V^s_{\emptyset}(\sigma) \quad (4.4)$$

4.3.3.1 Calculation of $D_{a(t)}(\sigma,\sigma')$

The first component $D_{a(t)}(\sigma,\sigma')$ denotes the change in packet loss probability due to queue overflow because of the action $a(t)$ and transition from state σ to state σ' . A transmission decision opens up a slot in the queue for a new packet. Therefore, each transmission decision reduces the future packet's dropping probability before it enters the queue. However, this reduction in packet loss probability is not same at all states.

The packet loss probability at state σ is expressed as $\Pr(Q(t') = L|\sigma)$ which denotes the probability of a queue becoming full at time t' given its current state σ at time t. Assuming service rate remains same, this probability is approximated based on the packet arrival rate as follows

$$D^{p}_{a(t)}(\sigma, \sigma') = (\lambda_p)^{L-\sigma_p} - (\lambda_p)^{L-\sigma'_p} \tag{4.5}$$

$$D^{s}_{a(t)}(\sigma, \sigma') = (\lambda_s)^{L-\sigma_s} - (\lambda_s)^{L-\sigma'_s}. \tag{4.6}$$

Here, σ_p and σ_s denote the number of packets waiting in the queue of the primary and secondary user at state σ. As the number of packets increases in the queue, the probability that the next packet will be dropped also increases. According to this function, if an action and change of state lead to fewer waiting packets, the event is rewarded. On the other hand, as the queue becomes full, the penalty increases. For example, consider a primary queue of length 10 and mean traffic arrival rate of 0.7. We calculate the reward component for two cases - (1) when the action leads to a state with one less packets waiting in the queue, (2) when the action leads to a state with one more packets waiting in the queue. Fig. 4.4 shows the two components for primary user only. The result shows that reducing the number of waiting packets is more highly rewarded as the queue gets fuller. Similarly, increasing the number of waiting packets is more highly penalized when the queue is fuller.

4.3.3.2 Calculation of $V_{a(t)}(\sigma)$

$V_{a(t)}(\sigma)$ denotes the probability of successful delivery of the packet at the head of the queue using the selected transmission decision $a(t)$ at state σ. Considering transmission deadline and packet length as Δt and len, we calculate the probability of successful delivery of any arbitrary packet in terms of the transmission rate R offered by $a(t)$ and waiting time ω. So, $\Pr(\omega + \frac{len}{R} \leq \Delta t|\omega)$

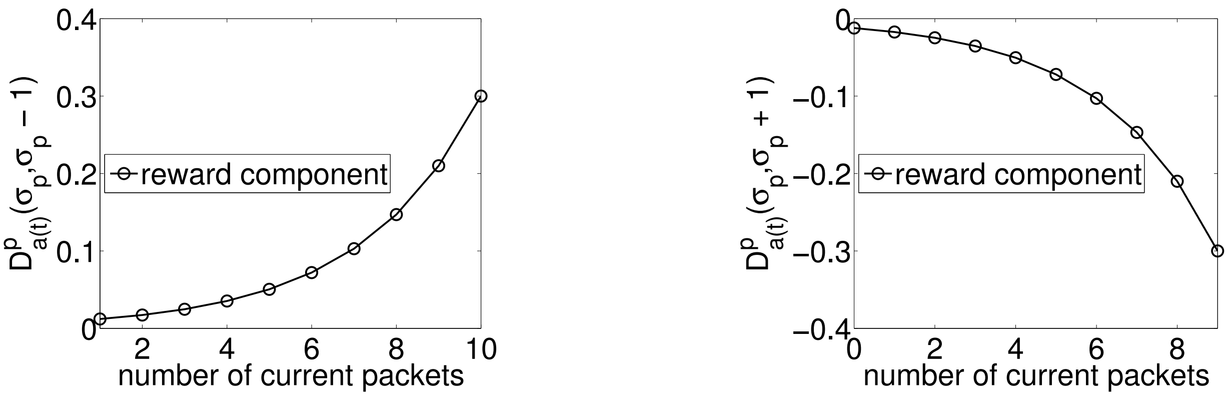

(a) change to a state with one less waiting packet

(b) change to a state with one more waiting packet

Figure 4.4: Reward component

$= \Pr(R \geq \frac{len}{\Delta t - \omega} | \omega) = \Pr(R \geq g(\omega)|\omega) = \Phi(R, g(w))$. Here, $g(\omega) = \frac{len}{\Delta t - \omega}$ is a function of waiting time that also denotes the minimum data rate required to deliver a packet successfully; $g(\omega)$ depends on the present state of the user and and the selected transmission approach. Note that the transmission rate R follows a distribution induced by the random channel gain and the transmission approach.

Based on the above equation, we express waiting time, transmission rate, and packet reception probability in terms of action $a(t)$ and the present system state σ. We denote the average waiting time of the first packet of primary user p and secondary user s at state σ as $\omega(\sigma_p)$ and $\omega(\sigma_s)$ respectively. We also denote transmission rate of primary user p and secondary user s with $R^p_{a(t)}$ and $R^s_{a(t)}$ and packet reception probability with $\Phi(R^p_{a(t)}, g(\omega(\sigma_p))$ and $\Phi(R^s_{a(t)}, g(\omega(\sigma_s))$ respectively.

$$V^p_{a(t)}(\sigma) = \Phi(R^p_{a(t)}, g(\omega(\sigma_p)) \quad = \quad \Pr\left(R^p_{a(t)} \geq g(\omega(\sigma_p)|w = \omega(\sigma_p))\right) \tag{4.7}$$

$$V^s_{a(t)}(\sigma) = \Phi(R^s_{a(t)}, g(\omega(\sigma_s)) \quad = \quad \Pr\left(R^s_{a(t)} \geq g(\omega(\sigma_s)|w = \omega(\sigma_s))\right) \tag{4.8}$$

4.3.3.3 Calculation of $W_{a(t)}(\sigma)$

The third reward component is applicable to only the primary user. We observe that a cooperative transmission decision of a primary user may increase the successful reception probability of the first packet at the cost of increasing waiting time of later packets. The longer the cooperation negotiation period, the higher the impact on remaining packets will be. Therefore, each cooperation decision must consider how it affects the chance of successful delivery of later packets in case there is no cooperation in the next state and packets are transmitted directly to the destination. So, this third component includes the success probability of remaining packets with cooperation overhead. We can express the net reward as follows

$$W^p_{a(t)}(\sigma) \;=\; \sum_{i=1}^{\sigma_p} \left[\Phi \left(R^p_{\emptyset}, g(\omega(i) + \Delta s) \right) \right]. \tag{4.9}$$

Here, Δs denotes the additional waiting time imposed on later packets because of the action taken at present state.

Next, we calculate R^p_{α} and $\Phi(R^p_{\alpha}, g(\omega(\sigma_p))$ for different values of $a(t) = \alpha$. Specifically, there are four cases we need to consider.

- $\alpha = \emptyset$: The primary user sends the packet at the rate R_1 and the secondary user opportunistically sends packet at rate R_5 that are calculated as follows:

$$R^p_{\emptyset} = R_1 = \log\left(1 + \frac{E_p \gamma_1}{\eta^2}\right),\; R^s_{\emptyset} = R_5 = \log\left(1 + \frac{E_s \gamma_5}{\eta^2}\right)$$

  For the direct transmission, the successful packet reception probability at respective destinations can be expressed as

$$\Phi(R^p_\emptyset, g(\omega(\sigma_p))) = exp\left(-d_1^\nu \frac{\eta^2}{E_p}\left(2^{g(\omega(\sigma_p))}-1\right)\right) \tag{4.10}$$

$$\Phi(R^s_\emptyset, g(\omega(\sigma_s))) = exp\left(-d_5^\nu \frac{\eta^2}{E_s}\left(2^{g(\omega(\sigma_s))}-1\right)\right). \tag{4.11}$$

- $\alpha = 0$: In this case, p lets s transmit s's packet which implies that $R^p_0 = 0$. Then s applies its full transmission power to send its packet at rate R_5 i.e. $R^s_0 = R_5$. However, allowing s the exclusive transmission opportunity increases waiting time of p's packets in addition to the negotiation time Δs.

$$R^p_0 = 0, R^s_0 = R_5 = \log\left(1 + \frac{E_s\gamma_5}{\eta^2}\right)$$

The successful packet reception probability of a primary and a secondary user at state σ can be expressed as

$$\Phi(R^p_0, g(\omega(\sigma_p))) = 0 \tag{4.12}$$

$$\Phi(R^s_0, g(\omega(\sigma_s))) = exp\left(-d_5^\nu \frac{\eta^2}{E_s}\left(2^{g(\omega(\sigma_s))}-1\right)\right). \tag{4.13}$$

- $\alpha = 1$: The primary user relays through secondary user and the secondary user applies its full transmission power to relay the primary signal to its destination. So, the effective primary transmission rate is minimum of the transmission rate from primary source to secondary source ($p \rightarrow s$) and from secondary source to primary destination ($s \rightarrow p'$).

$$R^p_1 = \frac{1}{2}\min\left(\log\left(1+\frac{E_p\gamma_2}{\eta^2}\right), \log\left(1+\frac{E_p\gamma_1 + E_s\gamma_4}{\eta^2}\right)\right)$$

We calculate $\Phi(R_1^p, g(\omega(\sigma_p)))$ as follows

$$\Phi\left(R_1^p, g(\omega(\sigma_p))\right) = \begin{cases} exp\left(\frac{-d_2^\nu \eta^2}{E_p}\left(2^{2g(\omega(\sigma_p)} - 1\right)\right), & \text{if } \gamma_2 \leq \gamma_4 + \gamma_1 \\ \frac{d_1^\nu}{d_1^\nu - d_4^\nu} exp(-y d_4^\nu) - \frac{d_4^\nu}{d_1^\nu - d_4^\nu} exp(-y d_1^\nu), & \text{otherwise} \end{cases}. \quad (4.14)$$

Here, $y = \frac{\eta^2}{E_p}(2^{2g(\omega(\sigma_p)} - 1)$.

- $0 < \alpha < 1$: The primary user relays through secondary user and the secondary user applies αE_s to relay the primary signal to its destination and applies $(1-\alpha)E_s$ to transmit its own signal. So, the effective primary transmission rate is minimum of the transmission rate from primary source to secondary source ($p \to s$) and from secondary source to primary destination ($s \to p'$).

$$R_\alpha^p = \frac{1}{2}\min\left(\log\left(1 + \frac{E_p\gamma_2}{\eta^2}\right), \log\left(1 + \frac{E_p\gamma_1}{\eta^2} + \frac{\alpha E_s \gamma_4}{(1-\alpha)E_s\gamma_4 + \eta^2}\right)\right)$$

We calculate $\alpha' = \frac{(\gamma_2 - \gamma_1)(1 + \frac{E_s\gamma_4}{\eta^2})}{\gamma_4 + (\gamma_2 - \gamma_1)\frac{E_s\gamma_4}{\eta^2}}$ which decides the effective transmission rate of the primary user.

$$\Phi\left(R_\alpha^p, g(\omega(\sigma_p))\right) = \begin{cases} exp\left(-d_2^\nu \frac{\eta^2}{E_p}\left(2^{2g(\omega(\sigma_p))} - 1\right)\right) & \text{if } \alpha \geq \alpha' \\ exp\left(-d_1^\nu \frac{\eta^2}{E_p}\left(2^{2g(\omega(\sigma_p))} - 1\right)\right) & \text{otherwise} \end{cases} \quad (4.15)$$

The successful packet reception probability of a secondary user will be calculated as follows:

$$\Phi\left(R_\alpha^s, g(\omega(\sigma_s))\right) = exp\left(-\frac{\eta^2}{(1-\alpha)E_s} d_5^\nu \left(2^{2g(\omega(\sigma_s))} - 1\right)\right) \quad (4.16)$$

4.3.4 Comparison

In this section, we evaluate how effectively the proposed model (referred to as 'rtCoop') represents the real-time system requirements. If a model captures the true characteristics of the underlying system, its selected action should lead to the optimum system performance, in this case, higher packet reception rate. In this regard, we also consider an existing model presented in [117] (referred to as 'prCoop') for comparison. In this model, reward functions are defined based on the cost of storing and relaying a primary packet. We assume that there are four different values of α ($\emptyset$, 0, 1, 0.65) to choose from.

Accordingly, we solve the MDP of each model using linear programming, run the simulation, and record different statistics e.g. the average waiting time, packet reception rate. Additionally, we include the direct transmission approach in the analysis where p transmits directly to p' and s transmits only when the primary queue is empty. We refer to the direct transmission as 'noCoop'.

To analyze the simulation results, we vary different system parameters e.g. distance between users, queue length, traffic rate. For each different configuration, we collect several statistics e.g. number of times a cooperative action is preferred over direct transmission, average waiting time ω_p experienced by p, and cumulative packet reception rate and compare the results.

First, we fix the primary and secondary traffic rate following a Bernoulli distribution, channel access probability ($q = 0.8$), queue size ($L = 5$). We vary the distance between p and s and p' and s' which are denoted as d_2 and d_4 respectively. All the distances are normalized to 1. We move the secondary user along the line between the primary transmitter and the destination i.e. we set $d_2 = 1 - d_4$ while keeping the distance between the secondary transmitter and the secondary destination fixed to 0.3. Fig. 4.5a and 4.6a show that rtCoop achieves higher cumulative packet reception rate and lower average primary waiting time compared to prCoop.

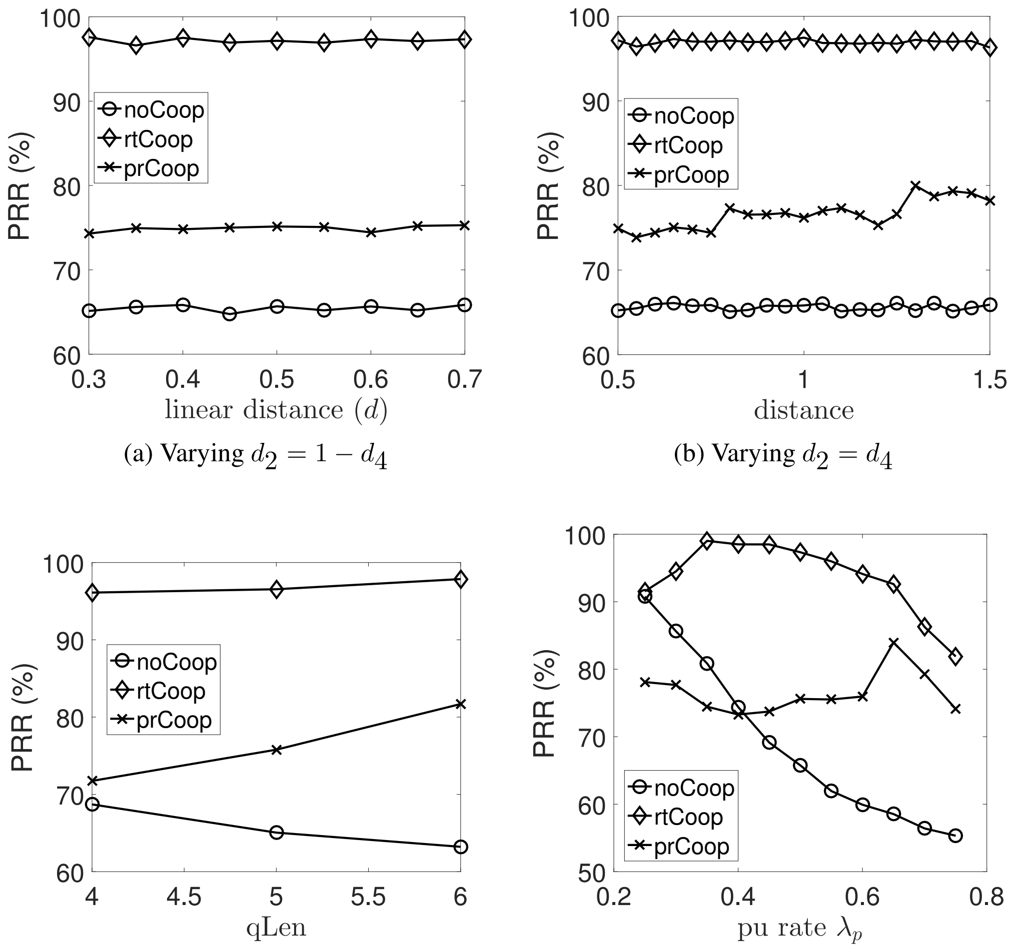

(a) Varying $d_2 = 1 - d_4$

(b) Varying $d_2 = d_4$

(c) Varying queueing length

(d) Varying λ_p

Figure 4.5: Comparison between cooperation models (packet reception rate)

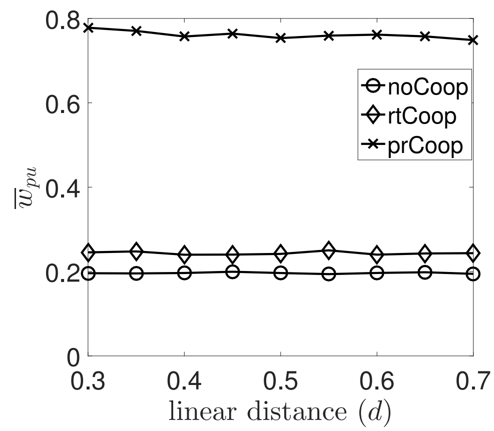

(a) Varying $d_2 = 1 - d_4$

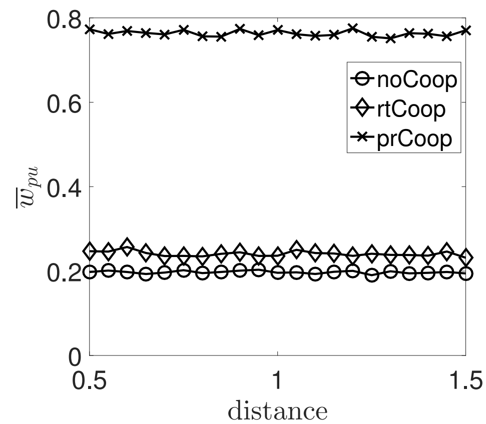

(b) Varying $d_2 = d_4$

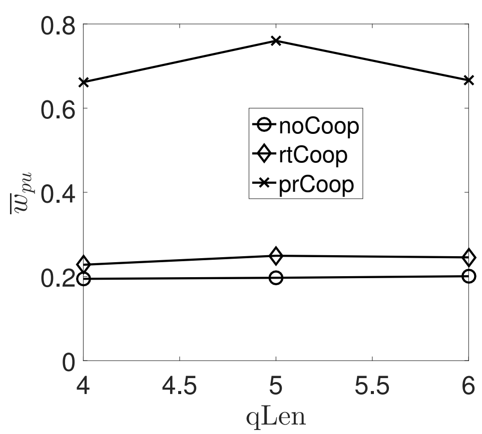

(c) Varying queueing length

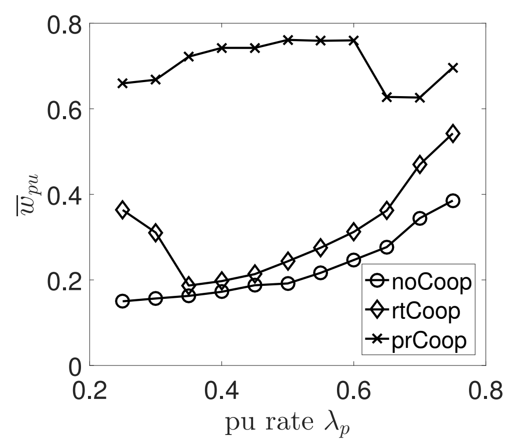

(d) Varying λ_p

Figure 4.6: Comparison between cooperation models (average pu waiting time)

Next, we put the secondary user away from the line between the primary transmitter and the destination and we set $d_2 = d_4$ and $d_5 = \frac{d_2}{2}$. We also vary the queue length, primary traffic rate, and secondary traffic rate while keeping all other parameters fixed. For each of these different configurations, we plot the packet reception rate and average waiting time of a primary packet in Fig. 4.5. The results show that the proposed cooperation model rtCoop improves the packet reception rate compared to prCoop and noCoop. We also record the average waiting time encountered by primary users and show the results in Fig. 4.6. In general, it shows that prCoop incurs higher waiting time compared to our proposed model. This is because the former approach does not take into consideration the communication overhead associated with cooperation that leads to wrong transmission decision and low packet reception rate.

4.4 Multi-user Cooperative Transmission Model

The cooperation model in multi-user setting adds some unique challenges to the single user model. First, in the single user analysis, we assume that changes occur at discrete time intervals and system parameters do not change in a state. However, in reality, the interaction between primary and secondary users is asynchronous. Packets arrive asynchronously at the user and transmission times may differ from user to user. Therefore, state transition may occur at different intervals. Second, we need to consider the interference between primary and secondary transmissions which was absent in the single user analysis. Furthermore, a user has no knowledge of other users' traffic and queue status, and has to decide solely based on its state parameters and cooperation offers received from its neighbors. Addressing these above issues, we present a distributed cooperative transmission model for making cooperation offers, negotiating terms of cooperation, selecting a transmission approach, and finally scheduling packet transmission. We explain these steps of the algorithm next.

4.4.1 Step 1: Pre-screening

In this step, a secondary user constructs an interference map which helps it to identify potential primary users that it can engage in cooperative transmissions. We assume that each secondary user is aware of the interference constraint of the primary network and knows the channel gain between itself and every primary receiver in the network. A secondary user may estimate the channel quality and link rate from overhearing the message exchange between primary transmitters and receivers and by applying standard training sequence methods [43] or by analyzing the received patterns [82]. Thus, a secondary user determines the maximum transmission power it can use for each primary user and builds the interference map.

Let $\mathcal{V}(s_j)$ denote the set of primary users within transmission range of s_j. The interference map has $|\mathcal{V}(s_j|$ entries and each entry represents the maximum transmission power $\alpha_{max}(p_i, s_j)$, s_j can use in relaying while cooperating with $p_i \in \mathcal{V}(s_j)$. s_j calculates its interference contribution to other ongoing transmission while cooperating with p_i and finds the maximum value it can use without interfering any of these transmissions. For example, to calculate $\alpha_{\max}(p_i, s_j)$ we calculate $\alpha_{\max}(p_i, s_j|p_k)$, the maximum transmission power s_j can use relaying p_i's traffic without interfering with p_k's transmission. Finally, the maximum power $\alpha_{max}(p_i, s_j)$ is set to the minimum of these maximum values.

$$\alpha_{max}(p_i, s_j) = \min_{\forall k \in \mathcal{P}} \alpha_{\max}(p_i, s_j|p_k) \tag{4.17}$$

On the other hand, a primary user by default operates in direct transmission mode. A primary user continuously monitors its queue size and packet loss rate, and if the change in packet loss exceeds beyond a threshold ϵ_p, it tunes to control channel, looks for cooperation opportunity, and enters into the negotiation step.

4.4.2 Step 2: Negotiation

At this step, the interested users tune to the common control channel for submitting or accepting its cooperation offer. A primary user's goal is to find a secondary user whose relaying will reduce packet loss. A secondary user's goal is to ensure transmission opportunity while spending less power in relaying and avoiding interference to others' transmission.

Accordingly, a secondary user consults its interference map, initiates the cooperation process, and sends an offer to one or more primary users from the list. A cooperation offer from a secondary user includes the value of α, and its transmission duration. To start with, s_j starts with an offer of the highest transmission power $\alpha_{max}(p_i, s_j)$ it can provide to p_i. This initial offer helps s_j in assessing its future cooperative transmission opportunities. The subsequent offers are modified using Eqn. 4.18. If its offer is accepted, the value of $\alpha_t(p_i, s_j)$ is changed at the rate of the change in queue. On the other hand, the value of $\alpha_{t-1}(p_i, s_j)$ is doubled in the next offer. Here, $\frac{dQ}{dt}$ denotes the change in the number of waiting packets with time.

$$\alpha_t(p_i, s_j) = \begin{cases} \min\left(\alpha_{t-1}(p_i, s_j) \times \left(1 + \frac{dQ}{dt}\right), \alpha_{max}(p_i, s_j)\right) & \text{if successful} \\ \alpha_{t-1}(p_i, s_j) \times 2 & \text{otherwise.} \end{cases} \tag{4.18}$$

A primary user willing to cooperate looks into the cooperation offers it has received. For each such potential offer, a primary user calculates its cooperation gain considering its impact on current and later periods in comparison with direct transmission. So, a primary user p_i receives offer from its neighboring secondary user s_j in the form of transmission power $\alpha_t(p_i, s_j)$ and transmission

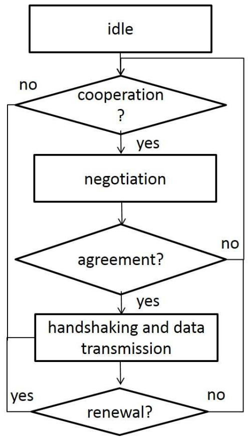

Figure 4.7: Cooperation life cycle of a user

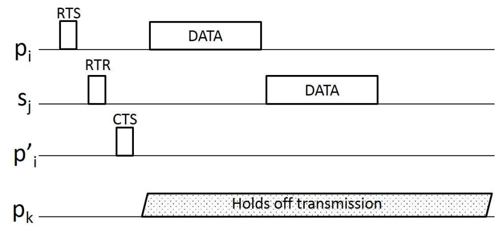

Figure 4.8: Handshaking protocol

time yt_j. For each offer from s_j, p_i estimates cooperative channel gain, calculates the expected relay transmission time and cooperation gain $\mathcal{G}_j(i)$, and compares it with direct transmission approach. Both immediate gain and future opportunities are considered in gain calculation and are weighed by the state of the queue. Given the remaining time to transmit a packet (rt_i), estimated direct transmission time (dt_i), and estimated offered transmission time (xt_j) and the requested transmission time (yt_j), p_i calculates the cooperation gain $\mathcal{G}_j(i)$ of a cooperation offer from s_j as follows:

$$\mathcal{G}_j(i)=\left(\frac{c_1\times(dt_i-rt_i)}{\max(rt_i,dt_i)}+\frac{c_2\times(rt_i-xt_j)}{\max(rt_i,xt_j)}+\frac{c_3\times(dt_i-xt_j)}{\max(dt_i,xt_j)}\right)\times\left(1-\frac{Q_i}{L}\right)+\left(1-\frac{yt_j}{xt_j}\right)\times\frac{Q_i}{L} \tag{4.19}$$

Here, c_1, c_2, and c_3 are constants that denote the relative weight factor of these subcomponents where $c_1+c_2+c_3=1$. Q_i denotes the number of packets waiting in the queue of p_i. p_i selects the secondary user with the highest gain for cooperation. Otherwise, it decides to transmit directly.

In the final step, a secondary user s_j receives confirmation from one or more primary users. If there is more than one reply, s_j picks the one that increases its cooperation gain i.e. achieves higher energy efficiency and less power consumption in relaying. s_j sends a confirmation message to the selected primary user, and both users start agree to cooperative transmission. Since primary users operate asynchronously, a user may receive cooperation offers from other users while it is in data transmission mode. However, all these offers during transmission mode are ignored. Fig. 4.7 shows the different phases of the cooperation life cycle of a typical user. Each user goes through this above negotiation procedure to make transmission decisions.

4.4.3 Step 3: Data Transmission

A primary user in cooperation agreement with a secondary user follows a modified RTS/CTS handshaking protocol before data transmission. In the traditional RTS/CTS handshaking protocol, the source and the destination sends small control packet to announce their next data transmission. Any user overhearing either of these packets backs off the transmission period and tries again.

In cooperative relayed transmission, an additional user involves in data transmission. Specifically, the secondary user receives a packet from the primary user and then relays the packet to the destination. With the traditional handshaking protocol, a successful packet delivery involves at least two handshaking periods - the first one from primary transmitter to secondary user, and the second one from secondary user to primary receiver. The primary packet needs to be stored in the secondary queue. In the proposed handshaking protocol, we introduce an additional control packet RTR (ready to relay) which will be sent by the cooperating secondary user. This ensures a primary packet spent minimum time in a secondary queue, and reduces the overhead of handshaking. Accordingly, when two cooperating users are ready to transmit, a primary user sends a RTS packet including the name of the secondary user it is cooperating with. The cooperating secondary user then sends a RTR packet denoting the address of both the sender and receiver. Finally, the primary receiver sends a CTS packet with cooperation duration. If each cooperating user involved in the cooperation agreement receives the other two control packets, it assumes that the channel is secured and data transmission starts. Any other user outside this cooperation agreement backs off the entire duration when it receives any of those control packets. Fig. 4.8 demonstrates a handshaking event between a cooperating primary and secondary user.

4.4.4 Step 4: Cooperation Renewal

The final step of the cycle is to determine the cooperation duration. If the duration is small, users have to frequently go through negotiation periods; the overhead associated with it may outweigh the cooperation benefits. On the other hand, while longer intervals reduce the communication overhead, users may miss cooperation opportunities which hurt the system reliability. So, it is important for a user to be able to adapt the cooperation duration with changing user and network conditions.

With this in mind, the proposed model allows a cooperating user to continue cooperative transmission without going through negotiation period. A primary user keeps record of the rate of change in queue status and the change in packet reception rate. If this ratio drops below a threshold (δ_p), it terminates the current cooperation period and switches to direct transmission. Otherwise, it continues to send its packet to the cooperating secondary user without additional message exchange. Similarly, a secondary user also keeps record of the rate of change in its queue status and cooperation gain in terms of energy consumption. If the ratio drops below a threshold (δ_s), the secondary user does not participate in handshaking. This way communication overhead is reduced without sacrificing significant cooperation benefits. The tradeoff is controlled by adjusting the parameters δ_p and δ_s.

4.5 Performance Evaluation

In this section, we evaluate the performance of the proposed cooperation model in a cognitive radio network to support real-time traffic.

4.5.1 Performance Metrics

We use three metrics to analyze the performance of the model. They are as follows:

- packet reception rate : Our primary evaluation metric is packet reception rate of the network. We define 'weighted packet reception rate' or 'weighted PRR', $\overline{PRR}$ as weighted sum of primary and secondary packet reception rate. So, $\overline{PRR} = \delta \times \sum_{i=1}^{m} \text{PRR}_i + (1-\delta) \sum_{j=1}^{n} \text{PRR}_j$. Here, PRR_i and PRR_j denote the packet reception rate of primary user p_i and secondary user s_j. Throughout our simulation, we use δ = 0.5 i.e. we consider equal priority to primary and secondary packets.

- cooperation overhead analysis: We introduce another metric that determines the overhead caused from exchanging message during negotiation procedure. We define 'pu overhead' as the number of times a primary user engages in cooperation negotiation (whether it is successful or not) during its lifetime.

- cost benefit analysis: We perform a cost benefit analysis for secondary users in terms of power consumption in relaying primary traffic. We define 'su cost per packet' as a ratio of the total power spent in relayed transmission and number of its packets it has transmitted.

4.5.2 Simulation Setup

We consider a $150m \times 150m$ simulation area where secondary users are randomly placed in the area between primary sources and destinations. Number of (primary and secondary) users are varied between 1 and 5. For each set of primary and secondary users, we create 20 random topologies and for each topology, we run the simulation on each topology 20 times; each case is simulated for 1000ms. In each topology, it was made sure that each primary (secondary) user has at least one secondary (primary) user within its transmission range. All results are summarized over these topologies and presented with 95% confidence interval. Each primary user is assigned a channel of bandwidth $20KHz$. The (maximum) primary and secondary transmission power, $E_p = E_s = E = 100$mW and the noise, N_0 is set to $10e^{-10}$ mW/Hz. Path loss ν is set to 4 and the size of the packet, len is set to 1Kb. We use additive interference model [59] to calculate mutual interference between ongoing transmissions.

We compare the performance of the proposed model in two different user settings with two different primary traffic model. In the first setting, we consider a single pair of primary and secondary users where primary traffic follows a Poisson distribution. In the second setting, we consider a multi-user setting where number of channels are less than the active primary users and two primary users may use the same channel.

4.5.3 Single User Setting

We select the power division approach proposed in [47] to compare the performance of our proposed cooperation model. We refer to the proposed cooperation model as ‘rtCoop’ and the basic power division approach in [47] as ‘prCoop0’. In this approach [47], the power distribution is optimized to reduce the outage probability of the primary systems. This approach does not take

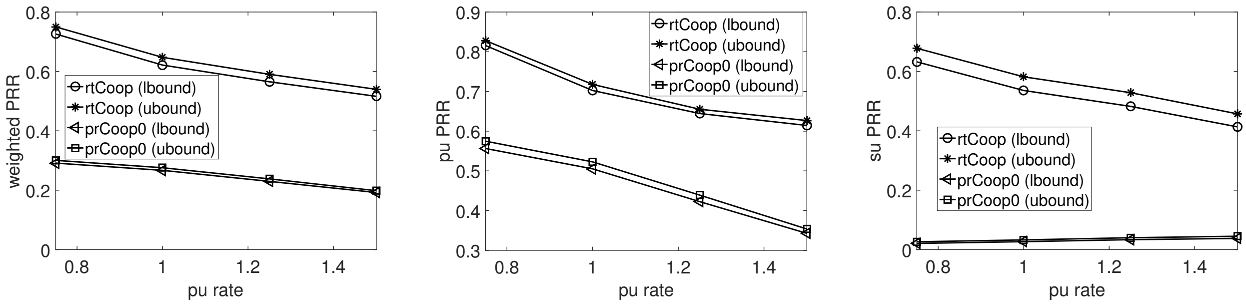

(a) weighted PRR (b) pu packet reception rate (c) su packet reception rate

Figure 4.9: Comparison between models of a single pair of primary and secondary users

into consideration the user's queue status and future opportunities. The network topology and simulation procedure remains same.

We consider that the primary traffic follows a Poisson distribution. We vary the mean primary traffic rate from 0.75 and 1.5, and record the packet reception rate for each cases. The result is shown in Fig. 4.9 where the proposed model outperforms the basic model [47]. This is because in our proposed approach, a secondary user has equal rights to select cooperation parameters and takes its decision from the perspective of real-time traffic.

4.5.4 Multi-user setting

To compare the performance of the proposed model in a multi-user setting, we consider the cooperation model proposed in [117]. In this model, a secondary user considers the cost of storing a packet in queue and spending power in relaying and sends cooperation offer accordingly. A primary user selects the secondary user that offers the highest transmission power. Upon negotiation, RTS/CTS handshaking protocol is used for data transmission. We consider two traffic models to evaluate the performance of the proposed model. The first one is a Markov modulated process presented in [49] which has three internal states and traffic generation rate varies between states. The second traffic model we consider here is a Poisson distribution. In both cases, secondary

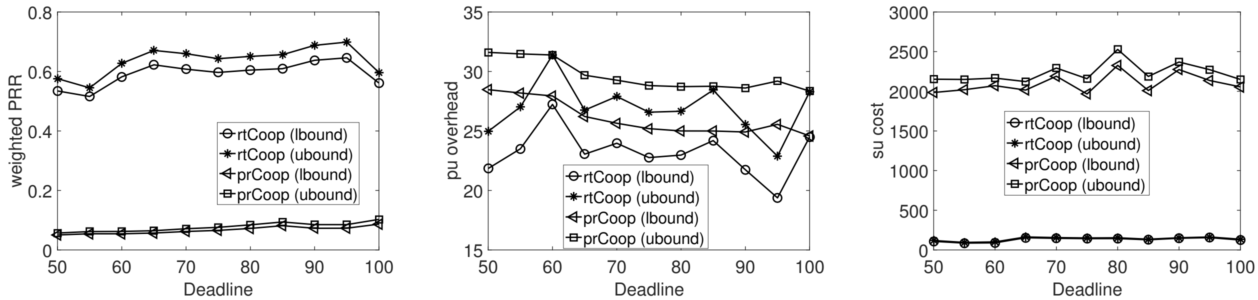

(a) weighted PRR (b) pu overhead (c) su cost

Figure 4.10: Markov three state traffic model with varying transmission deadline

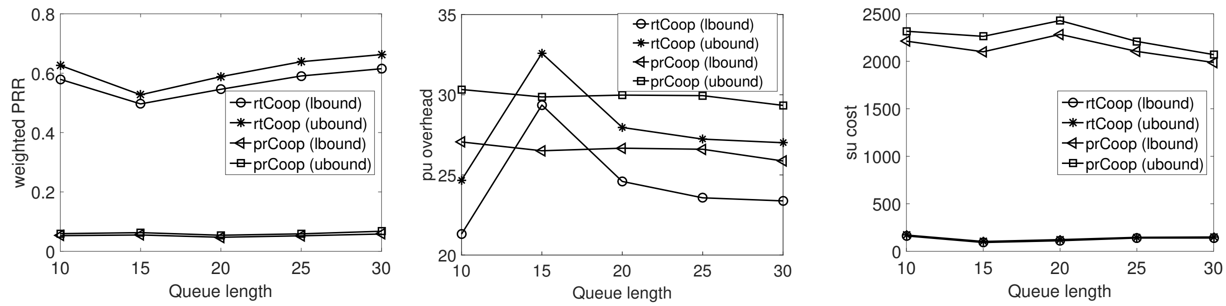

(a) weighted PRR (b) pu overhead (c) su cost

Figure 4.11: Markov three state traffic model with varying queue length

user's traffic follows a Poisson distribution. For each traffic model, we run simulation with varying transmission deadline and queue length and analyze the performance of the proposed model.

First, we vary the transmission deadline with Markov three state traffic model and plot the results in Fig. 4.10. The simulation result shows that rtCoop achieves higher packet reception rate than prCoop. However, both approaches exhibit high pu overhead because of the rate of change in queue size is not consistent which makes the cooperation duration small and triggers frequent cooperation negotiation. However, secondary users spend less power in rtCoop compared to prCoop. Next, we vary the queue length and plot the performance metrics in Fig. 4.11 which shows similar trend as with varying transmission deadline.

Next, we consider that primary traffic follows a Poisson distribution. The mean value of traffic

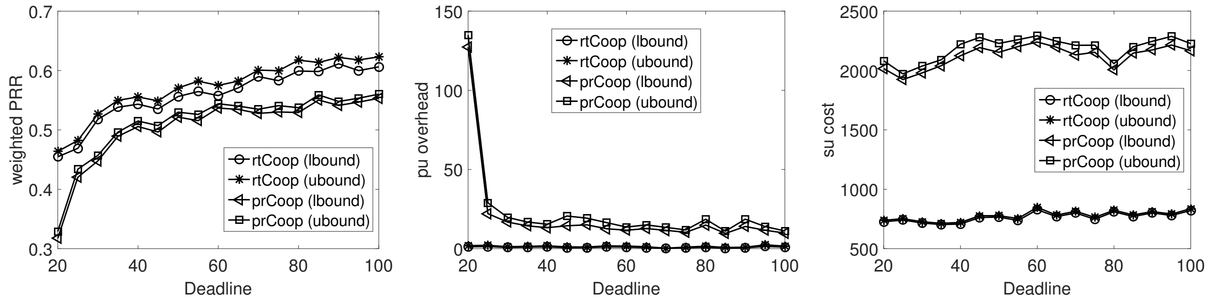

(a) weighted PRR (b) pu overhead (c) su cost

Figure 4.12: Poisson traffic model with varying deadline

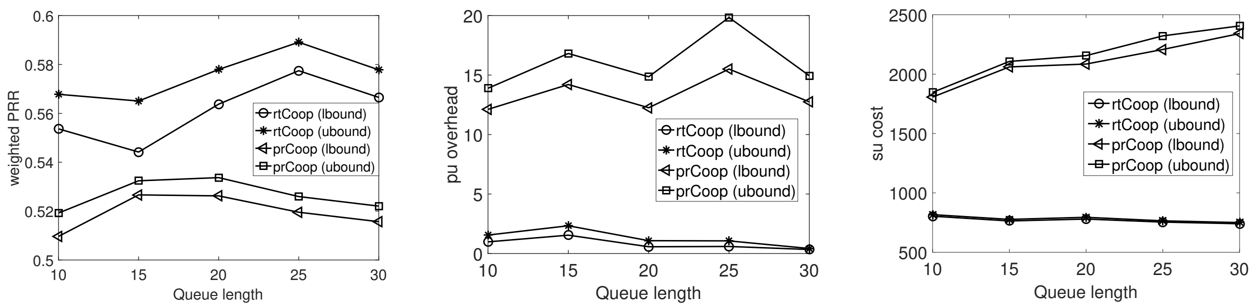

(a) weighted PRR (b) pu overhead (c) su cost

Figure 4.13: Poisson traffic model with varying queue length

is varied is set to 0.05. Again we vary the transmission deadline and plot three metrics in Fig. 4.12. As deadline increases, the packet reception rate increases, however, rtCoop ensures higher packet reception rate in all cases. The proposed model also achieves low primary overhead and less secondary cost per packet compared to prCoop. We also vary the queue length and the results are shown in Fig. 4.13. Again, the proposed model outperforms prCoop.

Next, we vary the mean value of Poisson distribution while keeping every other parameter fixed. The results are shown in Fig. 4.14. The results show that the proposed model achieves higher packet reception rate while ensuring low primary overhead and low energy per bit for a secondary user.

Finally, we vary the number of secondary users from 5 to 15 while keeping the number of primary users fixed to 5 to analyze the impact of cooperation overhead on the system performance.

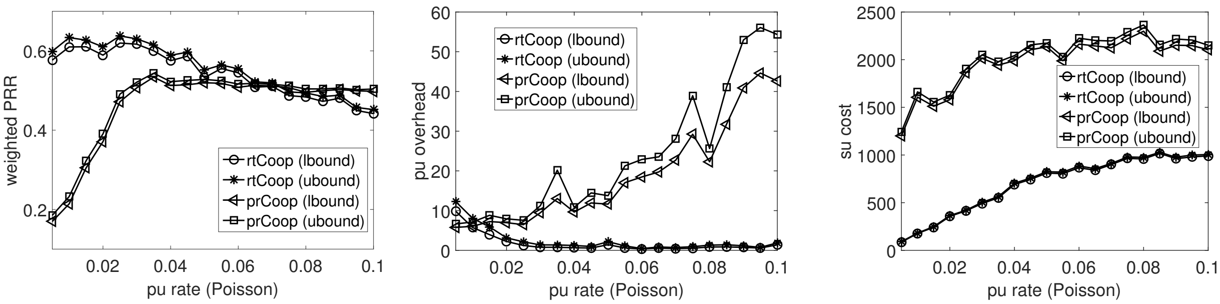

(a) weighted PRR (b) pu overhead (c) su cost

Figure 4.14: Poisson traffic model with varying pu rate

The simulation result shows that the cooperation overhead in the proposed algorithm increases very slowly compared to the existing models. This is because a secondary user in the proposed algorithm goes through a renewal step with almost no overhead instead of frequent negotiation in the existing algorithms.

4.6 Summary

In this chapter, we develop an interference aware cooperative cognitive radio network for real-time applications. We formulate the cooperation optimization problem into an MDP and define its states, action sets, transition matrix, and reward functions reflecting the tradeoff between cooperation overhead and cooperation benefits. We define the reward of a primary user in terms of successful packet reception probability subtracted by the cost of cooperation overhead. Likewise, we define the reward of a secondary user in terms of successful packet reception probability with respect to transmission power applied to relayed transmission. Our analysis of a single pair of primary and secondary users points out the fact that there is an effective cooperation region in terms of the distance among users. In a multi-user cooperation model, we define ‘cooperation gain’ that represents benefits of cooperation and selects pairs for transmission following a negotiation procedure. The cooperating pairs use a modified RTS/CTS handshaking protocol for data transmission. We perform extensive simulations under different network settings with varying different network parameters and compare the results with an existing model. The result shows that cooperative transmission ensures higher packet reception rate than the prior cooperation model. We perform a cost benefit analysis that represents the secondary user's cost in terms of energy consumption in relaying primary packet. We also perform an overhead analysis which demonstrates the effect of cooperation negotiation on primary users. The proposed model ensures low control overhead and low energy cost for cooperating primary and secondary users respectively.

Chapter 5

Cooperative Routing in Cognitive Radio Networks

As discussed in Chapter 4, relay based collaboration model brings a powerful means to combat channel fading, to achieve improved network capacity, and to provide efficient spectrum sharing among primary and secondary users. By exploiting cooperative diversity, a primary user (PU) appoints a secondary user to relay its packets, and improves its throughput, and a secondary user (SU) increases channel access opportunities in return for its services. The success in single hop relay model motivates the researchers to study and explore the collaboration model in multi-hop cooperative communication.

In this chapter[1], we study and analyze the multi-hop cooperative relay selection and scheduling problem. In a multi-hop cooperation model, a primary user intends to establish a stable routing path to its destination by selecting multiple secondary users as intermediate relays. A secondary user, on the other hand, participates in one or more routing paths to ensure its transmission opportunities while limiting power consumption in relaying. Exploiting time and space diversity over multiple hops, this model can offer an innovative solution for relaying the growing $3G/4G$ cellular traffic [128]. The emerging technology of cognitive sensor networks with limited transmission range and

[1]The work presented in this chapter has been published in the following research article:

(i) Chowdhury Sayeed Hyder, and Li Xiao. ”Cooperative Routing via Overlapping Coalition Formation Game in Cognitive Radio Networks”, in the 10th Workshop on Wireless Mesh and Ad-hoc Networking (WiMAN), Waikoloa, Hawaii, USA, Aug 4, 2016.

longer lifetime expectation also advocates an efficient mechanism for relaying traffic [79]. Finally, network model relying on spectrum sensing techniques may not provide satisfactory results due to imperfect sensing. On the other hand, cooperation among primary and secondary users eliminates the unintentional collision with PU transmission [127].

Although multi-hop cooperative relaying brings significant promises, we need to address several unique challenges to design the cooperation model and exploit its full benefits. The main challenge is to quantify the mutual interest of primary and secondary users into payoff and incorporate it in cooperation decision making. For example, while a secondary user as an intermediate relay may offer higher data rate, it also introduces delay in the same routing path. Therefore, a primary user's payoff must reflect the tradeoff between achievable throughput and path delay. On the other hand, unlike single hop relay model, a secondary user's cooperation benefit is defined not only by its own action but also by the action of other users in the routing path. Therefore, we must take into consideration the competition among the secondary users to meet their requirements. As a result, single hop relay based research ([64, 67, 76, 131, 136]) are not extensible to multi-hop scenarios.

In this regard, few work [79, 127] address the multi-hop cooperative relay selection problem and design a cooperation model focusing on primary users' interest only. For example, Xue et al. [127] present a scheduling algorithm for a single primary transceiver pair whose routing path consists of fixed and predetermined secondary relay nodes. However, the competition among multiple primary source-destination pairs is not addressed and the consideration of fixed routing path make the cooperation model impractical. Although Li et al. [79] have considered multiple primary users in their work, the model becomes unstable when users have to deal simultaneous requests. Furthermore, a secondary user acts only in response to primary users' specific requests, and each one may cooperate with at most one primary user. This limitation prevents a secondary user from exploring its cooperative transmission opportunity. Finally, we need to ensure the stability of the routing path and the scalability and complexity of the cooperation algorithm. An unscalable algorithm causes unstable routing path that leads to collision and packet loss, and the network output degrades significantly. Therefore, these proposed framework do not represent the true potential of a multi-hop cooperation framework. In this chapter, we analyze the multi-hop cooperation framework and present $mcRoute$, a multi-hop cooperation-based relay selection and transmission scheduling algorithm addressing the issues discussed above.

We consider coexisting primary and secondary users and analyze a multi-hop cooperation framework based on users' mutual interests. In this framework, we consider both primary and secondary users as 'active' participants which actively adopt strategies to decide when and how to accept cooperation from other users for improved system performance. This complex interaction and negotiation process is analyzed using an overlapping coalition formation game. The result from this analysis is then used to devise a cooperation based routing algorithm that handles simultaneous route discovery requests and ensures stable routing paths through coalition formation. Therefore, our network model is more general than others and exploits the full benefits of mutual cooperation.

The salient contributions of our work are summarized as follows.

- We formulate the multi-hop relay selection and scheduling problem as an overlapping coalition formation (OCF) game. Unlike existing approaches, this model involves active participation from both primary and secondary users where one secondary user can join more than one coalition. The user payoff functions in the game are defined reflecting their mutual interest on cooperation.

- We propose $mcRoute$, a cooperation based routing algorithm based on the properties of the

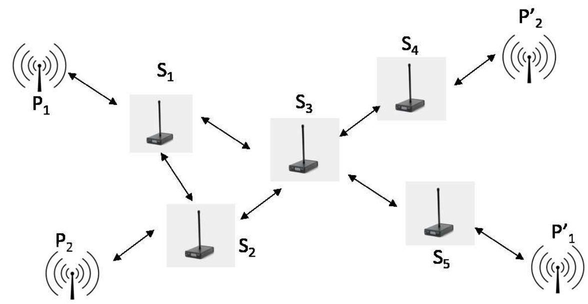

Figure 5.1: Network model

OCF game. Each primary transmitter initiates a route discovery request. When a secondary user receives such requests, it coordinates between multiple requests and carefully sets its cooperation parameters to show its interest to join in coalitions. After exchanging messages between users, the routing paths are guaranteed to converge and packets are scheduled for transmission in time domain.

- Finally, we develop the proposed joint routing and scheduling algorithm and compare our algorithm with an existing work [79] and show that our algorithm performs better than existing one. We also analyze our proposed algorithm in terms of various performance metrics.

5.1 System Model and Problem Formalization

5.1.1 System Model

We consider an OFDMA-based network consisting of m independent source-destination pairs of primary users (Fig. 5.1). The set of primary transmitters is represented as $\mathcal{P} = \{p_1, \ldots p_m\}$ while the set of corresponding receivers is represented as $\mathcal{P}' = \{p'_1, \ldots p'_m\}$. We assume the coexistence of an ad hoc secondary network with n secondary transmitters in set $\mathcal{S} = \{s_1, \ldots, s_n\}$ and their corresponding receivers in set $\mathcal{S}' = \{s'_1, \ldots, s'_n\}$. Each user (primary and secondary) is equipped with two radios – one is dedicated for data transmission and the other one is for exchange of control message.

To make the best use of the bandwidths available to the primary network, the orthogonal sub-carriers can be divided into data channels and control channels [73] [140]. Since our goal is to address the multi-hop relay selection and routing path formation via cooperation, this channel allocation technique among the primary users will not be discussed. For simplicity, we assume that each primary transmitter $p_i \in \mathcal{P}$ is allocated a subset of sub-carriers, and together they are referred to as 'sub-channel' for data transmission [79]. We consider that each sub-channel consists of an equal number of sub-carriers, thereby achieving equal bandwidth[2], B. Each secondary user $s_i \in \mathcal{S}$ can operate over any of the sub-channels of these primary users based on their cooperation agreement. A common control channel is also established for exchanging control message in time domain among the users.

We assume that users engage in cooperative transmission and share their resources in time domain [64, 67, 79] if it increases their profit. A primary user is interested in exploiting the cooperation diversity to build a routing path that provides improved network performance. Similarly, a secondary user's interest is to ensure enough transmission time to meet its rate requirement while spending as less power in relaying primary packets as possible. This mutual interest in achieving higher payoff drives the users to negotiate cooperation terms, share resources in time domain, and builds a multi-hop cooperation model.

Our goal here is to determine the terms of cooperation and design a multi-hop transmission model that maximizes users' payoff. To achieve this goal, we first formulate the relay selection problem as an overlapping coalition formation game. We start with a brief description on overlapping coalition formation game followed by step by step problem formalization.

[2] The model can be extended to users with variable bandwidth.

5.1.2 Preliminaries

Overlapping coalition formation game is a special type of cooperative game where players can participate in several coalitions. This theory has been used to model collaborative spectrum sensing in cognitive radio networks [119], interference management in small cell networks [139], and so on. In the context of relay selection in $CCRN$, we adopt the overlapping coalition formation game to model and analyze the behavior of the framework. We present the properties of the overlapping coalition formation game in the following definitions.

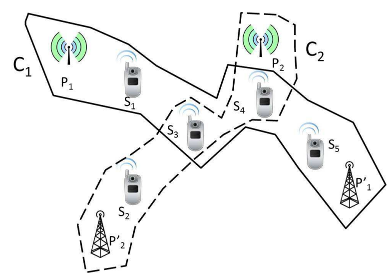

Figure 5.2: Overlapping coalition example

- **OCF Game**: An OCF game G with player set $\mathcal{N} = \mathcal{P} \cup \mathcal{S}$ is given by a characteristic function $U[0,1]^{m+n} \mapsto \mathbb{R}$, where $U(0^{m+n}) = 0$. The role of the characteristic function of a coalition game specifies the valuation of a coalition [139].

- **Coalition Structure**: An overlapping coalition structure over $\mathcal{N}$, denoted as $\mathcal{CS}$, is defined as a set $\mathcal{CS} = \{C_1, ..., C_m\}$ where m is the number of coalitions, $C_j \subset \mathcal{N}$ and $\cup_{j=1}^{m} C_j = \mathcal{N}$. The coalitions can be overlapping, and thus, the sets may not be disjoint.

- **Resource Vector**: A coalition $C_j \in \mathcal{CS}$ can also be represented as a resource vector $\mathbf{r}^j$. $\mathbf{r}^j$ is the cumulative resource contribution of each player in that coalition. So, $\mathbf{r}^j = [r_1^j \dots r_{(m+n)}^j]$ where r_i^j denotes the fraction of resource that player i allocates to coalition C_j. If $r_i^j = 0$, it means that user i does not belong to coalition C_j.

A coalition structure $\mathcal{CS}$ is also represented with a finite list of vectors $\mathbf{CS} = (\mathbf{r}^1, \ldots, \mathbf{r}^m)$ that satisfies (i) $\mathbf{r}^j \in [0,1]^{m+n}$; and (ii) $\sum_{j=1}^{m} r_i^j \leq 1$ for all $i \in \mathcal{N}$.

- **Payment Vector**: The characteristic function U defines a mapping from the resource vector **r** to payment vector **U** for all coalition $C_j \in \mathcal{CS}$. This is represented as $U(\mathbf{r}, \mathbf{CS}) = \mathbf{U} = [\mathbf{U}^1\ \mathbf{U}^2 \ldots \mathbf{U}^m]$.

  The payment vector of an individual coalition C_j can be represented as $U(C_j, \mathcal{CS}) = U(\mathbf{r}^j, \mathbf{CS}) = \mathbf{U}^j = [U_1^j\ U_2^j \ldots U_{m+n}^j]$.

  The payment of an individual player can be represented as a summation of payment from all the coalitions it has participated in. $U_i(\mathcal{CS}) = \sum_{j=1}^{m} U_i(C_j, \mathcal{CS}) = \sum_{j=1}^{m} u_i^j$.

5.1.3 Formulation

We formulate the cooperative relay selection and scheduling problem as an OCF game, G = $(\mathcal{N}, U)$ where $\mathcal{N} = \mathcal{P} \cup \mathcal{S}$, and $|\mathcal{N}| = m + n$, and U denotes the payoff function that converts a user's contribution in a coalition into its profit. We present the formulation into two steps - routing path construction as coalition formation and transmission scheduling as resource sharing in an OCF game.

5.1.3.1 Routing path Construction as Coalition Formation

In the context of cooperative relay communication, a primary user initiates a search for discovering a routing path to its destination. Nodes are added to the path based on their mutual interest (expressed as payoff function). Finally, a routing path between a primary transmitter (source) and a primary receiver (destination) is established that includes one or more secondary users as intermediate relay nodes (to receive packets from the previous one and forward packets to the next one in the path.)

The construction of routing path can be mapped to the coalition formation in an OCF game. Each primary transmitter $i \in \mathcal{P}$ starts the process, secondary users join the coalition if it increases their payoff, and a coalition C_i (i.e. a path between the primary transmitter and receiver) is formed. Thus, C_i represents the routing path starting with primary transmitter i, followed by one or more secondary transmitters from the set $\mathcal{N}$ based on their mutual needs - constructing a multi-hop routing path and creating transmission opportunities respectively. The payoff of a coalition is defined as the summation of the payoff of all its members earned from joining the coalition.

A coalition structure $\mathcal{CS}$ represents the set of m such coalitions (i.e. routing path of m primary users) where any of the secondary transmitters may participate in more than one coalition. So, $\mathcal{CS} = \{C_1, \ldots, C_m\}$. For example, there are two coalitions formed in Fig. 5.2. The first primary transmitter-receiver pair (p_1, p_1') forms a coalition C_1 with four secondary users s_1, s_3, s_4, and s_5. This implies the packets from primary user p_1 follows this path $p_1 \rightarrow s_1 \rightarrow s_3 \rightarrow s_4 \rightarrow s_5 \rightarrow p_1'$. The second primary transmitter-receiver pair (p_2, p_2') forms another coalition C_2 with three secondary users s_2, s_3, and s_4. There are two secondary users (s_3, s_4) overlapping in both the coalitions.

5.1.3.2 Scheduling as Resource Sharing

The packet transmission scheduling can be mapped to resource sharing in the coalition game. The resource contribution of individual user $i \in \mathcal{N}$ is denoted as r_i and the resource contribution to a coalition C_j is denoted as r_i^j and $r_i = \sum_{j=1}^{m} r_i^j$. The resource vector of a coalition C_j is denoted as $\mathbf{r}^j = [r_1^j \ldots r_{(m+n)}^j]$ where the first m entries represent resource contribution from primary users and the next n entries represent contribution from secondary users. Considering T time slots, each user has maximum T time slots to share it with other users in its coalition or schedule its own transmission.

A primary user only contributes to its own coalition and the resource contribution by a primary user $i \in \mathcal{P}$ is the total amount of time secondary users in its coalition transmit their own packets in its sub-channels.

$$r_i = r_i^i = \frac{1}{T}\sum_{t=1}^{T}\sum_{j\in C_i}\theta^i_{j\to j'}(t) \le 1, \forall\, i \in \mathcal{P} \tag{5.1}$$

Here, $\theta^j_{x\to y}(t)$ is an indicator function whose value can be $\{0,1\}$. $\theta^j_{x\to y}(t) = 1$ implies that user x sends packet to user y at time t in coalition C_j where $x, y \in \mathcal{N}$, 0 means no transmission. If $y = x'$, user x sends packet directly to its corresponding destination.

A secondary user contributes its resource to more than one coalitions. The resource contribution by a secondary user $i \in \mathcal{S}$ to a coalition C_j is the amount of time it engages in receiving and relaying packets of the primary user $j \in \mathcal{P}$ of that coalition.

$$r_i^j = \frac{1}{T}\sum_{t=1}^{T}\left[\sum_{k\in C_j}\theta^j_{i\to k}(t) + \sum_{q\in C_j}\theta^j_{q\to i}(t)\right], \forall\, i \in \mathcal{S} \tag{5.2}$$

For any user $i \in \mathcal{N}$ by definition, $r_i \le 1$.

In order to schedule users' transmission without interference, additional constraints must be satisfied. In general, any user $x \in \mathcal{N}$ cannot send to more than one user $y \in \mathcal{N}$. Also, it cannot receive from more than one user $y \in \mathcal{N}$.

$$\sum_{j=1}^{m}\sum_{y\in C_j}\theta^j_{x\to y}(t) \le 1, (x \in \mathcal{N}) \tag{5.3}$$

$$\sum_{j=1}^{m}\sum_{y\in C_j}\theta^j_{y\to x}(t) \le 1, (x \in \mathcal{N}) \tag{5.4}$$

Also, a user $x \in \mathcal{N}$ cannot send and receive packet simultaneously at the same time slot t.

$$\sum_{j=1}^{m} \left[\sum_{y \in C_j} \theta^{j}_{x \to y}(t) + \sum_{y \in C_j} \theta^{j}_{y \to x}(t) \right] \leq 1 \tag{5.5}$$

Furthermore, all the scheduled transmissions must be interference free. So, while a user in a coalition is receiving packet from another user in the same coalition, all other interfering users to that receiver in the same coalition cannot send any packet. Otherwise, the receiver will experience interference.

$$\theta^{j}_{x \to y}(t) + \sum_{z \in I_y} \sum_{q \in V_z} \theta^{j}_{z \to q}(t) \leq 1 \tag{5.6}$$

Here, I_y represents the set of nodes interfering to users y's transmission while V_z represents the set of nodes within transmission range of user z. Note that, a user's interference range is usually longer than its transmission range.

5.1.4 Payoff of a Primary User

The payoff of a primary user $i \in \mathcal{P}$ from a coalition C_i, $U^{p}_{i}(C_i, \mathcal{CS})$ is defined in terms of data rate profit $\Re_i(C_i)$ and path delay profit $\mathbb{D}_i(C_i)$ in Eqn. 5.7

$$U^{p}_{i}(C_i, \mathcal{CS}) = \alpha \Re_i(C_i) + (1 - \alpha)\mathbb{D}_i(C_i) \tag{5.7}$$

Here, the parameter α defines the characteristics of a primary user based on his preference between throughput and delay in payoff calculation. For example, $\alpha = 1$ means that a primary user's only focus is to maximize throughput while $\alpha = 0$ means that the user is delay sensitive and aims to minimize delay.

The data rate profit $\Re_i(C_i)$ of a primary user i in coalition C_i is calculated comparing cooperative transmission rate[3] $R_i(C_i)$ with $R_i(\{i\})$. $R_i(\{i\})$ denotes the effective transmission rate that the primary player i can achieve from direct transmission i.e. coalition has only one player. We can calculate $R_i(\{i\})$ directly from Eqn. 5.10.

$$\Re_i(C_i) = \frac{R_i(C_i) - R_i(\{i\})}{R_i(\{i\})} \tag{5.8}$$

Similarly, the delay profit $\mathbb{D}_i(C_i)$ of a primary user i in coalition C_i is calculated as a ratio of delay improvement compared to delay from direct transmission.

$$\mathbb{D}_i(C_i) = \frac{\Upsilon_i(\{i\}) - \Upsilon_i(C_i)}{\Upsilon_i(\{i\})} \tag{5.9}$$

We start our analysis with the calculation of data rate. We assume that the channel experiences white Gaussian noise, and the signal quality degrades due to path loss. The effective transmission rate R_{ij} from node i to node j is calculated following Eqn. 5.10 [44]. Thus, we calculate transmission rate between any link between two consecutive members in a coalition.

$$R_{ij} = B \log_2 \left(1 + \frac{E_{tx} G_t G_r (d_0/d)^\gamma}{N_0 B}\right) \tag{5.10}$$

where E_{tx}, G_t, G_r, and N_0 denote the transmission power of node i, transmitter gain, receiver gain, and power spectral density of noise respectively. Also, d is the distance between node i and node j, d_0 is the reference distance for the antenna far-field, and γ is the path loss exponent. The overall packet transmission rate of a primary user from a coalition is denoted as the minimum data

[3] $R_i(C_i)$ and $R_i(\mathcal{CS})$ are same for a primary user i

rate of any of the links in that coalition (since nodes have to receive the packet first and then send it to the next one, the effective transmission rate is factored by $\frac{1}{2}$). Consequently, the effective transmission rate of a primary user i in a coalition C_i is defined as,

$$R_i(C_i) = \min\left(R_i(\{i\}), \frac{1}{2}\min\left(\forall_{j,j+1 \in C_i}\left(R_{j,j+1}\left(C_i\right)\right)\right)\right) \tag{5.11}$$

Here, $R_{j,j+1}\left(C_i\right)$ denotes the data rate between two consecutive members in the coalition C_i.

Next, we present the delay analysis. According to [14], the delay in direct transmission ($\Upsilon_i(\{i\})$) is calculated considering $M/G/1$ queueing system by the following equation:

$$\Upsilon_i(\{i\}) = \frac{\lambda_i}{2\mu_i(\mu_i - \lambda_i)} + \frac{1}{\mu_i} \tag{5.12}$$

Here, λ_i and μ_i denote the packet arrival rate and packet transmission rate respectively and in steady state, $\lambda_i < \mu_i$.

On the other hand, the delay of the routing path is the summation of each link delay in the coalition.

$$\Upsilon_i(C_i) = \sum_{j,j+1 \in C_i} \Upsilon_{j,j+1}(C_i) \tag{5.13}$$

Here, $\Upsilon_{j,j+1}(C_i)$ denotes the delay between two consecutive secondary users in the coalition C_i.

We perform a queuing analysis to calculate the link delay $\Upsilon_{j,j+1}(C_i)$ between two consecutive users in a coalition C_i.

The queueing system in a secondary user can be modeled as an $M/G/1$ queue with vacation period. According to this queueing model a secondary user $j \in \mathcal{N}$ acts as a relay for c ($c \leq m$) primary users (i.e. coalitions). The user j receives packets from the primary users at rates following Poisson distribution with $\lambda_1, \ldots, \lambda_c$ and offers relay service times $y_{j,1}, \ldots, y_{j,c}$ respectively.

When the relayed transmission is finished, the secondary user starts transmitting its own packets in the vacation time (i.e. the bandwidth time it has earned through cooperation).

A secondary user precalculates required vacation time per cycle based on its transmission requirement. Let us consider that vacation time v is a random variable with distribution $F(v)$ and finite mean $\bar{v}$ and the service times are independent random variables drawn from a common distribution H_y and finite mean $\bar{y}$. Using Cobham's well-known formula for the waiting time of an arbitrary arrival in the higher priority queue, we can calculate the mean delay $\Upsilon_{j,j+1}(C_i)$ experienced by a packet of a primary user i from one secondary user j to another secondary user $j+1$ in the coalition C_i as follows [75]

$$\Upsilon_{j,j+1}(C_i) = \frac{\lambda E(y^2)}{2(1-\lambda\bar{y})} + \frac{E(v^2)}{2\bar{v}} \tag{5.14}$$

Here, $\lambda = \lambda_1 + \ldots + \lambda_c$.

5.1.5 Payoff of a Secondary Player

The payoff value of a secondary player j is defined in terms of the fraction of transmission period earned in return for relay period and power consumption in relaying. A secondary player's payoff is determined by the following equation:

$$U_j^s(C_i, \mathcal{CS}) = \frac{R_a \times \sum_{t=1}^{T} \theta^i_{j\to j'}(t)}{T \times \sum\limits_{k\in\mathcal{P}} w_{j,k} \times r_j^k} \tag{5.15}$$

Here, $\theta^i_{j\to j'}(t)$ denotes that user j transmits to its destination using sub-channels of primary user i in coalition C_i at time t, R_a denotes the transmission rate between secondary transmitter and secondary receiver which can be calculated using Eqn. 5.10, r_j^k denotes the packet relay time of primary user k, and $w_{j,k}$ denotes the transmission power spent in relaying traffic from primary user k per time unit. As it can be seen from the payoff function, a secondary user can increase its payoff either by asking for more bandwidth time from the primary user or spending less power in relaying primary traffic.

5.1.6 Problem Statement

Given the set of primary players $\mathcal{P}$ and secondary players $\mathcal{S}$ and their corresponding resources, the goal is to allocate resources into m coalitions such that individual payoff is maximized while satisfying the routing and scheduling constraints mentioned in Eqns. (5.1) - (5.6). Mathematically, we define the problem statement as follows:

$$\max_{\mathbf{r}} U_i^p, U_j^s \ \ \forall_{i \in \mathcal{P}, j \in \mathcal{S}} \tag{5.16}$$

such that Eqns. (5.1) - (5.6) are satisfied

The resulting profit maximization problem can be solved to find stable solutions using linear programming. However, this problem is NP-hard. The proof of the complexity relies on a reduction from a well known NP-hard problem e.g. multiple knapsack problem (MKP) [16]. Since it is not practical to coordinate between all users in a large network, we develop a distributed coalition formation algorithm in the next section.

5.2 Cooperative Routing Protocol

In this section, we present *mcRoute*, a distributed cooperative routing protocol. The routing protocol depends on message exchange between users to construct stable and profitable routing paths.

There are three types of message exchanged between users. The first message is $coalition\_join$ request $C_i(i)$ that denotes a coalition request initiated by primary user i. The second message is $coalition\_reply$ request $C_i(j)$ which is a response from secondary user j to the initiating primary user i. The third message is $coalition\_approval$, C_i which confirms secondary users in the selected routing path of primary user i.

Next, we explain the routing protocol from the perspective of both a primary and a secondary user. The primary user i initiates a $coalition\_join$ request $C_i(i)$ to search for a more profitable path than the direct transmission. Accordingly, it includes basic parameters e.g. direct transmission rate, traffic rate, and direct end to end delay in the message. The message is then sent to each user $j \in V_i$ where V_i denotes the set of secondary users within its transmission range. A primary user moves to a wait state to receive coalition offer from its neighbors. If no reply is received within a predefined time, the PU user continues transmitting directly to the destination. Otherwise, the primary user embraces the coalition offer that maximizes its payoff.

$$j^* = \arg\max_j U_i^p(C_i(j)) \tag{5.17}$$

Finally, the primary user sends a $coaltion\_approval$ C_i towards the selected secondary user j^*. The entire process of routing path construction continues until the parameter δ_d reduces below a predefined threshold ϵ (the update process of δ_d is discussed later). The protocol is summarized in Table 5.1.

An SU j receiving a $coalition\_join$ request $C_i(i)$ first checks whether the destination is reachable or not. Otherwise, it either drops the request from i (if it is not interested) or forwards it to its neighbor $k \in V_j$ and moves to wait state. Since a secondary user's success depends on other users on routing path, it first selects the best proposal from the coalition offers it has re-

Table 5.1: Algorithm $mcRoute$: for a PU user i

$C_i = \{i\}$, $U_i^p(C_i) = 0$
initiate a $coalition\_join$ request $C_i(i) = \{i\}$
repeat
    send $C_i(i)$ to each node $j \in V_i$
    receive $coalition\_reply$ $C_i(j)$ from each node $j \in V_i$
    select $j^* = \arg\max_j U_i^p(C_i(j))$
    if $U_i^p(C_i) < U_i^p(C_i(j^*))$ **then**
        select $C_i = C_i(j^*)$
        send the $coalition\_approval$ C_i to user j^*
    end if
    update δ_d, add j^* as next hop, and update the routing table
    advance round d
until $\delta_d \geq \epsilon$

ceived from its neighbors. It combines its own cooperation terms to the selected offer considering all other available requests from other primary users. We explain the parameter selection mechanism in Sec. 5.2.2. The combined offer is then sent in the upstream direction as a coalition offer $coalition\_reply$, $C_i(j)$ from user j. When secondary user j receives $coalition\_approval$ C_i, it updates its routing table, schedules its packet for transmission, and forwards the packet in the downstream direction. The protocol is summarized in Table 5.2.

We will further discuss the message format and the selection and modification process of coalition offer.

5.2.1 Message Format

A coalition message contains some important parameters to represent the coalition offer. The parameters can be classified into three main categories. The basic category contains the initiator id (*SrcID*), the destination id (*DstID*), packet type (*pktType*), and packet id (*Round*). The second category represents the primary user's information e.g. its direct data rate (R_0), end-to-end delay (D_0), and the traffic rate (λ_0). The third category contains the cooperation offer in the form that

Table 5.2: Algorithm $mcRoute$: for SU user j

repeat
  for each $coalition\_join$ request $C_i(i)$ **do**
    initialize $C_i(j) = \{j\}$
    if destination is not reachable **then**
      forward the packet $C_i(i)$ to each node $k \in V_j$
      receive $coalition\_reply$ packet $C_i(j)$ from each node $k \in V_j$
      select $j^* = \arg\max_k U_i^p(C_i(k))$
      combine $C_i(j) = C_i(j*) \cup C_i(j)$
    end if
    calculate $U_j^s(C_i(j)), U_i^p(C_i(j))$ with its own offer
    send $coalition\_reply$ packet $C_i(j)$ in upstream and move to wait state
    if $coaltion\_approval$ C_i is received **then**
      forward the $coalition\_approval$ packet C_i in downstream
      update routing table
    end if
  end for
until no more $coalition\_join$ packet has been received

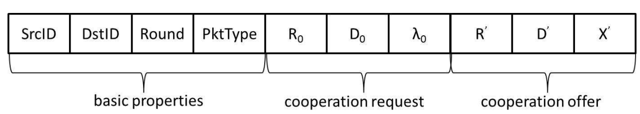

Figure 5.3: Message format

is understandable to the primary user. The fields in the coalition offer category are as follows: R': the cooperative data transmission rate through secondary path, D': the cooperative delay through secondary path, and X': the cumulative transmission time demanded from the primary transmitter.

5.2.2 Coalition Offer and Payoff Calculation

When a secondary user $j \in \mathcal{S}$ receives coalition proposals from its neighbors in response to a $coalition\_join$ $C_i(i)$, it selects the cooperation offer that provides the most profitable path for the initiating primary user $i \in \mathcal{P}$. Let us assume that the offer, $C_i(k)$ from user $k \in V_j$ is selected. The user j next selects two parameters as its cooperation terms to add into the chosen cooperation offer $C_i(k)$. The first parameter denotes the cycle time it allocates for relaying the corresponding primary user and the second parameter denotes the bandwidth time it requests from the coalition of primary user i.

In order to select these two parameters, the user checks the offers it made to other primary users. In the first round, it selects parameters for each coalition request proportional to the power consumption in relaying the corresponding primary traffic. Based on its success at previous rounds, a secondary user either (i) reduces its demand for bandwidth time while relay time remains unchanged, (ii) requests more bandwidth time while relay time is unchanged. (iii) approves more relay time to the primary user with the request of the same unchanged transmission time, or (iv) reduces relay time with unchanged transmission time.

Finally, the cooperation offer of a secondary user is converted to a form that is understandable to a primary user that expects the offer in the form of cooperative data rate and end-to-end delay (see Fig. 5.3). Accordingly, an SU j calculates the primary user i's payoff as follows using Eqn. 5.11.

$$R_i(C_i(j)) = \min(R_{j,k}, R_i(C_i(k)))$$

The intermediate path delay (Eqn. 5.14) introduced by a secondary user j in a coalition S_i is as follows:

$$D_j(C_i) = \frac{\sum_{t=1}^{T} \sum_{x=1}^{m} \left(\theta_{j \to x}^{x}(t) + \theta_{x \to j}^{x}(t) \right) \times len}{\sum_{t=1}^{T} \theta_{j \to i}^{i}(t) \times R(C_i)}$$

$$D_i(C_i(j)) = D_i(C_i(k)) + D_j(C_i)$$

Here, len denotes the length of the packet. Also, the payoff of a secondary user j is calculated based on the resource sharing with the primary users using Eqn. 5.15.

5.2.3 Stability of Coalitions

In order to ensure stable coalitions, we control the search for coalition by two parameters. A primary user maintains a convergence parameter, δ_d. The value of this parameter determines whether the user will initiate another round of route discovery or not. The initial value of the parameter is set to 1. After each round d, the user calculates the change in payoff over total rounds and if the value drops lower than the threshold (ϵ), the user stops the route discovery process. The value of ϵ is a system defined parameter. The parameter δ_d at round d is calculated as follows:

$$\delta_d = \begin{cases} |\Delta U_d|/d & \text{if } d > 1 \\ 1 & \text{otherwise} \end{cases} \tag{5.18}$$

where ΔU_d denotes the difference between user i's payoff at round d and at round $d-1$. As the number of round increases, δ_d decreases to a value below the threshold and primary user becomes stable with its coalition. Also, each secondary user cannot request transmission time lower than δ_s. When a secondary user's request with minimum transmission time to a primary user fails, it stops participating in that coalition. Thus, the usage of δ_d and δ_s controls the convergence speed, and the routing paths become stable.

When users are on a stable routing path, the channel states may change that may reduce the payoff valuation of one or more users on the path. To avoid continuing on a less profitable path, all participants continuously monitor the payoff value. If the payoff drops significantly from the agreed one, the primary user may switch to direct transmission and initiate the search for the routing path while a secondary user may remove itself from the path and search for a new opportunity.

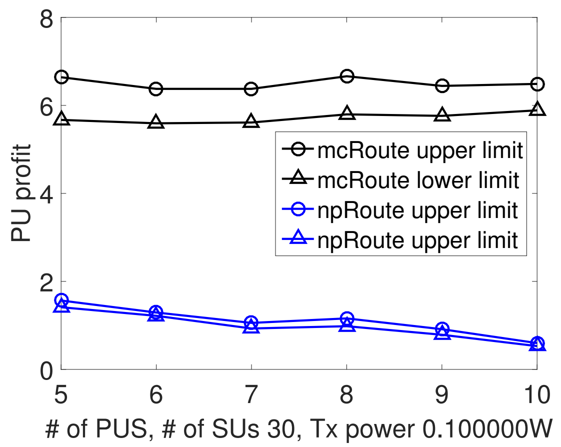

(a) average PU profit

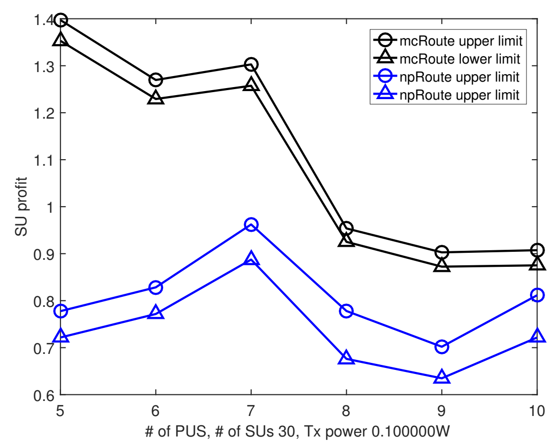

(b) average SU profit

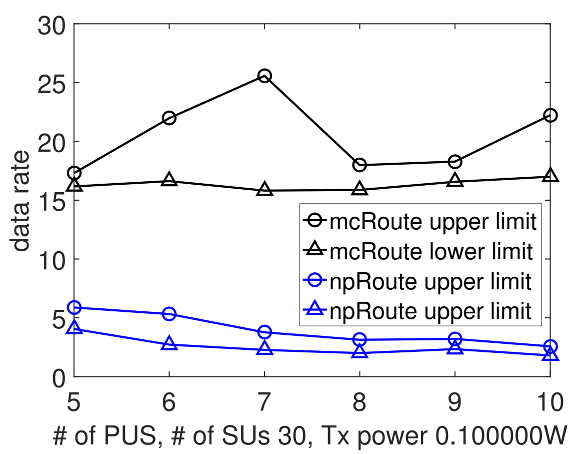

(c) average data rate

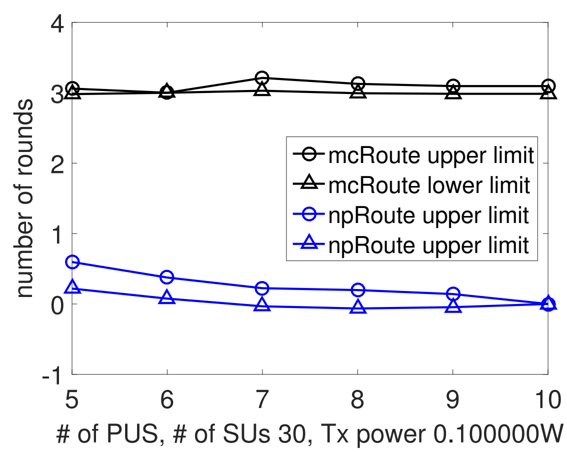

(d) number of rounds

Figure 5.4: Comparison between mcRoute and npRoute [79]

5.3 Performance Evaluation

In this section, we analyze the performance of coalition based multi-hop cooperative routing algorithm. We simulate a cognitive radio network located in an area of $5000\text{m} \times 5000\text{m}$. We deploy different number of primary source-destination pairs (5 to 10). Each primary source node is assigned a channel with 20KHz bandwidth. The transmission cycle time is normalized to one unit and a secondary user requires $1/10$th of its cycle time is for supporting its minimum rate requirement. In order to evaluate the impact of cooperation in the routing path selection, we vary the

Table 5.3: Simulation parameters

Parameters	Value
Bandwidth (B)	$20KHz$
Transmitter and Receiver Gain (G_t, G_r)	1
Power spectral density of Noise (N_0)	10^{-10} W/Hz
Transmission Power (E_{tx})	100mW
Path loss exponent (γ)	2
Base distance (d_0)	$10m$ [44]
Threshold (ϵ)	0.001
Packet length (len)	1024bits

number of primary users, secondary users, and transmission power. The simulation parameters are listed in Table 5.3.

5.3.1 Topology

The primary source and destination nodes are randomly and uniformly deployed in the network area. Secondary users are also randomly and uniformly deployed in the area so that each user has at least one neighbor. We also made sure that each pair of primary source and destination node is connected, and there exists at least one path between primary source-destination pairs through secondary users. For each set of input configuration, we have generated as many as 50 sample scenarios and the statistics are recorded for each set. Finally, for statistical confidence, we take an average of results of all sets to represent the outcome of each scenario.

5.3.2 Performance Comparison with Prior Work

To compare with an existing algorithm, we implement a modified version of the algorithm proposed in [79]. We have chosen [79] over [127] since the latter one assumes fixed routing path. Unlike [79], in the modified version, a secondary user may receive simultaneous coalition requests from more than one primary user. A secondary user processes multiple concurrent cooperation requests, selects one of them randomly, and participates in routing path of only one primary user at a time. We refer to this algorithm as 'non-overlapping routing' in short 'npRoute'.

We calculate PU and SU profit (with 95% confidence interval) with the varying number of primary users while the transmission power is set to 0.1W and number of secondary users is set to 30. Fig. 5.4a and 5.4b show that the proposed cooperation algorithm achieves higher PU and SU payoff than those of npRoute. In mcRoute, PU profit stays almost constant with the increase in the number of PUs. This is because each primary user on average cooperates with same number of secondary users and increasing number of primary users does not increase the average PU profit. On the other hand, SU profit decreases due to increasing competition among them. We also show in Fig. 5.4c that the cooperative data rate achieved through mcRoute is higher than npRoute. Also, we investigate average number of rounds [119] that reflects the stability and convergence speed. Fig. 5.4d shows that npRoute converges to a local maxima when it handles multiple cooperation offers simultaneously. On the other hand, mcRoute goes through few more rounds to achieve higher data rate and higher PU and SU payoff.

Similarly, we also vary the number of secondary users and calculate PU and SU profit (with 95% confidence interval). mcRoute creates more cooperation opportunity for secondary users than npRoute and increases the number of secondary users involved in cooperation and their profits as well.

To better understand the multi-hop cooperation behavior in cognitive networks, we further investigate the following properties of the proposed mechanism in addition to average to PU and SU profit. First, average length of the routing path (i.e. number of relays on each path of PU); it also indicates the average participation of secondary users in each routing path. Second, number of overlapping secondary users (i.e. number of SUs involved in more than one routing paths of PUs in comparison to total participating SUs).

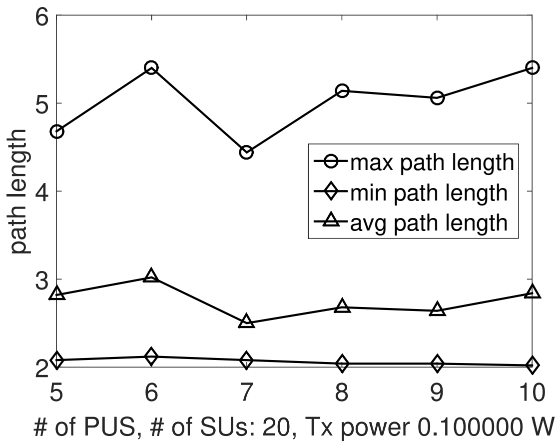

(a) path length vs. number of PUs

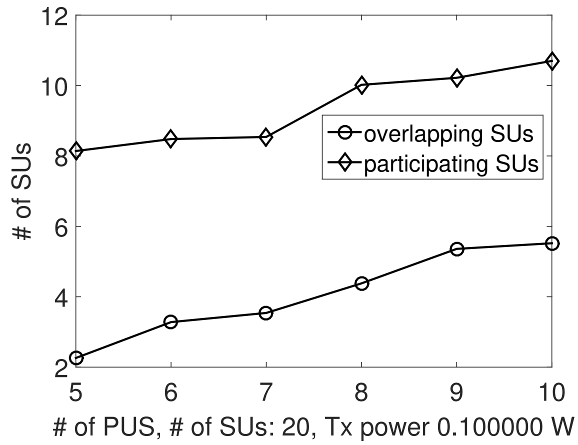

(b) number of overlapping SUs vs. number of PUs

Figure 5.5: Results with varying PUs

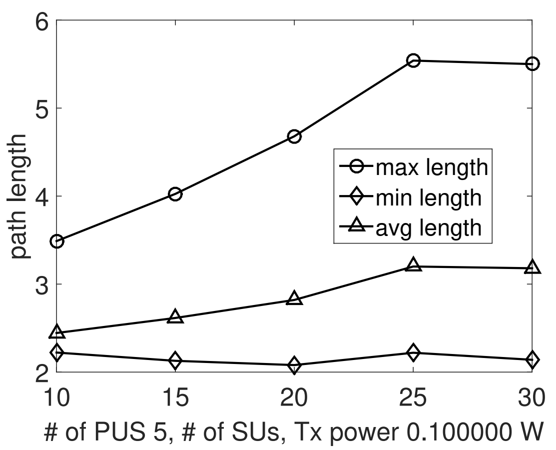

(a) path length vs. number of SUs

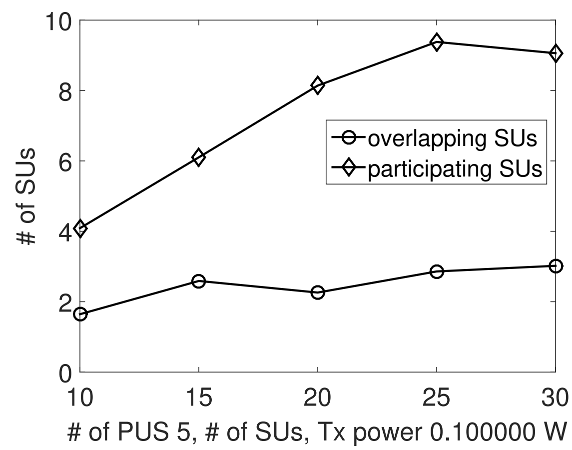

(b) number of overlapping SUs vs. number of SUs

Figure 5.6: Results with varying SUs

5.3.3 Results with Varying Number of PUs

We first vary the number of primary users from 5 to 10 pairs while the number of secondary users is fixed to 20. Figure 5.5 shows the routing path length, and the number of the overlapping nodes participating in the cooperation. Although the length of the routing path does not vary with the number of primary users (Fig. 5.5a), the number of the participating and overlapping secondary users increases almost linearly (Fig. 5.5b).

5.3.4 Results with Varying Number of SUs

Next, we perform the same set of experiments but with varying number of SUs from 10 to 30. The number of primary users is fixed to 5 pairs. All other parameters are kept the same. The results are depicted in Fig. 5.6. The path length increases with an increase in the number of secondary users (Fig. 5.6a). As expected, the number of cooperating SUs increases with varying number of SUs (Fig. 5.6b). We also evaluate the impact of transmission power on cooperation by varying the transmission power from $0.1W$ to $0.5W$.

5.3.5 Results with Algorithm Parameters

We investigate the impact of changing two key parameters in relay selection and coalition formation. The first parameter α denotes the tradeoff between throughput and delay in the payoff of a primary user in Eqn. 5.7. We vary the value of α between 0 and 1 and record the change in user payoff, path length, and number of cooperating secondary users. The result is shown in Fig. 5.7. As the value of α reaches to 1, the primary user is more interested in increasing data rate and achievable throughput and ignoring the delay cost introduced by relaying secondary users. Therefore, number of participating secondary nodes (Fig. 5.7a) and path length (Fig. 5.7b) increases with the increase in value of α. This also increases PU profit almost linearly and opens more opportunity for secondary users to increase their payoff (Fig. 5.7c). Next, we select ϵ to investigate the stability of the algorithm. Fig. 5.7d shows that more rounds are needed to reach stable coalitions with smaller values of ϵ. Thus, these two parameters control the cooperation opportunity and convergence speed of the routing paths.

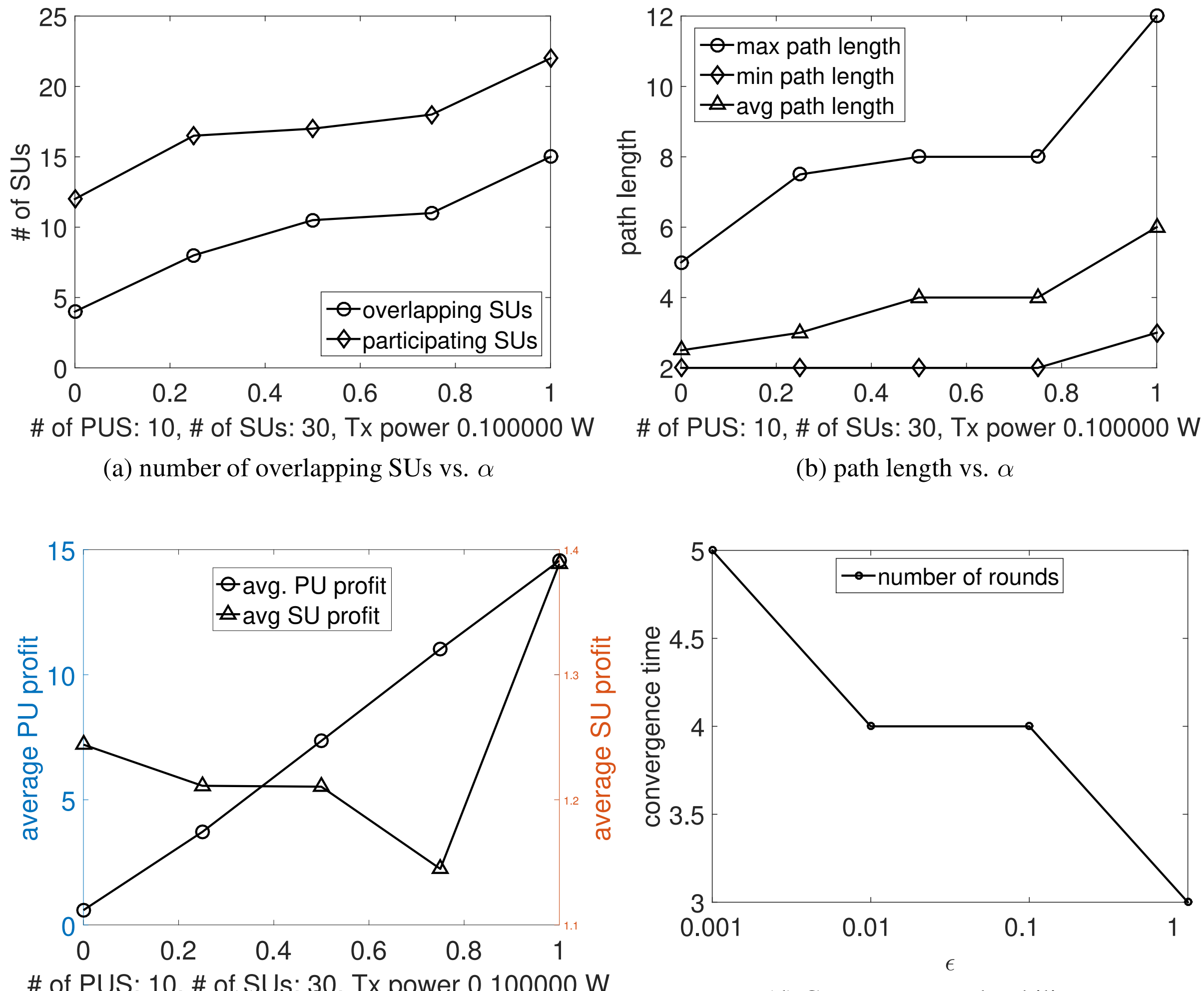

(a) number of overlapping SUs vs. α

(b) path length vs. α

(c) profit vs. α

(d) Convergence and stability

Figure 5.7: Results with varying algorithm parameters

5.4 Summary

In this chapter, we formulate the cooperative routing path formation problem as an overlapping coalition game where secondary users actively participate in multiple routing paths. A PU's payoff is defined as a combination of data rate profit and path delay. An SU's payoff is defined as bit per energy spent in relaying. Based on the payoff functions defined in an OCF game, we devise a distributed multi-hop routing and scheduling protocol. Both primary and secondary users go through rounds of exchanging messages and negotiating on cooperation terms to build stable routing paths. We compare our algorithm with an existing work and the simulation results show that our approach outperforms the existing work in terms of PU and SU profit. Our algorithm provides stable routing paths that is also verified through simulation. We have considered single path routing between each primary source destination pair. We will investigate the impact of cooperative behavior in the case of multi-path routing and possible cooperation strategy with secondary users in future work.

Chapter 6

Truthful Online Spectrum Auctions

In previous chapters, we have discussed spectrum sharing techniques under sensing and relay based collaboration models. In the sensing based collaboration model, secondary users share their sensing reports to take a joint decision without primary users' participation. The success in spectrum utilization depends on the accuracy of PU detection techniques and their collaborative decision. In the relay based collaboration model, PUs actively coordinate with SUs to improve their signal performance with cooperative diversity. When the PUs are idle with no pending transmission requests they have no incentive in sharing their unused spectrum with spectrum hungry secondary users. In this chapter, we explore auction based collaboration models[1] that have recently been investigated as a means to encourage these users into sharing their unused spectrum and earning revenue in return. Recent initiatives from FCC also indicate the prospect of auction based collaboration model. According to this model, PUs can sell their unused licensed spectrum units in temporal, spectral, and/or spatial domains for different durations while the buyers like small wireless networks, individual infrastructure networks, or home networks can bid for the share of the spectrum [22]. These

[1] The work presented in this chapter has been published in three research articles:

(i) Chowdhury Sayeed Hyder, Thomas D. Jeitschko, and Li Xiao. Bid and Time Truthful Online Spectrum Auctions with Dynamic User Arrival and Dynamic Spectrum Supply, in the 25th International Conference on Computer Communication and Networks, Waikoloa, Hawaii, USA, Aug 1 - 3, 2016.

(ii) Chowdhury Sayeed Hyder, Thomas D. Jeitschko, and Li Xiao. Truthful Online Double Auctions with Real-time Stochastic Arrival of Demand and Supply, in the 25th International Conference on Computer Comminca-tion and Networks, Waikoloa, Hawaii, USA, Aug 1 - 3, 2016.

(iii) Chowdhury Sayeed Hyder, Thomas D. Jeitschko, and Li Xiao. Towards a truthful online spectrum auction with dynamic demand and supply. in Military Communications Conference (MILCOM), pp 413 – 418, Tampa, Florida, USA, October 26 - 28, 2015.

users' spectrum demand may vary depending on the application type, user traffic, and user mobility. For example, a user with delay-tolerant applications can defer its transmission whereas a user with delay-sensitive applications may require immediate transmission.

Auction based collaboration models have been studied in the context of spectrum (re-)allocation, with particular attention being paid to the resulting efficiency of spectrum use (both within and across locations, because for a given geographical location, non-interfering users can be allocated the same spectrum to increase both coverage and capacity [114]), the revenue or profit generated in the process of (re-)allocation [31, 129], demand satisfaction [135, 143], and other performance metrics. Similar to these single auction mechanisms, double auction mechanisms have been designed with auxiliary motivations of improving efficiency, increasing revenue, etc. [22,31,40,143]. There are additional practical concerns: for instance, by exploiting the inherent characteristics of wireless networks, a bidder may overhear or intercept the bidding information of competitors and gain an advantage [138]; and, thus, considerable attention has been given to assuring that the auction mechanism induces participants to truthfully report their needs and requirements, rather than have them misrepresent their underlying supply or demand considerations in order to "game" the system and thereby increase their own benefits at the expense of others [142].

This auction based research constitutes a significant advancement in the potential for effective spectrum management. However, most work focuses on static (or off-line) settings with known number of bidders and supplies, thereby suppressing the inherent dynamic aspects of spectrum availability and spectrum needs discussed at the outset. Also, existing work considers users with no transmission deadlines and therefore, the proposed auction mechanisms are only bid truthful. Unfortunately, given the transmission flexibility the users may manipulate the outcome of these auctions by tweaking their deadlines even in the case of a single unit demand per user (explained with examples in Sec. 6.1.4). An exception to this is some recent work (e.g., TRADE [141], Topaz [30], and Tofu [125]) that considers dynamic arrival of bidders and addresses online single auction mechanisms based on the ideas presented in [45]. The bidders in these auctions place their bids to compete for a fixed number of spectrum units. However, the supply uncertainty i.e., the dynamics in spectrum availability has not been analyzed in these studies. On the other hand, the study in [114] and TORA [63] analyze the single auction mechanism considering the dynamics in spectrum availability while the number of bidders is fixed throughout the auction. TODA [118] presents a double auction mechanism considering stochastic arrival of users without considering spectrum reusability which is one of the distinct features of spectrum auction. A more recent paper, LOTUS [20] considers a double auction model consisting of a fixed number of users with dynamic demand and fixed number of spectrum. Although this work considers a double auction with dynamic user demand, the bidders have no transmission deadlines and the number of sellers is fixed. As a result, LOTUS fails to satisfy the truthfulness property when it is applied in an online setting since users may gain benefits by lying about their deadlines.

In contrast, we investigate auction based collaboration models in which both spectrum availability and demand are stochastic throughout the auctions, and users' urgency for transmission is also random. We first analyze this dynamic setting from the single auction perspective, discuss its challenges, and develop the truthful mechanism. We further extend our analysis to an online double auction setting where both bidders and sellers stochastically join the auction with different deadlines and valuations. An online double auction better represents the secondary spectrum market than the single auction since double auctions accommodate diversity in sellers' reserve prices and offer flexibility to the auction design. In presence of such diversity, an auctioneer has to make online decisions on spectrum allocation and pricing without the knowledge of future participants and their demand and supply. This online feature makes the spectrum auction easily vulnerable to bid and deadline manipulation. A bidder or seller may gain benefit over others by misreporting its arrival, deadline, or its valuation. Therefore, the mechanism must behold the truthfulness property. Additionally, the mechanism must support the allocation of same spectrum unit to non-interfering bidders to improve the spectrum utilization rate. Our goal here is thus to explore such dynamic settings and design online mechanisms for both single and double auctions that conform to these requirements. Summary of our contributions in online auction settings is:

- We study the spectrum allocation problem to secondary users in an auction setting where idle channels arrive stochastically and the total channel supply is unknown; and bidders with random lifetimes (transmission deadline) arrive at the auction stochastically with the total number of bidders being unknown. We identify the challenges associated with the dynamic auction model and show the vulnerabilities of existing research in such settings.

- We present our analysis of this dynamic setting in three steps. In the first step, all bidders (and sellers) have the same valuations. In the second step, we relax this restriction and consider diversity in bidders' valuations. In the third step, we also consider the sellers with different valuations. Our analysis of these auction settings is based on an endogenous priority value function that determines the priority of a bidder at each period given its value and urgency for transmission if the auctioneer has distribution knowledge. We prove that our proposed mechanism adheres to truthfulness and individual rationality.

- Consequently, we present three auction algorithms. The first algorithm is derived based on the priority function to develop a distribution aware truthful single auction mechanism. The second algorithm is also derived based on the priority function and develop a distribution aware truthful double auction mechanism. Finally, we present a distribution unaware mechanism for a truthful double auction. We introduce a bid-independent 'debt factor' that adjusts the payment amount of a winner depending on the number of users interfering with it over

Figure 6.1: Auction with dynamic bidder and supply

its lifetime. The users go through a candidate screening phase followed by a debt calculation phase, and finally winners are selected adhering to pricing rules in the algorithm.

- Finally, we present simulation results to analyze the performance of these algorithms under different auction settings. We evaluate the efficiency of the proposed mechanisms. We compare the performance of the auction mechanisms with an off-line mechanism and existing work e.g. Topaz [30] in terms of revenue, demand satisfaction, and spectrum utilization.

6.1 Online Dynamic Auctions

In this section, we explain the different components of the auction model and highlight the design challenges to achieve a truthful online auction mechanism.

6.1.1 The Auction Entities

We consider periodic spectrum auctions where users' arrivals and spectrum availability occur only at the beginning of a period (see Fig. 6.1). The period length is fixed across time. The three entities involved in a spectrum auction are primary users as sellers, secondary users as bidders, and an auctioneer.

Sellers: Primary users put their unused spectrum resources for sale at the auction in units of fixed spectrum bandwidth. The sales units are identical; however, each seller has its own valuation of its spectrum units. A spectrum unit remains at the auction for sale for one period only. A sales request of a typical seller j contains its reserve price, commonly referred to as the 'ask' that denotes the minimum price a seller will accept per spectrum unit. We represent a sales request with $\phi_j^p = (a_j)$ where a_j denotes the seller j's ask for its spectrum unit.

A seller's utility is calculated by subtracting its value from the payment it received at the auction. So, seller j's utility $U_j = x_j \times$ (ψ_j^p - v_j) where $x_j \in \{0, 1\}$ denotes whether seller j has won ($x_j = 1$) or not ($x_j = 0$), v_j denotes seller's valuation, and ψ_j^p denotes seller j's payment when it wins in the auction.

Bidders: Secondary users submit their spectrum requirements in the form of bid requests. A bid request of a bidder i is represented as $\phi_i = (g_i, o_i, d_i, b_i)$ where g_i denotes its location information, o_i denotes the time of arrival at the auction, d_i ($\geq o_i$) denotes the transmission deadline, i.e., the maximum time a bidder stays in the auction, and b_i denotes the maximum value a bidder is willing to pay for one spectrum unit. Each bidder has unit demand and has no particular preference over any spectrum unit since all units are identical.

A bidder's lifetime denotes its transmission deadline, and it is expressed in terms of number of periods a bidder can stay in the auction to win a spectrum unit. If the bidder cannot win by its deadline, it exits the auction. The lifetime l_i of a bidder i with arrival time o_i and departure time d_i is expressed as $l_i = d_i - o_i + 1$. Bidder i's utility is $U_i = x_i \times$ ($v_i - \psi_i^s$) where $x_i \in \{0, 1\}$ denotes whether bidder i has won ($x_i = 1$) or not ($x_i = 0$), v_i denotes the bidder's valuation, and ψ_i^s denotes bidder i's payment when it wins the auction.

Auctioneer: The auctioneer is responsible for conducting per-period auctions. At each period, the auctioneer applies an algorithm to select winners and determine their prices. The auctioneer's utility is referred to as the revenue it makes from the auction that is calculated by subtracting the total amount of sellers' payment from the total amount of bidders' payment. The auctioneer's utility, U_A is thus defined as, $U_A = \sum_i \psi_i^s$ - $\sum_j \psi_j^p$ where ψ_i^s represents the payment received from bidder i and ψ_j^p denotes the payment made to seller j.

6.1.2 Auction Properties

Definition 1 *An online auction mechanism is truthful if and only if no bidder i can improve its utility U_i by reporting $b_i' \neq v_i$, or falsely reporting its location $g_i' \neq g_i$, or arrival time $o_i' \neq o_i$, or deadline $d_i' \neq d_i$, or any combination of them and no seller j can improve its utility U_j by reporting its ask $a_j' \neq v_j$ [30].*

Definition 2 *An auction mechanism is "ex ante weakly individual rational" if all agents' expected utility from the mechanism when entering into the auction are non-negative. An online auction mechanism is "ex ante strongly individual rational" if the expected utility of all agents when entering into the auction are positive. An online auction mechanism is "ex post weakly individual rational" if all agents' realized utility from the mechanism is non-negative. An online auction mechanism is "ex post strongly individual rational" if all agents' realized utility from the mechanism is positive. This implies that for any bidder i, $U_i \geq 0$ and for any seller j, $U_j \geq 0$.*

Definition 3 *The budget balance refers to non-negative utility of the auctioneer. An auction mechanism is budget balanced if in each period the total payments received from all buyers is no less than the total amounts paid to all sellers. This implies that the utility of the auctioneer $U_A \geq 0$.*

6.1.3 Design Challenges

An online auction in dynamic environments poses several challenges in designing the mechanism. We present three key design challenges as follows:

(a) Online decision with demand and supply uncertainty: The primary challenge is to take an online decision without knowing the exact number of supply and bidder in future periods. The mechanism must take into consideration the tradeoff between present opportunity and future uncertainty for efficient spectrum allocation.

(b) Spectrum reusability: Unlike traditional auctions, same supply (i.e., spectrum) can be sold to multiple non-interfering bidders in spectrum auctions. This unique property makes it more challenging to achieve a truthful mechanism.

(c) Time and bid based cheating: Due to the online demand and supply nature of the spectrum auction, bidders may report their bids, arrival time, and deadline untruthfully, and gain advantage in the form of increased utilities [30]. The auction mechanism must provide safeguard against any such attempt of cheating from bidders.

6.1.4 Illustration

Before explaining our auction design, we demonstrate how bidders can gain advantage by misreporting their information e.g. their arrival times or deadlines in an online dynamic auction setting. Using illustrative examples, we show that existing static or partially dynamic models cannot ensure truthfulness in such cases. For the sake of simplicity, we have only shown bidders with different valuations in the following examples.

We start with a simple example where each participant reports truthfully. Bidders A, B, and C arrive at time t_1 and bid $\$100$, $\$80$, and $\$50$ respectively. One unit of spectrum also becomes available at the same time. We assume that all three bidders are interfering to each other. The lifetime of bidders is $[t_1, t_4)$, $[t_1, t_2)$, $[t_1, t_5)$ respectively. We apply static auction rules presented in [142] where the highest bidders win and the price is determined by the next highest losing

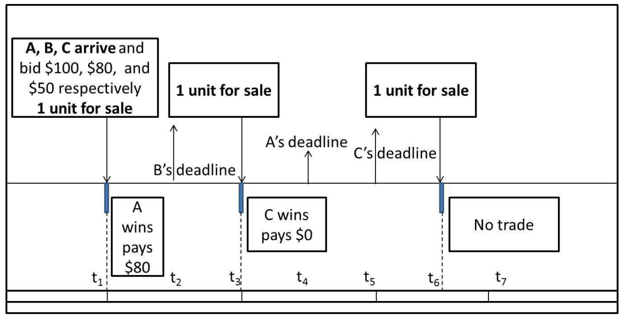

Figure 6.2: Applying static auction rules [142] in dynamic environments

bidder in its neighborhood. Accordingly, bidder A wins, and pays $\$80$. At time t_2, B leaves the auction, and at time t_3, another spectrum unit becomes available. So, C wins next and pays $\$0$. Finally, another spectrum unit arrives at t_6 but remains unsold. So, the auction efficiency becomes $\$150$ ($\$100 + \$50$), revenue becomes $\$80$ ($\$80 + \$0$), bidders' satisfaction ratio becomes $2/3$, and spectrum utilization rate becomes $2/3$. Fig. 6.2 demonstrates the arrival and departure of bidders in the auction and also notes down the decision made by the auctioneer at each period following rules in [142].

Next, we show that a bidder can lie about its arrival time and increase its utility while static rules [142] are applied in an online dynamic environment. In the same previous example, consider bidder A reports its arrival time at t_3 instead of t_1 ($t_3 > t_1$) and thus avoids competition with higher valued bidders. As a result, bidder B wins at t_1, pays $\$50$, and leaves the auction. At time t_3, bidder A wins and pays $\$50$, and thus increases its utility by $\$30$. Again, there is no trade at time t_6. So, the bidder satisfaction ratio and spectrum utilization rate remain unchanged, but efficiency and revenue become $\$180$ ($\$100 + \$80$) and $\$100$ ($\$50 + \$50$). Fig. 6.3 demonstrates this auction scenario. From this instance, it is clear that static auction rules cannot be applied to online auctions in dynamic environments.

Finally, we select a partially dynamic model Topaz [30] and show how a bidder misreports its information and increases its utility in dynamic environments. In the same example, consider

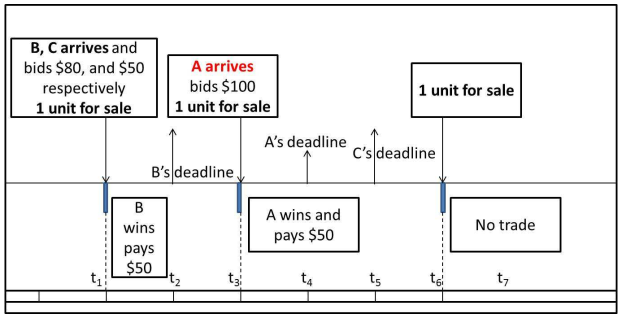

Figure 6.3: Late arrival manipulation by a bidder while applying static auction rules [142]

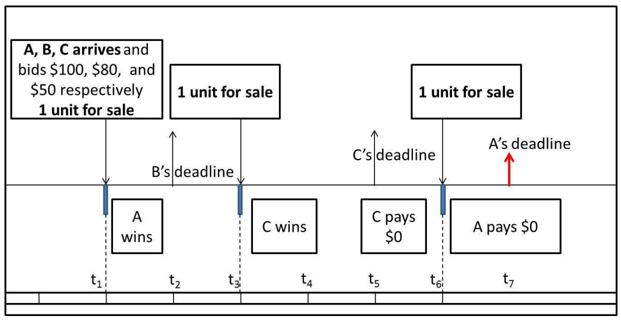

Figure 6.4: Late departure manipulation by a bidder while applying Topaz [30]

that bidder A reports its deadline t_7 instead of t_4 ($t_4 < t_7$). According to Topaz rules, the price is determined at the end of a winner's deadline that is set to the minimum of the critical price at any period over its lifetime. By reporting late deadline, A wins a spectrum unit, pays $\$0$ and increases its utility to $\$100$. The auction revenue reduces to $\$0$ while all other parameters remain unchanged. Fig. 6.4 demonstrates the decision made by the auctioneer at each period following rules in [30]. Therefore, these rules cannot ensure truthfulness.

From the above demonstration, it is clear that existing static or partially dynamic model based mechanisms cannot ensure truthfulness in fully dynamic environments. Next, we discuss the design principles behind our proposed mechanism and explain its components.

6.2 Auction Design

To prevent any attempt of strategic manipulation of information (explained in previous section), an auction mechanism must take into consideration the possible winning opportunity of a bidder in future periods of its lifetime. As explained in [60], bidders in sequential auctions bid their values for the object discounted by the "option value" of future auctions. Similarly in this case, since a bidder has the option of winning a spectrum unit in later periods of its lifetime, a bidder's valuation of a unit at earlier periods is different from its actual valuation. Therefore, an auctioneer must consider a bidder's option value of future periods while determining its value at present period in order to assure truthful reporting of values.

Accordingly, we derive a function, **Prank** that takes into consideration the "option value" at future periods and given a bidder's information, this function determines the rank of a bidder of winning spectrum at any period of its lifetime. We refer to this rank value as its 'priority' and to the **Prank** function as 'priority function'. This priority value also represents the amount the bidder is willing to pay in that period. An auctioneer uses the priority values of bidders instead of its bid during spectrum allocation. This consideration in priority calculation prevents a bidder from misreporting its bid and attempting any kind of time based cheating. We express the priority of a bidder i of value v_i at time t as a function of the following parameters — the set of active bidders $\mathcal{A}(t)$, the auction state from the viewpoint of bidder i, and the set of distribution information $\mathcal{F}$.

$$\beta_{i,t} = \beta_\tau(v_i) = \textbf{Prank}(\mathcal{A}(t), \sigma_i(t), \mathcal{F}) \tag{6.1}$$

$$\text{where } \tau = d_i - t + 1$$

Prank works on the basis of this generic Eqn. 6.2 which states that a bidder's priority value at any period is equal to its true valuation subtracted by the expected payoff from remaining periods of its lifetime.

$$\beta_\tau(v_i) = v_i - \sum_{x=1}^{\tau-1}\left(\prod_{y=x+1}^{\tau} L_y(v_i)\right)\mathbb{E}[\pi_x(v_i)] \tag{6.2}$$

Here, $\beta_\tau(v_i)$ denotes the priority value of a bidder of value v_i with τ remaining periods in its lifetime. Also, $\mathbb{E}[\pi_\tau(v_i)]$ and and $L_\tau(v_i)$ denote bidder i's expected payoff and the losing probability with τ remaining periods of its lifetime l_i. Next, we will derive different components of the priority function.

We assume that the auctioneer knows the distribution of spectrum availability F_m, the distribution of arrival of bidders F_n, and the distribution of bidders' lifetime F_k. Throughout our analysis, we assume that the support of distribution F_k is $\{1, \ldots, \overline{k}\} \subset \mathbb{N}$, and the support of distribution F_m is $\{\underline{m}, \ldots, \overline{m}\} \subset \mathbb{N}$.

6.2.1 Prank - I (Same Valuation Case)

Prank - I assumes that all bidders have the same valuation (i.e. $\forall_{i\in\mathcal{A}(t)}\ v_i = v$ and sellers do not have any set value for their units. So, the priority function can be simplified to

$$\beta_\tau(v) = v - \sum_{x=1}^{\tau-1}\left(\prod_{y=x+1}^{\tau} L_y(v)\right)\mathbb{E}[\pi_x(v)]. \tag{6.3}$$

Here, $\beta_\tau(v)$ denotes the priority value of a bidder of value v with τ remaining periods in its lifetime. Also, $\mathbb{E}[\pi_\tau(v)]$ and and $L_\tau(v)$ denote bidder i's expected payoff and the losing probability with τ remaining periods of its lifetime l_i.

If a bidder i with τ periods to live wins, the winning price is set by the priority rank of any bidder $j \in \mathcal{A}(t)$ with y periods to live where $\overline{k} \leq y \leq \tau$ and $\overline{k}$ denotes the maximum lifetime of any bidder:

$$\mathbb{E}[\pi_\tau(v)] = \sum_{y=\tau}^{\overline{k}+1} \big(v - \beta_y(v)\big) \Pr\big(\psi_i^s = \beta_y(v)\big)\,. \tag{6.4}$$

Here, ψ_i^s is the price bidder i pays when it wins. The probability $\Pr\big(\psi_i^s = \beta_y(v)\big)$ is calculated by considering three possible cases. First, if the total number of bidders is less than the number of available spectrum units, the bidder wins at no cost. Considering m units of spectrum available following distribution F_m, we express the probability of such an event as follows:

$$\Pr\left(\psi_i^s = 0\right) = \Pr\left(m > \sum_{x=1}^{k} n_x\right) = 1 - F_m\left(\sum_{x=1}^{k} n_x\right) + f_m\left(\sum_{x=1}^{k} n_x\right) = 1 - \mathcal{N}_k \tag{6.5}$$

where $\mathcal{N}_y = F_m\left(\sum_{x=1}^{y} n_x\right) - f_m\left(\sum_{x=1}^{y} n_x\right)$.

Second, if the total number of oldest bidders (bidders with only one period to live) are more than the number of supply items, the bidder pays the highest value and earns zero utility. So, the payment is set by the priority rank of a bidder $j \in \mathcal{A}(t)$ with 1 period to live:

$$\Pr\left(\psi_i^s = \beta_1(v)\right) = \Pr\left(m < \sum_{x=1}^{1} n_x\right) = F_m\left(\sum_{x=1}^{1} n_x\right) - f_m\left(\sum_{x=1}^{1} n_x\right) = \mathcal{N}_1. \tag{6.6}$$

Apart from the first two cases, the winning price is set by a bidder $j \in \mathcal{A}(t)$ and is given by:

$$\begin{aligned}\Pr\big(\psi_i^s = \beta_y(v)\big) =& \Pr\left(\sum_{x=1}^{y-1} n_x \le m < \sum_{x=1}^{y} n_x\right)\\ =& \left[F_m\left(\sum_{x=1}^{y} n_x\right) - f_m\left(\sum_{x=1}^{y} n_x\right)\right] - \left[F_m\left(\sum_{x=1}^{y-1} n_x\right) - f_m\left(\sum_{x=1}^{y-1} n_x\right)\right]\\ =& \mathcal{N}_y - \mathcal{N}_{y-1}. \end{aligned} \tag{6.7}$$

Letting $\mathcal{N}_0 = 0$, $\mathcal{N}_{\overline{k}+1} = 1$ and combining all three cases, we rewrite the pdf of the winning price as

$$\Pr\left(\psi_i^s = \beta_y(v)\right) = \mathcal{N}_y - \mathcal{N}_{y-1}. \tag{6.8}$$

Eqn. 6.4 can then be simplified to

$$\begin{aligned}\mathbb{E}[\pi(\tau)] =& \sum_{y=\tau}^{\overline{k}+1} \left(v - \beta_y(v)\right)\left(\mathcal{N}_y - \mathcal{N}_{y-1}\right) \\ =& v\left(1 - \mathcal{N}_{\tau-1}\right) - \sum_{y=\tau}^{\overline{k}+1} \beta_y(v)\mathcal{C}_y;\end{aligned} \tag{6.9}$$

where $\mathcal{C}_y = \mathcal{N}_y - \mathcal{N}_{y-1}$.

Next, we calculate the losing probability of a bidder i with τ periods to live. The losing probability depends on the population of bidders who are older than the bidder (i.e., have fewer periods to live). There are two components. The first component determines the probability that the number of available spectrum units is strictly less than the number of bidders with τ periods to live but greater than the number of bidders with $\tau - 1$ periods to live. The second component deals with the case when there are not enough units to provide all bidders with τ periods to live, and so each of them are equally likely to win or lose the auction.

$$\begin{aligned}\mathcal{L}_\tau(v) =& \Pr\left(\sum_{x=1}^{\tau-1} n_x < m < \sum_{x=1}^{\tau} n_x\right)\left(\frac{\sum_{x=1}^{\tau} n_x - m}{n_\tau}\right) + \Pr\left(m \leq \sum_{x=1}^{\tau-1} n_x\right) \\ =& \Delta_\tau + F_m\left(\sum_{x=1}^{\tau-1} n_x\right).\end{aligned} \tag{6.10}$$

Here, Δ_τ denotes the losing probability of bidder i with τ periods to live while the winning price is set by the priority rank of a bidder j with τ periods to live. Summarizing the above equations, we rewrite Eqn. 6.3 as:

$$\beta_\tau(v) = v - \sum_{y=1}^{\tau-1} \left(\prod_{x=y+1}^{\tau} \mathcal{L}_x(v) \left(v \left(1 - \mathcal{N}_{y-1}\right) - \sum_{x=y}^{k+1} \beta_x(v)\mathcal{C}_x \right) \right). \tag{6.11}$$

Finally, bidder i's priority rank with $1 \leq \tau \leq \overline{k}$ periods to live is expressed as a weighted summation of its priority rank in different periods from the first to the last period:

$$\begin{aligned} \beta_\tau(v) =& v \left[1 - \sum_{y=1}^{\tau-1} \left(\prod_{x=y+1}^{\tau} \mathcal{L}_x(v) \left(1 - \mathcal{N}_{y-1}\right) \right) \right] + \sum_{y=1}^{\tau-1} \left(\sum_{z=1}^{y} \prod_{x=z+1}^{\tau} \mathcal{L}_x(v) \right) \beta_y(v)\mathcal{C}_y \\ &+ \sum_{y=\tau}^{\overline{k}} \left(\sum_{z=1}^{\tau-1} \prod_{x=z+1}^{\tau} \mathcal{L}_x(v) \right) \beta_y(v)\mathcal{C}_y. \end{aligned} \tag{6.12}$$

Solving $\overline{k} - 1$ polynomial equations, we determine the priority ranking bid of a bidder i in all $\overline{k}$ periods.

6.2.2 Prank - II (Single Auction Case)

Prank - II assumes that bidders have different valuations and the auctioneer is aware of the distribution of valuation F_v. A bidder's true valuation of a single spectrum unit is considered to be a discrete random variable from the range $\{\underline{v}, \ldots, \overline{v}\} \subset \mathbb{N}$ following cdf F_v. We express the priority of a bidder i of value v_i at time t as a function of these parameters.

$$\begin{aligned} \beta_{i,t} = \beta_\tau(v_i) = \textbf{Prank-II}(\mathcal{A}(t), \sigma_t^i, F_v, F_m, F_n, F_k) \\ \text{where } \tau = d_i - t + 1 \end{aligned} \tag{6.13}$$

Here $\sigma_t^i(\mathbf{n}, m)$ denotes the auction 'state' concerning the rivals of user i at time t, and it is represented by a $\overline{k}$-dimensional matrix $\mathbf{n} = [n_{\overline{k}}, \ldots, n_1]$ and the number of spectrum units (m)

available in that period. Here, n_x denotes the expected number of bidders with x periods to live within the interference range of user i. Note that, σ_t^i changes depending on user location and the rival bidders' density in that area.

Next, we calculate these two subcomponents in the priority function (see Eqn. 6.2) - expected payoff and losing probability. A bidder's expected payoff at any given period will be the summation of expected payoff conditioning on the available spectrum units m multiplied by the probability of the availability of that number of units (f_m).

$$\mathbb{E}[\pi_\mathcal{T}(v_i)] = \sum_{m=\underline{m}}^{\overline{m}} f_m \mathbb{E}[\pi_\mathcal{T}(v_i|m)] \tag{6.14}$$

The conditional expected payoff, $\mathbb{E}[\pi_\mathcal{T}(v_i|m)]$ depends on the winner's payment which can be any value between 0 and its priority value at that period $\beta_\mathcal{T}(v_i)$ (since price is set by highest losing bidder). Accordingly, we express $\mathbb{E}[\pi_\mathcal{T}(v_i|m)]$ in terms of the probability of all possible prices. $\Pr(X^{(m)} = z)$ denotes the probability that mth highest priority value is equal to z in the remaining population.

$$\mathbb{E}[\pi_\mathcal{T}(v_i|m)] = \sum_{z=0}^{\beta_\mathcal{T}(v_i)} (v_i - z) \Pr\left(\psi_i^s = z\right) = \sum_{z=0}^{\beta_\mathcal{T}(v_i)} (v_i - z) \Pr\left(X^{(m)} = z\right) \tag{6.15}$$

The pricing probability $\Pr\left(X^{(m)} = z\right)$ can be expressed as differences between cdfs $F_X^{(m)}(z)$ and $F_X^{(m)}(z-1)$. $F_X^{(m)}(z)$ denotes the cdf of the highest priority value among the remaining population. Simplifying the results in Eqn. 6.15, we obtain as follows

$$\mathbb{E}[\pi_\mathcal{T}(v_i|m)] = (v_i - \beta_\mathcal{T}(v_i))\, F_X^{(m)}(\beta_\mathcal{T}(v_i)) + \sum_{z=0}^{\beta_\mathcal{T}(v_i)-1} F_X^{(m)}(z) \tag{6.16}$$

Similarly, we calculate the losing probability of a bidder with τ remaining periods conditioning on the number of available spectrum units.

$$L_\tau(v_i) = \sum_{m=\underline{m}}^{\overline{m}} f_m L_\tau(v_i|m) \tag{6.17}$$

Here, $L_\tau(v_i|m)$ denotes the probability that a bidder of value v_i with τ periods to live does not win the auction. This probability is equal to the probability that the price is higher than the bidder's priority value $\beta_\tau(v_i)$.

$$L_\tau(v_i|m) = 1 - \Pr\left(X^{(m)} \leq \beta_\tau(v_i)\right) = 1 - F_X^{(m)}\left(\beta_\tau(v_i)\right) \tag{6.18}$$

Both Eqns. 6.16 and 6.18 depend on the cdf value, $F_X^{(m)}(z)$ that denotes the cdf of the m-th highest priority value among the remaining population of active bidders.

$$F_X^{(m)}(z) = \Pr\left(X^{(m)} \leq z\right) = \sum_{i=0}^{m-1} \Pr\left(N(z) = i\right) \tag{6.19}$$

Here, $\Pr(N(z) = i)$ denotes the probability that there are exactly i bidders in the population with priority value greater than z. Since the population consists of bidders with different remaining periods, these i bidders (with priority value greater than or equal to z) may come from any of these bidder groups. Therefore, we take all possible combinations of i bidders with priority value greater than or equal to z from the population.

$$\Pr\left(N(z) = i\right) = f(a) \Pr\left(N_1(z) = a_1\right) \ldots \Pr\left(N_{\overline{k}}(z) = a_{\overline{k}}\right) \text{ such that, } \sum_{j=1}^{\overline{k}} a_j = i \tag{6.20}$$

Here, $f(a)$ represents the probability of having this exact combination $[a_1 \ldots a_{\overline{k}}]$ from $\overline{k}$ groups.

$\Pr\left(N_j(z) = a_j\right)$ denotes the probability that there are exactly a_j bidders (with j remaining periods in their lifetimes) whose priority value is greater than z. Here, $F_j(z)$ denotes the cdf of priority value of bidders with j remaining periods of their lifetimes.

$$\Pr\left(N_j(z) = a_j\right) = \binom{n_j}{a_j} \left(1 - F_j(z)\right)^{a_j} \left(F_j(z)\right)^{n_j - a_j} \tag{6.21}$$

Finally, we combine the results from these Eqns. 6.16, 6.18, and 6.21 into Eqn. 6.2 to get the priority value of a bidder of value v_i with τ remaining periods of its lifetime. Based on this priority function **Prank - II**, we calculate priorities of bidders of different values and at different periods of their lifetimes. The values are recorded in a priority table $\mathcal{PT}$.

6.2.3 Prank - III (Double Auction Case)

In addition to bidders' valuations, **Prank - III** assumes that a seller's valuation of a single spectrum unit is a discrete random variable on $\{\underline{a}, \ldots, \overline{a}\}$ following cdf F_a which is known to the auctioneer.

The priority of a bidder i of value v_i at time t becomes

$$\begin{aligned}\beta_{i,t} = \beta_\tau(v_i) = \textbf{Prank-III}(\sigma_t^i, F_n, F_k, F_v, F_m, F_a)& \\ \text{where,} \tau = d_i - t + 1.& \end{aligned} \tag{6.22}$$

Here $\sigma_t^i(\mathbf{n}, m)$ denotes the auction 'state' concerning the rivals of user i at time t, and it is represented by a $\overline{k}$-dimensional matrix $\mathbf{n} = [n_k, \ldots, n_1]$ and the number of spectrum units (m) available in that period. Here, n_x denotes the expected number of bidders with x periods to live within the interference range of user i. Note that, σ_t^i changes depending on user location and the rival bidders' density in that area.

We use the same Eqn. 6.2 to calculate the priority of bidders and sellers. The priority of a bidder at the last period of its lifetime is equal to its value. Since each seller lasts only one period, the priority of a seller is always equal to its value. For winner selection, we followed a modified approach proposed by McAfee [88]. McAfee proposed a truthful double auction mechanism for static settings. Please see Sec. 2.1.7 for detail algorithm. It can be shown that McAfee rules cannot ensure truthfulness in dynamic settings. From now on, we refer to this mechanism as 'MRules(**T**,**S′**)'. As stated, a bidder's utility depends on the price it pays to the auctioneer. A bidder i with τ remaining periods wins if the winning price at that period is less than or equal to its priority value $\beta_\tau(v_i)$. So, the expected utility $\mathbb{E}[\pi_\tau(v_i)]$ can be expressed as

$$\mathbb{E}[\pi_\tau(v_i)] = \sum_{z=0}^{\beta_\tau(v_i)} (v_i - z) \Pr\left(\psi_i^s = z\right). \tag{6.23}$$

Here, $\Pr(\psi_i^s = z)$ denotes the probability that the bidder i's payment is equal to z. The winner's payment in a given period is determined according to McAfee rules (see in Sec. 2.1.7) which depends on the order statistics of the distribution of valuations of bidders and sellers. Therefore, we calculate the probability over all possible matches and the expected sum of these probabilities defines the probability $\Pr(\psi_i^s = z)$. Let us represent the h-th highest priority value and h-th lowest ask as $X^{(h)}$ and $Y_{(h)}$ in the auction respectively.

$$\begin{aligned}
\Pr(\psi_i^s = z) &= \sum_{m=\underline{m}}^{\overline{m}} f_m \sum_{h=2}^{m} \Pr\left(X^{(h)} = z\right) \Pr\left(Y_{(h)} \leq z|m\right) \Pr\left(Y_{(h+1)} > z|m\right) \\
&= \sum_{m=\underline{m}}^{\overline{m}} f_m \sum_{h=2}^{m} \Pr\left(X^{(h)} = z\right) F_Y^{(h)}(z|m) \left(1 - F_Y^{(h+1)}(z|m)\right)
\end{aligned} \tag{6.24}$$

The first term f_m denotes the pdf of spectrum availability at an auction period. The second term $\Pr\left(X^{(h)} = z\right)$ in the above equation denotes the pdf of the h-th order statistic of bidders' priorities which can be calculated using Eqn. 6.19. The third and forth terms depend on $F_Y^{(h)}(z|m)$ that denotes the conditional cdf of the h-th lowest order statistic of sellers' asks. We calculate the cdf $F_Y^{(h)}(z|m)$ conditioning on the number of available spectrum units as

$$F_Y^{(h)}(z|m) = \sum_{j=0}^{m-h} (1 - F_a(z))^j \, (F_a(z))^{m-j} \, . \tag{6.25}$$

Combining Eqns. 6.24, 6.25, 6.19, we calculate priorities of a bidder at different periods of its lifetime and record them in a priority table, $\mathcal{PT}$.

6.3 Distribution Aware Auction Algorithms

In this section, we devise auction mechanism based on the priority functions discussed in Sec. 6.2. We present two algorithms focusing on single and double auctions respectively.

6.3.1 SOADE: Online Single Auction Algorithm

We explain the auction mechanism SOADE (**S**econdary **O**nline **A**uction in **D**ynamic **E**nvironments) constructed around the priority function **Prank - II**. At each period, the auction mechanism consists of four steps.

Step 1 (prescreening): In this step, a bidder's identity is validated by the auctioneer before its entrance to the auction. Each bidder is required to be registered offline with a centralized database that the auctioneer has access to. On successful registration, bidder i is assigned an encryption key $\mathcal{K}_i$. Any lightweight encoding algorithm e.g. Paillier's homomorphic encryption [51] can be used for this purpose. A new bidder submits its encrypted bid request to the auctioneer with its credentials and upon approval from the auctioneer, it enters the auction.

Table 6.1: Algorithm SOADE: Secondary Online Auction in Dynamic Environments

screen and validate new bidders with bid requests
B = $\emptyset$
for each active bidder $i \in \mathcal{A}(t)$ **do**
  get $\beta_{i,t}$ from $\mathcal{PT}$
  update B = **B** $\cup \{i\}$
end for
B = sort(**B**), **C** = $\emptyset$
while B $\neq \emptyset$ **do**
  i = Top (**B**)
  if (ch = NextAvailable(i, $G_i(t)$)) $\neq 0$ **then**
    assign ch to i, **C** = **C** $\cup \{i\}$
  end if
  B = **B** $\setminus \{i\}$
end while
while C $\neq \emptyset$ **do**
  i = Top (**C**)
  if (q = NotAllocatedNeigh(i, $G_i(t)$)) = 0 **then**
    ψ_i = 0
  else
    ψ_i = $\beta_{q,t}$
  end if
  C = **C** $\setminus \{i\}$
  send an encrypted message $\mathcal{K}_i(i, \psi_i)$ to bidder i
end while

Step 2 (ranking): At the beginning of each period t, the auctioneer considers only the active bid requests in $\mathcal{A}(t)$ where $\mathcal{A}(t) = \{\phi_i | o_i \leq t \leq d_i\}$. New bidders are added after prescreening and the conflict graph $G(t)$ is updated as well. The conflict graph $G(t)$ represents the interference relationship among the active bidders at time t and $G_i(t)$ represent the list of active bidders who are within the interference range of user i at time t.

$$G_i(t) = \{j | G(i,j) = 1 \wedge i, j \in \mathcal{A}(t)\} \tag{6.26}$$

Note that the conflict graph is updated at the arrival of new bidder (also, at the departure of a winner or losing bidder). For each active bidder, its priority value is accessed from from the priority table, $\mathcal{PT}$ which is populated based on the function **Prank - II** (explained in Section 6.2.2). The active bidders are then stored in **B** in a non-increasing order of their priority values. Bidders are considered for spectrum allocation in this order.

Step 3 (allocation): The allocation process starts with an empty set **C**. For each bidder $i \in$ **B**, the auctioneer checks the list of its interferers $G_i(t)$ and finds the lowest index channel that is not assigned to any of its interferers. Here, $G_i(t)$ denotes the list of active users interfering with bidder i. If there is an unassigned channel available, it assigns the channel ch to user i and it is moved in **C**. The function *NextAvailable(i,* $G_i(t)$*)* takes user i and its interferer list $G_i(t)$ as input, and returns the lowest available channel index.

Step 4 (pricing): In the final step, the winning price is determined for each winner. Each winner $i \in$ **C** pays the amount equal to the highest priority value of a bidder $j \in G_i(t)$ that has not won the auction. If there are more channels than the number of interferers, the user wins at no cost. The function *NotAllocatedNeigh(i,* $G_i(t)$*)* searches through the neighbor list to find the highest priority bidder from its neighborhood $G_i(t)$ that has not been allocated any channel. A bidder leaves the auction immediately if it wins a spectrum unit or stays in the auction until its lifetime expires.

The auctioneer sends an encrypted message to the winner containing the winner id and payment amount. The winner decrypts the message, pays the price, and uses the spectrum. Any other user overhearing the message cannot decrypt the message. Thus, the winning price and winner identity are not revealed to all. All the steps of the auction mechanism is summarized in Table 6.1 for convenience.

Example: To illustrate how the algorithm works we solve the Eqns. for $n \sim$ Poisson(2), $m \sim U[0, 2]$, and $k \sim U[1, 3]$, and determine the priorities of bidders. We reenact the example scenario in Fig. 6.2. At time t_1, the effective bid of bidder A, B, and C will be their priority values $\$58$, $\$80$, and $\$41$ respectively. According to Algorithm SOADE (Table 6.1), bidder B wins and pays $\$58$. Similarly, the effective bid of bidder A and C at time t_2 are $\$67$ and $\$43$. So, bidder A wins and pays $\$43$. Note that, bidder B wins before bidder A although B's actual value is smaller than A's. This is because B's priority is higher than A's priority at t_1. Auction efficiency is $\$180$ ($\$100 + \$80$) and revenue is $\$101$ ($\$58 + \$43$).

6.3.2 Analysis of SOADE

We analyze the characteristics of the priority value function **Prank - II** and prove the useful properties of the auction mechanism.

Theorem 1 *The priority value of bidder i at different periods in its lifetime l_i is monotonic i.e., $\beta_{l_i}(v_i) \leq \cdots \leq \beta_1(v_i)$.*

By construction, for any period in its lifetime, a bidder's expected payoff $\mathbb{E}[\pi_\tau(v_i)] \geq 0$. The priority value of a bidder at any period is calculated by subtracting the cumulative expected payoff of remaining periods from its true valuation, and since each remaining period contributes a non-negative component to the total, $\beta_{l_i}(v_i) \leq \cdots \leq \beta_1(v_i)$.

Theorem 2 *The priority value function $\beta_\tau(v)$ is a strictly non-decreasing step function with concave envelope with respect to v.*

Let us consider two bidders of value v_1 and v_2 and $\tau = 1$ where $\underline{v} \leq v_1 < v_2 \leq \overline{v}$. We know that at the last period of its lifetime, a bidder's priority is equal to its true valuation. Therefore, $\beta_1(v_1) < \beta_1(v_2)$. Next, we consider the case of $\tau = 2$.

$$\beta_2(v) = v - \mathbb{E}[\pi_1(v)] = v - \sum_{z=0}^{v} (v - z) \Pr(\psi_i^s = z)$$

Due to their different valuations, the expected payoff at the last period of their lifetime will be different. Given everything remains same, the higher the valuation of a bidder, the less competition it faces from the young bidders. This implies that a bidder with higher value (v_2) expects higher payoff than that of a bidder with lower value (v_1) at the same period. As a result, the priority of a bidder of value v_2 cannot be lower than that of a bidder of value v_1. So, $\beta_2(v_1) \leq \beta_2(v_1)$. As the value increases, the change in priority value of bidders at their second last period with respect to their values decreases. By the same argument, we can generalize the statement for $\tau > 2$.

Theorem 3 *The proposed auction mechanism SOADE is truthful.*

Let us consider bidder i with a manipulated bid request (g_i', o_i', d_i', v_i'), its remaining lifetime at time t, $\tau' = d_i' - t + 1$ and its priority value at time t is $\beta_{\tau'}(v_i)$. The manipulator can lie about one or more parameters in its bid request. We prove that lying about any of its information (location, arrival time, value, and deadline) does not bring any benefit to the manipulator.

(a) $o_i' > o_i$: This means that a manipulator reports late arrival time and pretends not to be available when it is actually active. The manipulator cannot learn about the auction state during those periods since the winner information is encrypted. So, the manipulator will not have any added advantage for later periods. On the contrary, it will miss an opportunity to win spectrum in the skipped periods. Therefore, reporting late arrival will not benefit the manipulator.

(b) $o_i' < o_i$: The priority value of a bidder is always determined based on its value and departure time. Therefore, claiming early arrival time in bid request will not change its priority. Also, if the manipulator reports $o_i' < o_i$, it pretends to be active in a period when it was not actually present. So, even if the manipulator is considered as a winner at that period, it cannot use the spectrum unit. Furthermore, it will lose any opportunity to win it in later periods. So, reporting early arrival will not benefit the manipulator.

(c) $d_i' > d_i$: There are possible two cases while a manipulator reports longer deadline.

- Case 1: the manipulator wins the auction at $d_i' \geq t > d_i$ i.e., after the actual deadline has expired. Although the manipulator wins, it has no use of the spectrum unit but still has to pay. This results in negative utility.

- Case 2: the manipulator wins at $t \leq d_i$. Since $\tau < \tau'$, according to Lemma 1, $\beta_{\mathcal{T}}(v_i) \geq \beta_{\mathcal{T}'}(v_i)$. If a manipulator wins an auction with priority value $\beta_{\mathcal{T}'}(v_i)$, its payment p must be less than or equal to its priority value. So, the relationship holds as follows: $\beta_{\mathcal{T}}(v_i) \geq \beta_{\mathcal{T}'}(v_i) \geq p$. If the manipulator wins, the truthful bidder also wins and achieves the same utility. Therefore, a bidder will not gain any advantage by reporting $d_i' > d_i$.

(d) $d_i' < d_i$: When a manipulator reports earlier deadline ($d_i' < d_i$) we need to consider three cases.

- Case 1: the manipulator does not win by $t = d_i'$. Although its actual deadline is not over, the manipulator will no longer be considered in the auction from the next period. Had the bidder reported its deadline truthfully, it could have won in later periods $d_i' < t \leq d_i$ and could have achieved positive utility.

- Case 2: the manipulator wins at $t \leq d_i'$ and $\psi_i^s \leq \beta_{\mathcal{T}}(v_i)$. This implies that the bidder would have won if it reported its deadline truthfully since the payment is also less than the priority value of the truthful bidder at that period.

- Case 3: the bidder wins at $t \leq d_i'$ and $\psi_i^s > \beta_{\mathcal{T}}(v_i)$. According to Lemma 1, $\beta_{\mathcal{T}'}(v_i) \geq$

$\beta_{\mathcal{T}}(v_i)$. We calculate the expected payoff of the manipulated bidder at time t,

$$\mathbb{E}[\pi_{\mathcal{T}'}(v_i)] = \sum_{z=\beta_{\mathcal{T}}(v_i)+1}^{\beta_{\mathcal{T}'}(v_i)} (v_i - z) \Pr\left(X^{(m)} = z\right) \leq \sum_{z=\beta_{\mathcal{T}}(v_i)+1}^{v_i} (v_i - z) \Pr\left(X^{(m)} = z\right) \tag{6.27}$$

The truthful bidder would not win the auction in the current period; however, its expected payoff from remaining periods of its lifetime is greater than that of a manipulator. The truthful bidder's expected payoff at the last period is

$$\mathbb{E}[\pi_1(v_i)] = \sum_{z=0}^{v_i} (v_i - z) \Pr\left(X^{(m)} = z\right) \geq \sum_{z=\beta_{\mathcal{T}}(v_i)+1}^{v_i} (v_i - z) \Pr(X^{(m)} = z) \tag{6.28}$$

Thus, a truthful bidder's expected payoff is higher than that of a manipulator.

$$\mathbb{E}[\pi_1(v_i)] \geq \mathbb{E}[\pi_{\mathcal{T}'}(v_i)] \tag{6.29}$$

Therefore, a manipulator will not gain any advantage by reporting its deadline incorrectly.

(e) $v_i' > v_i$: Without loss of generality, let us assume that a bidder i wins an auction with τ remaining periods of its lifetime. According to Lemma 2, the priority value of a manipulator ($\beta_{\mathcal{T}}(v_i')$) is higher than that of a truthful bidder ($\beta_{\mathcal{T}}(v_i)$) i.e., $\beta_{\mathcal{T}}(v_i') > \beta_{\mathcal{T}}(v_i)$. Three possible scenarios may occur based on when the bidder i wins and how much it pays ψ_i^s.

- Case 1 ($\psi_i^s \leq \beta_{\mathcal{T}}(v_i)$): In this case, the truthful bidder also wins and achieves the same payoff. So, the bidder will not gain any advantage by misreporting its value.

- Case 2 ($\psi_i^s > \beta_\mathcal{T}(v_i)$, $\tau = 1$): In this case, the manipulator wins and pays more than its true valuation that will result in negative payoff.

- Case 3 ($\psi_i^s > \beta_\mathcal{T}(v_i)$, $\tau > 1$): In this case, the manipulator only wins because it overbids in that auction period. The expected payoff of the manipulator at this period is

$$\mathbb{E}[\pi_\mathcal{T}(v_i')] = \sum_{z=\beta_\mathcal{T}(v_i)+1}^{\beta_\mathcal{T}(v_i')} (v_i - z)\Pr(X^{(m)} = z) \leq \sum_{z=\beta_\mathcal{T}(v_i)+1}^{v_i} (v_i - z)\Pr(X^{(m)} = z) \tag{6.30}$$

  On the other hand, the truthful bidder loses the current auction; however, its expected payoff from the remaining periods will be higher than that of the manipulator. The truthful bidder's expected payoff at the last period only is higher than that (see Eqn. 6.28).

$$\mathbb{E}[\pi_1(v_i)] \geq \mathbb{E}[\pi_\mathcal{T}(v_i')] \tag{6.31}$$

(f) $v_i' < v_i$: According to Lemma 2, the priority value of a truthful bidder is higher than the value of the manipulator i.e., $\beta_\mathcal{T}(v_i') \leq \beta_\mathcal{T}(v_i)$. Therefore, if a manipulator underbids, its priority value at any period of its lifetime will always be lower than or equal to that of the truthful bidder. This implies that if a bidder wins by underbidding, it could have also won by bidding truthfully.

From Eqn. 6.27, 6.28, 6.30, we find that the expected payoff of a bidder with either manipulated value or manipulated deadline is smaller than that of a truthful bidder at the last period of its lifetime. This result also holds when a bidder combines any of these manipulated information (arrival time, deadline and value). Based on the above discussion, we conclude that a bidder will not benefit by misreporting its location, bid, arrival time, and deadline, and the proposed mechanism is time and bid truthful.

Theorem 4 *The proposed auction mechanism SOADE is ex ante strongly individually rational.*

There are two entities (sellers and bidders) in the auction, and we have to prove the rationality for both the entities. Let us calculate the expected payoff $\mathbb{E}[\pi_j]$ of seller j. The seller's payoff depends on the price range (between 0 and $\overline{v}$ inclusive) a bidder pays to win an auction.

$$\mathbb{E}[\pi_j] = \sum_{z=0}^{\overline{v}} z \Pr(\psi_j^p = z) > 0$$

Similarly, bidder i's expected payoff $\mathbb{E}[\pi_\tau(v_i)]$ with τ remaining periods in its lifetime can be calculated using Eqn. 6.16 which is also greater than 0. Therefore, both the entities in the auction achieve positive utility, and thus the proposed mechanism is ex ante strongly individual rational.

Theorem 5 *The proposed auction mechanism SOADE is ex post weakly individually rational.*

There can be three possible auction outcomes from the perspective of bidder i with τ remaining periods of its lifetime. First, the bidder departs without winning and earns zero utility. Second, the bidder wins and pays ψ_i^s. Since the winning price of a bidder is always less than its priority value at that period and the highest priority of a bidder is equal to its valuation v_i, $\psi_i^s \leq v_i$. So, the bidder achieves utility equal to $v_i - \psi_i^s \geq 0$. Similarly, it can be shown that the proposed auction mechanism is ex post individually rational from the perspective of a seller. Therefore, both the entities in the auction achieve non-negative utility, and thus the proposed mechanism is ex post weakly individual rational.

6.3.3 distAware: Online Double Auction Algorithm

The distribution aware online double auction mechanism works based on the priority function, **Prank - III**. At the beginning of each period, the priority value of each active bidder is taken from the priority table $\mathcal{PT}$. An active bidder refers to a bidder with at least one period to live that has not won a spectrum unit in earlier periods of its lifetime. Sellers only have lifetimes of one period. Bidders are sorted based on their priority value in list $\mathbf{B'}$. For each bidder $i \in \mathbf{B'}$, a list $\mathbf{T}$ of active bidders interfering with i is created using the conflict graph G. The auctioneer applies McAfee rules to find the critical price for bidder i at time t, $CP(i,t)$, which indicates the minimum value bidder i's priority should be to win the auction at that period. If bidder i wins, it pays the amount equal to the priority value of h-th bidder in i's neighborhood. The auctioneer allocates spectrum using $nextAvailableChannel()$ which finds the lowest index spectrum that has not been allocated to any of its interfering bidders. Similarly, sellers' payments are determined according to McAfee rules. Note that, sellers are paid multiple times at different amounts due to spectrum reusability. The winners from both bidders and sellers are removed from the active bidder list; the losing bidders move on to the next period with one less period to live. The entire algorithm is presented in Table 6.2.

6.3.4 Analysis of distAware

Theorem 6 *The distribution aware online double auction mechanism is truthful.*

According to the definition of truthfulness, we need to show that a participant cannot increase its utility by reporting incorrect arrival time, deadline, and/or bid. Let us denote the true bidder i's bid request as $\phi = (g_i, b_i, o_i, d_i)$ and its utility as U_i where $b_i = v_i$. Let us also denote the manipulator i' and its bid request as $\phi' = (g'_i, b'_i, o'_i, d'_i)$, its utility as U'_i and where $g'_i \neq g_i$, $b'_i \neq b_i$, $a'_i \neq a_i$,

Table 6.2: Algorithm distAware: Distribution Aware Online Double Auction

for i $\in$ **B** **do**
  assign priority $\beta_{i,t} = \mathcal{PT}[v_i, d_i - t + 1]$
end for
sort bidders according to priority, $\mathbf{B}'$ = sort($\mathbf{B}$)
$W = \emptyset$
while $\mathbf{B}' \neq \emptyset$ **do**
  i = Top($\mathbf{B}'$)
  $\mathbf{T}$ = $\{i\} \cup \{j|G(i,j) = 1 \wedge j \in \mathbf{B}\}$
  find h = MRules($\mathbf{T}$, $\mathbf{S}'$), $CP(i,t) = \beta_{\mathbf{T}(h)}$
  if $\beta_{i,t} > CP(i,t)$ **then**
    j = nextAvailableChannel(i);
    $W = W \cup \{i\}$;
    $\psi_i^s = CP(i,t)$, chn(i) = j, $\psi_j^p = \psi_j^p + a_{\mathbf{S}'(h)}$
  end if
  $\mathbf{B}' = \mathbf{B}' - \{i\}$
end while

$d_i' \neq d_i$. Note that, if a bidder reports an incorrect location, it will be allocated spectrum in that location which does not help the manipulator to gain benefits. Therefore, a manipulator does not report incorrect location. We will show that any combination of other manipulated information from i' does not increase its utility.

(a) First, we consider the case where $b_i' < v_i$. Based on the priority function, $\forall t \in l_i$, $\beta_t(b_i')$ $\leq \beta_t(v_i)$ i.e., at any period t in its lifetime, the priority of a bidder is no less than that of a manipulator. Therefore, given everything else remains the same, if a manipulator wins at period t, the true bidder also wins at that period and the manipulator does not gain any benefit by underbidding.

(b) Second, we consider the case where $b_i' > v_i$. If the manipulator wins at the last period and pays $\psi_i^s > v_i$, it pays more than its actual valuation which incurs negative utility. If $\psi_i^s < v_i$, a true bidder also wins given everything remains the same. If the manipulator wins at an earlier period, there are again two possible cases. Let us consider that a manipulator wins at period t. Since the manipulator overbids, the manipulator's priority is higher than a true bidder's priority, i.e., $\beta_t(b'_i) > \beta_t(v_i)$. If $\psi_i^s < \beta_t(v_i)$, the manipulator does not gain since it would have won by bidding truthfully. If $\beta_t(b'_i) > \psi_i^s > \beta_t(v_i)$, the true bidder could not win at t. However, it can be shown (Eqn. 6.32) that a true bidder's expected utility from its last period only is higher than that of a manipulator which discourages a manipulator to overbid.

$$\mathbb{E}[\pi_t(b'_i)] = \sum_{z=\beta_t(v_i)+1}^{\beta_t(b'_i)} (v_i - z)\Pr(\psi_i^s = z) \leq \sum_{z=0}^{v_i}(v_i - z)\Pr(\psi_i^s = z) = \mathbb{E}[\pi_1(v_i)] \tag{6.32}$$

(c) Next, we consider the case where a manipulator informs late arrival ($o'_i > o_i$) or early departure ($d'_i < d_i$) which implies shorter deadline. In both cases, a manipulator misses winning opportunity either at its earlier periods or later periods of its lifetime. However, by reporting late arrival or early departure, a manipulator implies shorter deadline for the reported periods of its lifetime. So, a manipulator's remaining period (τ') is always smaller than that of a true bidder (τ) i.e., $\tau' < \tau$; a manipulator's priority is, therefore, higher than that of a true bidder i.e. $\beta_\tau(v_i) < \beta_{\tau'}(v_i)$. If $\psi_i^s < \beta_\tau(v_i)$, manipulator does not gain any benefit since it would have also won by truthfully reporting its time. If $\beta_{\tau'}(v_i) > \psi_i^s > \beta_\tau(v_i)$, the true bidder could not win at that period. Using similar argument, we show (Eqn. 6.33) that a true bidder's expected utility from its last period only is higher than that of a manipulator which discourages a manipulator to report late arrival and early departure.

$$\mathbb{E}[\pi_{\tau'}(v_i)] = \sum_{z=\beta_\tau(v_i)+1}^{\beta_{\tau'}(v_i)} (v_i - z)\Pr(\psi_i^s = z) \leq \sum_{z=0}^{v_i}(v_i - z)\Pr(\psi_i^s = z) = \mathbb{E}[\pi_1(v_i)] \tag{6.33}$$

(d) Finally, we consider the case where a manipulator informs early arrival ($o_i' < o_i$) or late departure ($d_i' > d_i$) which implies a longer deadline. In both cases, a manipulator may end up winning a spectrum unit beyond its valid periods which results in negative utility. Also, in valid periods, the manipulator's priority will be lower than that of a true bidder. So, if a manipulator wins a true bidder also wins in the same period which discourages a manipulator to report early arrival and late departure. Using similar approach, it can be shown that a manipulative seller does not gain any benefit by underbidding or overbidding.

Theorem 7 *The distribution aware online double auction mechanism is individually rational.*

By construction, a seller either fails to sell its spectrum and earns zero utility or sells its spectrum according to McAfee rule which guarantees non-negative utility. On the other hand, a bidder may fail to earn a unit which results in zero utility. Otherwise, a bidder may win at any period of its lifetime, and its payment is always less than or equal to its priority value of that period. Since a bidder's highest priority value is equal to its actual valuation, a winning bidder never pays more than its valuation. This proves that the mechanism is individually rational.

Theorem 8 *The distribution aware online double auction mechanism is budget balanced.*

At any period, all matches between bidders and sellers are determined according to McAfee rules. This guarantees the balanced budget property of the mechanism.

6.4 Distribution Free Online Double Auction Algorithm

The algorithm in Sec. 6.3 requires distribution knowledge which may not be easily available to reflect the real auction scenario. In this section, we therefore present an auction mechanism that requires no knowledge of the underlying distributions of bidders and sellers.

In this algorithm, a bidder wins at an auction period only when a bidder's bid is higher than the critical price of that period. The calculation of the critical price is somewhat different from the distribution aware algorithm. A bidder i's critical price at time t, $CP(i,t)$ has two components - one component is derived according to McAfee rules, $MP(i,t)$ and the second component is calculated based on the 'debt factor', $DP(i,t)$ (will be described later in this section). Bidder i's final payment is determined as the lowest critical price over all periods of its lifetime. A seller's critical price is determined solely based on McAfee rule.

$$\psi_i^s = \min_{t \in [o_i, d_i]} CP(i,t) \tag{6.34}$$

The algorithm has three phases. In the screening phase, the algorithm identifies the candidates of potential winners from the list of active bidders (sellers) and determines the minimum amount they need to pay (to be paid) according to McAfee rules described in Sec. 2.1.7. In the debt calculation phase, the algorithm calculates the debt factor of each candidate considering the interfering bidders that have won at previous periods but their lifetimes have not expired yet. In the final phase, the algorithm determines the critical price of that period for each bidder, selects winners from the list of active bidders and sellers of this period, and if applicable, changes the payment amount of the previous winners.

For convenience, we summarize all symbols used in both algorithms in Table 6.3 and brief function descriptions are in Table 6.4.

6.4.1 Candidate Screening (Phase 1)

First, the active bidder list **B** is sorted based on their bid (from high to low) in **B**$'$. The spectrum (or seller) list **S** is also sorted based on their ask (low to high) in **S**$'$. For each bidder $i \in$ **B**$'$, an

Table 6.3: Symbols used in the algorithm

symbols	meaning
$\mathbf{B}$, $\mathbf{B}'$	unsorted and sorted active bidder list
$\mathbf{S}$, $\mathbf{S}'$	unsorted and sorted active seller list
$\mathcal{P}$, $\mathcal{P}'$	unsorted and sorted active pender list
$\mathbf{A}$	candidate bidder list
$\mathbf{A}'$	candidate pender list
W	winners' list
$\beta_{\mathbf{T}(h)}$	the priority of the h-th bidder in the list $\mathbf{T}$
$b_{\mathbf{T}(h)}$	the bid of the h-th bidder in the list $\mathbf{T}$
$a_{\mathbf{S'}(h)}$	the ask of the h-th bidder in the list $\mathbf{S}'$
$pp(i,t)$	denotes intermediate McAfee price of pender i
G	Conflict graph or Interference graph G(i,j) = 1 if i and j interfere, 0 otherwise

Table 6.4: Functions used in the algorithm

function	description
chn(i)	the spectrum unit assigned to bidder i
Top(**B**)	returns the top element from the list **B**
NextAvailableChannel(i)	returns the spectrum unit with the lowest ask which has not been assigned to any of the neighbors of bidder i
count(i)	number of bidders in neighborhood sharing the debt of pender i

Table 6.5: Algorithm distFree: Candidate Screening (Phase 1)

while $\mathbf{B}'$ is $\neq \emptyset$ **do**
  i = Top($\mathbf{B}'$)
  T = $\{i\} \cup \{j | G(i,j) = 1 \wedge j \in \mathbf{B}\}$
  find h = MRules(**T**, $\mathbf{S}'$), $MP(i,t)$ = $b_{\mathbf{T}(h)}$
  if $b_i > MP(i,t)$ **then**
    j = nextAvailableChannel(i)
    A = **A** $\cup \{i\}$
    ψ_i^s = $MP(i,t)$, $x_i = 1$, chn(i) $= j$, ψ_i^p = $a_{\mathbf{S}'(h)}$
  end if
  $\mathbf{B}'$ = $\mathbf{B}'$ - $\{i\}$
end while

interferer list **T** is created based on the conflict graph G. Given the list **T** and $\mathbf{S}'$ at time t, we apply McAfee rules to identify the winning potential of bidder i and the first component of its payment amount, McAfee price $MP(i,t)$. It also keeps record of the corresponding seller's payment. If bidder i is selected as a potential winner, a function $nextAvailableChannel()$ finds the lowest index channel available for bidder i that is not allocated to any of its neighbors. Thus, at the end of the first phase, each bidder is either moved to the list **A** of candidate of winners or removed from consideration for the current auction period. The first phase of the algorithm distFree is presented in Table 6.5.

6.4.2 Debt Calculation (Phase 2)

In the second phase, we review the list $\mathcal{P}$ of pending winners from previous periods whose lifetimes have not expired yet (referred to as 'penders') to calculate the debt amount in the current period. Accordingly, penders are sorted in order of their bids (from high to low) in $\mathcal{P}'$. For each pender, an interferer list **T** is constructed using the conflict graph G. McAfee rule is applied to determine whether the pender would win at the current period if it had not won before. In case of winning, it calculates the price it would have paid in the current period. If this price is higher than its

Table 6.6: Algorithm distFree: Debt Calculation (Phase 2)

```
while 𝒫′ ≠ ∅ do
    i = Top(𝒫′)
    T = {i} ∪ {j|G(i, j) = 1 ∧ j ∈ B}
    find h = MRules(T, S′), MP(i, t) = b_T(h)
    if MP(i, t) < ψ_i^p then
        DP(i, t) = ψ_i^p - MP(i, t)
        A′ = A′ ∪ {i}
    end if
    pp(i, t) = MP(i, t), 𝒫′ = 𝒫′ − {i}
end while
```

current payment, no further action is needed. If the pender's calculated price is lower than its current payment but higher than the corresponding seller's payment, we set the current payment to the calculated price. If the calculated price is lower than the corresponding seller's payment, the difference in payment is considered to be 'debt' and must be compensated by the mechanism to maintain 'budget balance' property. The pender is moved to list $\mathbf{A}'$ for next phase analysis. The second phase of the algorithm distFree is presented in Table 6.6.

6.4.3 Critical Price and Winner Selection (Phase 3)

In the final phase, we calculate the 'debt factor' for each candidate winner $i \in \mathbf{A}$. For each pender $j \in \mathbf{A}'$, we find the bidders from $\mathbf{A}$ who are in its interference range, and the debt of pender j is equally shared among its interferers. So, the debt of a bidder i at time t is the total debt factor from all penders $DP(i,t)$. If the critical price $CP(i,t)$ of bidder $i \in \mathbf{A}$ exceeds its valuation b_i, i is removed from $\mathbf{A}$ and the debt amount is recalculated for all the existing candidate bidders in $\mathbf{A}$. This process continues until all the bidders in $\mathbf{A}$ are removed or the bidders in $\mathbf{A}$ settle in sharing debts with the penders in $\mathbf{A}'$. If all the bidders are removed, there will be no winners in that period and the payment amount of penders will not change. Otherwise, the payment amount of the penders is updated based on their critical price of that period.

Table 6.7: Algorithm distFree: Critical Price Determination (Phase 3)

```
while isConverged = false and A ≠ ∅ do
    isConverged = true
    for i ∈ A do
        for j ∈ A′ do
            if G(i,j) = 1 then
                DP(i,t) = DP(i,t) + x_i × DP(j,t)/count(j)
            end if
        end for
        if ψ_i^s + DP(i,t) ≥ b_i then
            A = A − {i}, x_i = 0
            isConverged = false
        end if
    end for
end while
for i ∈ A′ do
    ψ_i^s = min (ψ_i^s, pp(i,t) + DP(i,t))
end for
for i ∈ A do
    ψ_i^s = b_i^s + DP(i,t)
    P = P ∪ {i}
end for
```

Finally, if the lifetime of any pender $j \in \mathcal{P}$ expires, it is removed from $\mathcal{P}$. The winning bidders at the current period whose lifetime has not expired yet are moved from **A** to $\mathcal{P}$. The final phase of the algorithm distFree is presented in Table 6.7.

6.4.4 Analysis of distFree

In this section, we provide a theoretical analysis of the proposed algorithms and show that both these mechanisms satisfy all three auction properties.

Theorem 9 *The distribution free online double auction mechanism is truthful.*

According to the definition of truthfulness, we need to show that a participant cannot increase its utility by reporting incorrect arrival time, deadline, and/or bid. Let us denote the true bidder i's bid request as $\phi = (g_i, b_i, o_i, d_i)$ and its utility as U_i where $b_i = v_i$. Let us also denote the manipulator i' and its bid request as $\phi' = (g_i', b_i', o_i', d_i')$, its utility as U_i' and where $g_i' \neq g_i$, $b_i' \neq b_i$, $a_i' \neq a_i$, $d_i' \neq d_i$. Note that, if a bidder reports an incorrect location, it will be allocated spectrum in that location which does not help the manipulator to gain benefits. Therefore, a manipulator does not report incorrect location. We will show that any combination of other manipulated information from i' does not increase its utility.

(a) First, we suppose that manipulator i' underbids, i.e., $b_i' < v_i$ to increase its utility. Since spectrum is allocated in non-decreasing order of their bids, a higher valued bidder always wins before a lower valued bidder given everything else remains the same. Therefore, i' does not gain any advantage by underbidding.

(b) Second, we consider the case where a manipulator overbids, i.e., $b_i' > v_i$. Let us assume that a manipulator wins at an earlier period t, and the true bidder does not win at that period. So, the manipulator's payment is set to $\psi^s_{i'} = CP(i', t) > v_i$. In this algorithm, a bidder's final price is determined as the minimum critical price of any period over its lifetime. So, if the final price $\psi^s_{i'} < v_i$, it implies that the critical price at a later period t' of its lifetime is smaller than its value, $CP(i', t') < v_i$. Given everything else remains the same, the true bidder i would also win at that same period t' and would achieve the same utility. Otherwise, the manipulator's final price will be higher than its actual valuation. In that case, a true bidder does not win and has zero utility, however, the manipulator ends up paying more than its valuation which results in negative utility.

(c) Next, we consider that i' reports late arrival ($o'_i > o_i$). Since a true bidder gets more opportunity to win an auction and reduce its payment amount, i' does not gain any advantage over i. Next, we consider that manipulator i' reports early deadline $d'_i < d_i$. By submitting deadline earlier than its actual deadline, a manipulator may miss an opportunity to reduce its payment amount. But it does not get any advantage by reporting early deadline since spectrum allocation does not take bidder's deadline into consideration. Therefore, reporting earlier deadline does not help a manipulator in increasing utilities. Finally, if a manipulator reports early arrival or late departure the manipulator may end up paying when it no longer needs a spectrum unit. Therefore, a manipulator does not report early arrival or late departure.

Using a similar approach, it can be shown that a manipulative seller j' cannot gain any advantage by submitting higher or lower ask than its true valuation of the unit.

Theorem 10 *The proposed distribution free double auction mechanism is individually rational.*

Let us first consider the utility U_i of a bidder i. If a bidder does not win, it does not pay anything and its utility, $U_i = 0$. There are two cases when a bidder wins. First, a bidder wins at the last period of its lifetime. In the 3rd part of the algorithm, a bidder is selected as a winner only if the bidder's bid is higher than the critical price at that period. So, $U_i \geq 0$. Second, a bidder wins at an early period of its lifetime. In this case, the bidder is moved to the pending list. A pender's final payment is set to the minimum of the critical prices of later periods in its lifetime. So, in subsequent periods, the payment will never go up. Therefore, $U_i \geq 0$.

Let us consider the utility U_j of a seller j. If a seller does not win, it is not paid anything. So, $U_j = 0$. If a seller wins, the payment is decided according to McAfee rule which guarantees that the winning seller is paid no less than its ask.

Theorem 11 *The distribution free online double auction mechanism is budget balanced.*

Let us suppose that the bidder's lifetime is only one period. When both bidders and sellers live for only one period, the mechanism reduces to the McAfee mechanism in each period. Therefore, the mechanism is budget balanced. When a bidder's lifetime is more than one period and wins at an earlier period, its payment may be reduced at later periods; however, a seller's payment does not change afterwards. There may be two possible cases. First, the bidder's payment is reduced to not lower than the corresponding seller's payment. In that case, condition for balanced budget still holds. Second, the payment is reduced to below the corresponding seller's payment. However, in that case, the difference is equally shared among its winning neighbors (which is referred to as 'debt factor'). So, the auctioneer's utility will not be negative and the mechanism is budget balanced.

6.5 Performance Evaluation

We organize this section into two parts. In the first part, we analyze the priority functions presented in Sec. 6.2. Specifically, we investigate how the priority of a bidder changes with the change in the distribution parameters and explain their properties. In the second part, we compare the performance of the proposed algorithms with an off-line mechanism with or without spectrum reusability.

6.5.1 Priority Analysis

As presented in Sec. 6.2, we consider two versions of priority function — **Prank-II** and **Prank-III**. We consider different configuration of auction environments by varying bidders' arrival rate F_n, supply availability F_s, bidders' lifetime F_k, bidders valuations F_v, and sellers' valuations F_a. For a specific configuration of the auction environment, we solve the priority value functions to find the priority value of a bidder at different periods of its lifetime. To start with, we assume that the bidders' priority is equal to their valuation independent of their lifetime. We simulate the auction for 10000 time periods and if the estimated priority values match with the simulation outcome, we stop the simulation, and the results are recorded. Otherwise, the next iteration starts with the result of previous iteration and continues until the result converges. For statistical confidence, the entire process was repeated 10 times, and we take an average over all these runs to construct the priority table. Note that, according to Strong Law of Large Numbers, we use the sample mean as the actual mean for bidders' population with different periods to live, and use it in priority calculation. The same process is repeated for different auction configuration, and all simulation results are calculated following this process.

6.5.1.1 Prank - II

Prank-II is a distribution aware ranking function that calculates the priority of a bidder given its value and lifetime in an online single auction setting. We present the simulation results of the priority value function **Prank - II** and investigate how the priority value of a bidder changes with changes in bidders' arrival rate, supply availability, and bidders' lifetime (see Fig. 6.5).

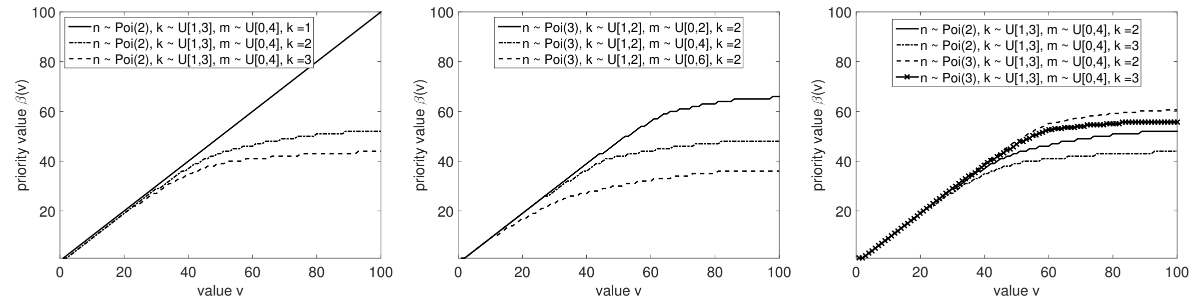

(a) priority value at different periods (b) priority value with varying supply rate (c) priority value with varying bidder arrival rate

Figure 6.5: Priority value with varying parameters (**Prank - II**)

First, we consider an auction environment where new bidders arrive following a Poisson distribution with a mean value of 2 and lifetime of the bidders are uniformly distributed over $\{1, 2, 3\}$. Also, number of available spectrum units at each period is uniformly distributed over $\{0, \ldots, 4\}$ with a mean value of 2. Fig. 6.5a shows the priority value of a bidder at different periods of its lifetime under this setting. For example, the priorities of a bidder of value $\$100$ are $\$40$, $\$45$, and $\$100$ with 3, 2, and 1 period to live. As expected, a bidder's priority value increases as it approaches the end of its lifetime.

Next, we set the bidder arrival rate following a Poisson distribution with a mean value of 3 and the lifetime of the bidders are uniformly distributed over $\{1, 2, 3\}$. We vary the supply availability rate $\{0, 1, 2\}$, $\{0, \ldots, 4\}$, $\{0, \ldots 6\}$ with mean 1, 2, and 3 respectively. Fig. 6.5b shows a decrease in the priority value of a bidder with an increase in supply rate. This is because more supply per period increases winning probability at early periods, and the expected payoff from remaining lifetime periods increases which decreases the priority value of the bidder.

Third, we vary the mean value of the bidder arrival rate while the lifetime of the bidders are uniformly distributed over $\{1, 2, 3\}$. We plot the priority value of a bidder with 2 and 3 remaining periods of its lifetime in Fig. 6.5c. The mean arrival rate are considered 2 and 3. The result shows that the priority value of a bidder at the same period increases with an increase in the bidder arrival

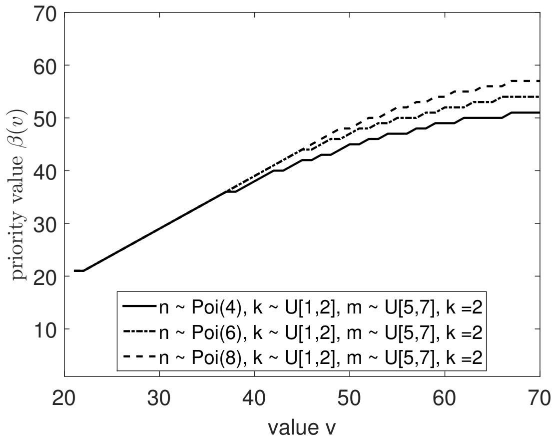

Figure 6.6: Priority values with varying parameter (**Prank-III**)

rate. This is because with the arrival of more bidders, the auction gets more competitive, and the winning probability decreases. This leads to a decrease in the expected payoff which is followed by a higher priority value.

6.5.1.2 Prank - III

Prank-III is a distribution aware ranking function that calculates the priority of a bidder given its value and lifetime in an online double auction setting. In this section, we analyze the properties of **Prank-III**. We take a closer look at the priority values of a bidder at different periods of its lifetime. We consider a setting where bidders have either 1 or 2 periods of lifetime. We assume that bidders' arrivals follow a Poisson distribution with mean value varying between 4 and 8. The priority values of a bidder at the second to last period are shown in Fig. 6.6 across different valuations. The result shows that the priority value of a bidder increases with the increase in bidders' arrival rates and increase in bidders' valuations. This is because priority is calculated based on the expected utility of future periods, and with the increase in bidders' arrival rates, a bidder has to compete with more bidders which reduces the expected utility at future periods.

6.5.2 Algorithm Performance

We consider two different auction settings. In the first setting, all bidders are located inside each other's interference range. Thus, the interference relationship between users forms a complete graph. So, a spectrum unit cannot be allocated to more than one user. In the second setting, the users are randomly deployed. So, each user may experience different number of interferers that may make it possible to allocate the same spectrum unit to more than one user. The first setting is referred to as 'setting with no reusability' and the second one is referred to as 'setting with reusability'. For each setting, we have considered the following four performance metrics to evaluate the performance of the auction algorithms

(i) spectrum utilization rate - it denotes the ratio between the number of bidders who won a spectrum unit and the number of spectrum units auctioned for sale.

(ii) bidder satisfaction rate - it denotes the ratio between the number of bidders who won a spectrum unit and the number of bidders who participated in the auction.

(iii) average value of winner - it denotes the average valuation of a winning bidder which is related to the efficiency of the auction.

(iv) revenue per winner - it denotes the average price a winning bidder pays for a spectrum unit.

6.5.3 Single Auction Algorithm

In this section, we simulate different auction settings to verify the properties and analyze the performance of the proposed auction mechanism. We assume that both the bidders' arrival and spectrum availability follow a Poisson distribution [30]. Also, the bidders' lifetime follows a Uniform distribution while the bidders' valuation follows a Uniform distribution with support $\{1, \ldots, 100\}$.

To the best of our knowledge, this is the first work addressing both the dynamic arrival of bidders and dynamic spectrum supply. For performance comparison, we select Topaz [30] that successfully handles the dynamic arrival of bidders but considers a fixed number of available spectrum units. It allocates spectrum to the bidders in the non-decreasing order of their bids whenever a new bidder arrives. In order to handle the dynamic supply, we also invoke the allocation procedure when new spectrum arrives at the auction. Note that, Topaz is not truthful since a bidder can gain benefit by reporting a longer deadline (see in Fig. 6.4). Additionally, we have considered an auction setting where spectrum supply is fixed. We have also included the results from an off-line algorithm where the auctioneer has complete information of bidder arrival and spectrum supply in future periods. Thus the off-line algorithm serves as a benchmark solution to analyze the performance of SOADE.

6.5.3.1 Results on Setting with No Spectrum Reusability

We evaluate the performance of the proposed single auction algorithm in the setting with no spectrum reusability (defined in Sec. 6.5.2). In this setting with no reusability, we assume that the bidders arrive following a Poisson distribution, and their lifetime is uniformly drawn from the set $\{1, 2, 3\}$. We change the mean arrival rate of the bidders between 2.0 and 3.0. We assume that supply arrive at each period following a Uniform distribution from the set $\{0, 1, 2\}$.

Under the setting with no spectrum reusability, Fig. 6.7 shows the simulation results of four performance metrics of SOADE and Topaz. In the case of spectrum utilization rate (Fig. 6.7a) and the bidder satisfaction rate (Fig. 6.7b), SOADE performs marginally better than Topaz. This is because in SOADE, a bidder with smaller value and shorter lifetime may have higher priority than a bidder with larger value and longer lifetime and wins over it. Also, as expected, the spectrum utilization rate increases, and the bidder satisfaction rate decreases with the increase in bidders'

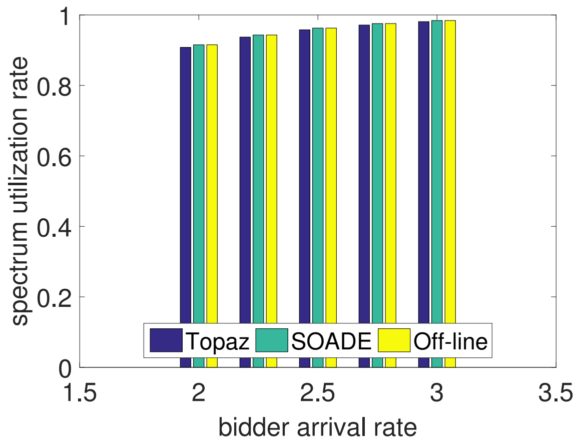

(a) spectrum utilization rate

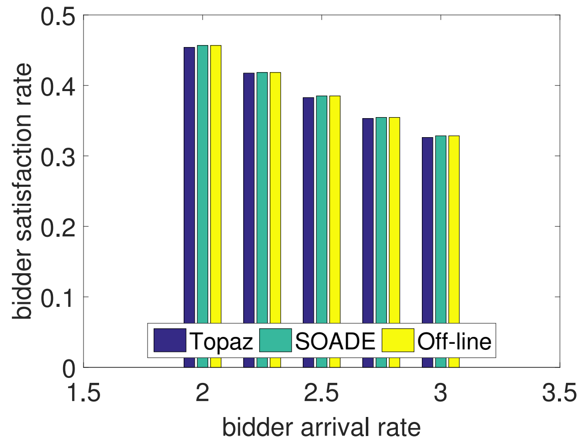

(b) bidder satisfaction rate

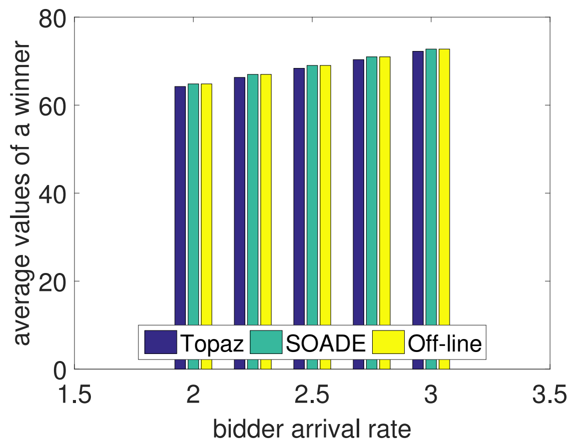

(c) average value of a winner

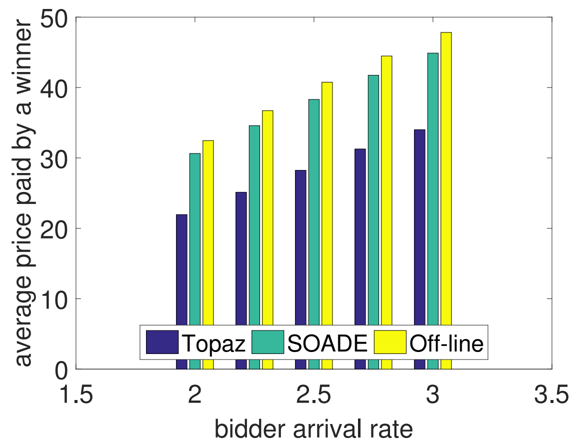

(d) revenue per winner

Figure 6.7: Topaz vs. SOADE on setting with no reusability

arrival rate. The next figure (Fig. 6.7c) reflects the auction efficiency of the auction. Both the approaches show similar result where the average value increases with the increase in bidders' arrival rate. Finally, we compare the winner's payment (denoted as auction revenue) in Fig. 6.7d. The result shows that revenue increases with the increase in arrival rate due to the presence of more competitors in the auction. For a fixed user arrival rate, SOADE generates more revenue than Topaz but less than the off-line algorithm. This is because winning price in SOADE depends on the priority values of the participating bidders on the same auction period.

6.5.3.2 Results on Setting with Spectrum Reusability

We also evaluate the performance of the proposed single auction algorithm in the setting with spectrum reusability (defined in Sec. 6.5.2). Under this setting with spectrum reusability, we allocate the same spectrum to more than one users as long as they are not interfering each other. We consider that nodes are randomly distributed within $250m \times 250m$ area. The interference range of a user is set to 50m i.e., two nodes will interfere each other if they are less than or equal to 50m apart. In other words, two users located 50m apart from each other can use the same spectrum unit without any interference. As before, the bidders' lifetime is uniformly drawn from the set $\{1, 2, 3\}$ while the mean bidders' arrival rate is changed between 16 and 24. We also consider that the spectrum unit is uniformly drawn from the set $\{0, 1, 2\}$ with mean 1. The simulation result is presented in Fig. 6.8. The result shows similar pattern to the first setup and SOADE generates revenue closer to that of the off-line algorithm. We have also considered an auction environment with fixed number of spectrum supply per time period. We get similar results where SOADE achieves higher revenue and higher bidder satisfaction rate than that of Topaz[2].

In summary with fixed or dynamic spectrum supply, with or without spectrum reusability, SOADE generates auction revenue close to off-line revenue in addition to slightly increasing spectrum utilization rate, bidder satisfaction rate, winners' valuations while preserving truthfulness in comparison to Topaz.

6.5.4 Double Auction Algorithms

In this section, we analyze and evaluate the performance of the proposed algorithms under different auction setting. For convenience, we refer to the distribution aware online double auction

[2]Due to the its similarity with Fig. 6.7, results are not shown here

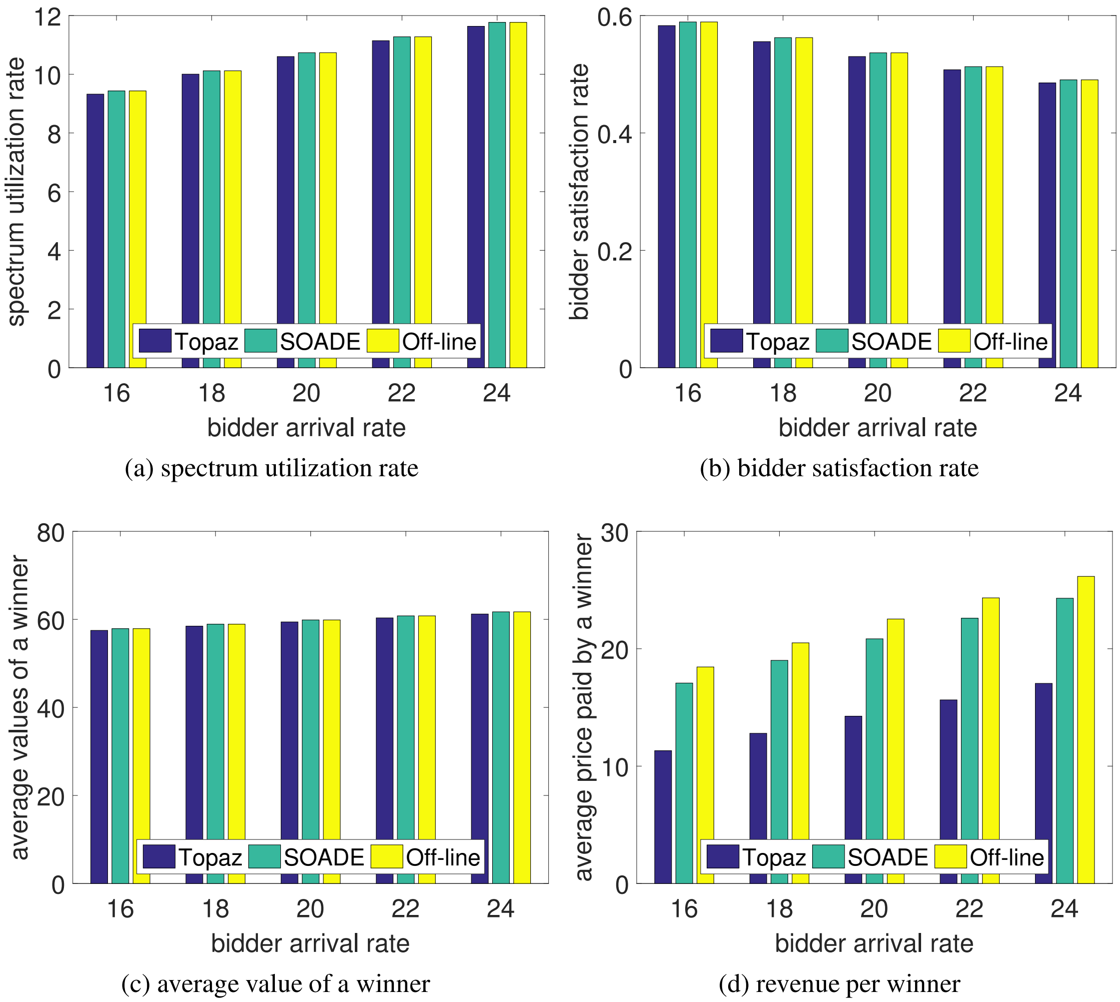

(a) spectrum utilization rate

(b) bidder satisfaction rate

(c) average value of a winner

(d) revenue per winner

Figure 6.8: Topaz vs. SOADE on setting with spectrum reusability

mechanism as 'distAware' and the distribution unaware mechanism as 'distFree'.

We consider bidders' arrival follows a Poisson distribution and spectrum becomes available following a Uniform distribution [118] [30]. In all following simulations, spectrum availability per period is uniformly drawn from $\{5, 6, 7\}$. Bidders' valuations are uniformly drawn from $\{21, \ldots, 70\}$ while sellers' valuations are uniformly drawn from $\{1, \ldots, 50\}$. For any auction setting, we run the simulation 5 times and each time, the simulation runs for 5000 time periods. For statistical confidence, we take an average of all these runs. Similar to single auction performance analysis, we use two different auction settings.

6.5.4.1 Results on Setting with No Spectrum Reusabililty

We evaluate the performance of the proposed double auction algorithm in the setting with no spectrum reusability (defined in Sec. 6.5.2). To the best of our knowledge, existing research cannot ensure truthfulness in an online dynamic setting. Therefore, we compare our algorithms with an off-line algorithm. Note that the off-line auction benchmark is necessarily counter-factual in that it is not possible to implement it without knowing the future realizations of the distributions. However, it serves as a good benchmark in that it gives the best possible outcome. We consider an auction setting where all bidders are interfering to each other. Bidders' arrivals follow a Poisson distribution with a mean value varying between 4 and 6 and bidders' lifetimes are uniformly drawn from $\{1, 2, 3\}$.

Under the setting with no spectrum reusability, we observe that both distAware and distFree show almost as high bidder satisfaction rate and spectrum utilization rate as the off-line approach when the mean arrival rate of bidders is close to the mean number of spectrum units. We also plot the total payment made by bidders (Fig. 6.9c) and total payment made to the sellers respectively. The results show that distAware generates revenue closer to the off-line approach than distFree

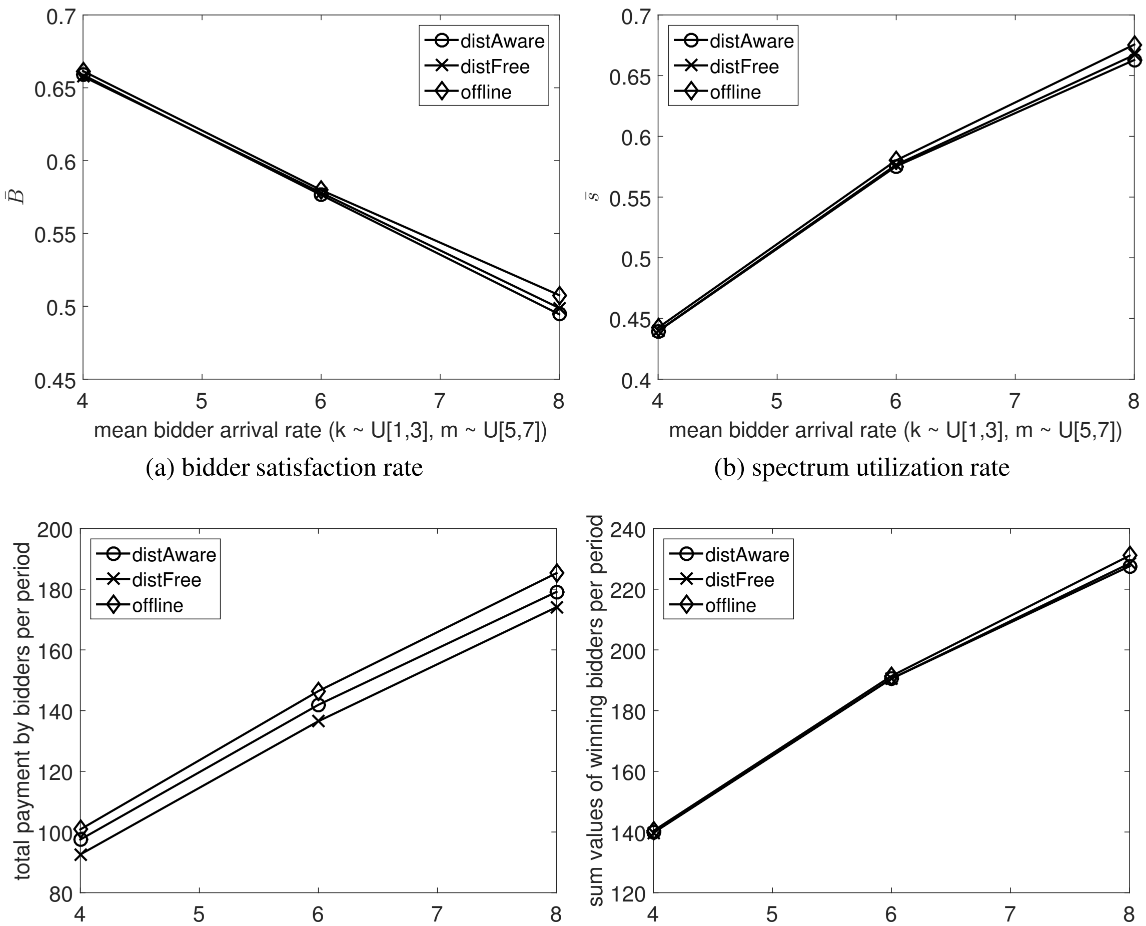

(a) bidder satisfaction rate (b) spectrum utilization rate

(c) bidders' payment (d) winning bidders' valuations

Figure 6.9: Performance comparison on setting with no reusability

with varying mean arrival rates. Finally, we plot the winning bidders' valuations in Fig. 6.9d. It shows that both algorithms give almost the same result as in the off-line algorithm.

6.5.4.2 Results on Setting with Spectrum Reusability

Like single auctions, we investigate the performance of the double auction algorithms in the setting with spectrum reusability (defined in Sec. 6.5.2). Under the setting with spectrum reusability, the same spectrum is allocated to non-interfering bidders. We consider the network in which the secondary users are scattered randomly within an area of $100\text{m}\times100\text{m}$. The interference range

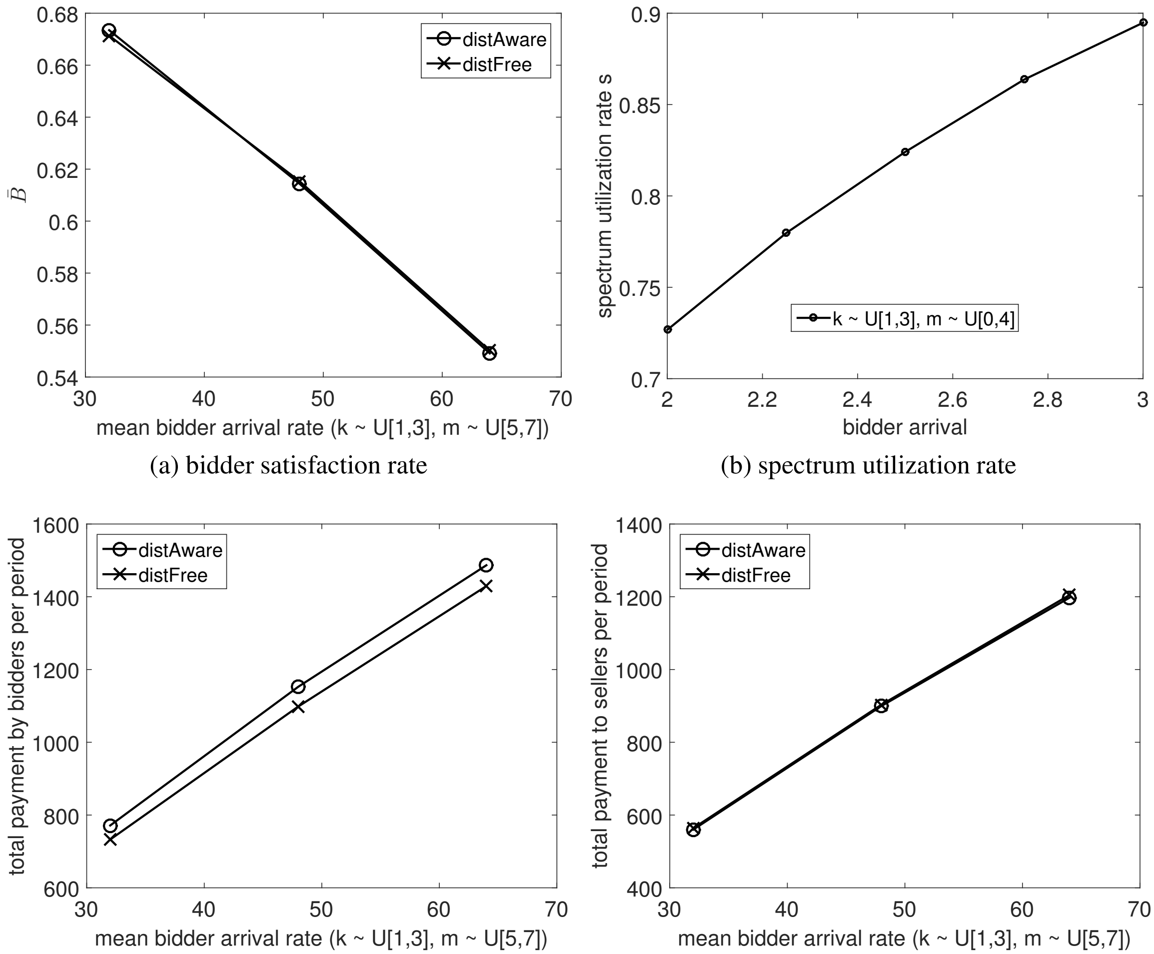

(a) bidder satisfaction rate

(b) spectrum utilization rate

(c) bidders' payment

(d) payment to winning sellers

Figure 6.10: Performance comparison on setting with spectrum reusability

of a secondary user is set to 20m. Two users located 20m apart can use the same spectrum unit without any interference. An interference graph G is constructed based on the user's transmission range. In the simulation, bidders' arrivals follow a Poisson distribution with mean value varying between 32 and 64, and their lifetimes are uniformly drawn from $\{1, 2, 3\}$.

Under the setting with spectrum reusability, we first plot bidder satisfaction rates in Fig. 6.10a. The result shows that with the increase in bidders' arrival rates, the winning rate of bidders decreases. However, the distFree algorithm achieves the same satisfaction rate as the distAware algorithm. We also calculate the winning probability of a bidder given its value, referred to as

$\Pr(x_i = 1|v_i)$. As expected, the higher valued bidders have higher probabilities to win and the winning probability decreases with the decrease in bidders' valuations. Also, the distAware algorithm shows a slight increase in the winning probability for higher valued bidders compared to the distFree algorithm.

Next, we plot the spectrum utilization rate ($\bar{s}$) in the auction in Fig. 6.10b. The arrival of more bidders in the auction increases spectrum reusability, however, the rate of change in spectrum utilization diminishes at higher arrival rates of bidders. We also calculate the winning probability of a seller given its valuation and the result shows that the lower the ask of a seller is, the more it is likely to win.

Fig. 6.10c shows the average payment a bidder pays according to the proposed algorithms, while Fig. 6.10d shows the the average payment a seller receives. The results show that bidders' payments are lower in the distFree algorithm than in the distAware algorithm while the sellers' payments are almost same in both cases. Also, the number of trades increases as the bidders' arrival rates increase, however, the rate of change in the number of trades diminishes. The auctioneer's balance is higher in the distAware algorithm than in the distFree algorithm.

6.6 Summary

In this chapter, we investigate online single and double auction for spectrum allocation in the dynamic secondary market. In this spectrum market, both bidders and sellers arrive dynamically with different lifetimes and different valuations. We first present an online single auction mechanism to allocate the randomly available spectrum among the bidders according to their value and urgency of transmission, such that bidders with higher values and shorter lifetimes of demand receive a higher priority. By allocating the same spectrum unit to non-interfering bidders, we achieve spectrum reusability. We formally prove that the mechanism is individually rational for all agents ensuring truthful reporting by both sellers and bidders, including bidders' valuations and lifetime reports. The proposed mechanism is simulated under various distributional settings, and auction revenue and bidder satisfaction rate are significantly increased compared to existing work. Second, we present two algorithms for winner selection and price determination in an online double auction setting. The first algorithm assumes that the underlying distributions of arrival of bidders and sellers are known to the auctioneer. Using this information in a priority function, the auctioneer determines the winning opportunity of a bidder at different periods of its lifetime. The second algorithm works without any distribution knowledge and determines the critical price for a bidder based on McAfee rules and active bidders in its neighborhood. Both mechanisms are proved to be truthful, individually rational, and budget balanced. We compare the performance of these algorithms with an off-line algorithm. The simulation results show that these algorithms provide almost the same bidder satisfaction rate and spectrum utilization rate compared to the off-line mechanism when the number of bidders and supplies are equal on average. We also compare results in terms of auction revenue, bidders' valuations, and sellers' valuations and find that both these algorithms achieve results very close to the off-line mechanism.

Chapter 7

Conclusion

Cognitive radio network has provided promising means of spectrum sharing to address the limitations of the traditional fixed allocation system. With the flexibility and adaptability of the CRN, the primary and secondary users adopt various collaboration models for efficient spectrum management. In this dissertation, we have explored three collaboration models between the primary and secondary users — sensing based, relay based, and auction based. We have identified the challenges in these models and addressed some of these challenges towards the development of efficient spectrum sharing algorithms. We also provide a list of research topics for our future study.

7.1 Summary of Contributions

In this section, we summarize our contributions on solving different problems in three different collaboration models.

7.1.1 Contribution on Sensing based Collaboration Model

In the sensing based collaboration model, secondary users share their sensing reports among themselves to detect free channels without primary users' knowledge. Based on this model, an IEEE 802.22 standard is developed for wireless regional area network. We address a well known vulnerability in sharing sensing reports in IEEE 802.22, propose a prevention mechanism, and validate its effectiveness through simulations.

7.1.1.1 The SSDF Attack and Proposed Solution

The report sharing vulnerability in IEEE 802.22 is referred to as spectrum sensing data falsification (SSDF) attack. According to the IEEE 802.22 guidelines, all SUs send their sensing reports to the base station, and the BS makes a decision about the PU presence based on all the reports. We have identified that in the SSDF attack, a malicious secondary user may send false sensing reports to fool the base station. We have shown that a malicious user may convince the BS to make a wrong decision about the PU presence and afterwards, it can use the free channel without sharing it with others. This attack is proven to be harmful to promote effective spectrum sharing.

To further analyze the SSDF attack, we have discussed how a malicious user may exploit this vulnerability in the network independently and collaboratively and may gain benefits from that. We have considered three different types of group attacks. In the first type of group attack, malicious secondary users form different subgroups. The members in the same subgroup alter reports with the same probability and report to the BS; however subgroups are independent and may opt to alter sensing reports with different probability. In the second type of group attack, the malicious users falsely report the exact opposite of the actual sensing report of majority of the users. This way, the attackers try to maximize their chances of success to manipulate the BS while avoiding detection by the BS. In the third type of group attack, malicious users follow an adaptive attacking strategy where an attacker changes its attacking probability based on the outcome of its action and adapts accordingly.

To defend against such individual and group attacks of malicious secondary users, we have presented an adaptive reputation based clustering algorithm, ARC. In this algorithm, the BS keeps record of recent sensing reports from the secondary users. A number of virtual clusters are formed based on their sensing reports and their reputation using k-medoid clustering. The decision about the PU presence is made in a two step voting. In the first step, each cluster determines its decision about the PU presence. To calculate the cluster vote, current report of each member of the cluster is normalized by the inverse of the distance between the member and the medoid of the cluster. Thus, depending on a user's distance from the mediod, its voting contribution varies. A user closer to the medoid has more power to influence the cluster's decision than the one far away from it. In the second step, the base station takes a majority vote among the clusters to make a final decision. The final decision is then used to adjust the reputation of the users in the same way. A user closer to the medoid of its cluster experiences more changes in reputation than a user away from the medoid. Thus, the honest and malicious users are separated in the BS, and SSDF attacks in IEEE 802.22 are prevented.

7.1.1.2 Performance Evaluation

To verify the efficacy of the proposed algorithm ARC, we have used three performance metrics - error rate, recall, and false alarm rate. Error rate denotes the number of times the BS makes a wrong decision in percentage. Recall denotes the ratio of number of attackers detected by the proposed algorithm in comparison to the actual number of attackers in the network. The false alarm rate denotes the number of honest users tagged as attackers in comparison to the total number of users tagged as attackers in the network. We have performed simulation varying the attacking probability, changing the number of attackers, and adopting different attacking strategies with the algorithm in [8]. The simulation results show that our proposed algorithm lowers the error rate than [8]. It also detects many of the attackers in the process and the false alarm rate is almost negligible compared to [8]. The performance of our proposed algorithm can be explained as follow. Whenever the number of attackers in the network or their attacking probability increases, the virtual distance between honest and malicious users is also increased. This results in two cases. First, the honest and malicious users end up in separate clusters. As long as total number of malicious users are smaller than the number of honest users, malicious users cannot take over majority of the clusters and their influence on the BS is reduced. Second, the malicious users coexist with the honest users in different clusters. But the virtual distance between the honest and malicious users in the same cluster becomes significantly large. Therefore, the malicious users cannot influence most of the cluster's vote and the error rate drops significantly. Thus, the proposed algorithm ARC neutralizes the harmful impact of the malicious users on the BS decision.

7.1.2 Contribution on Relay based Collaboration Model

In relay based collaboration model, the primary users share their spectrum in time and/or frequency domain in exchange for relaying service from the secondary users. The secondary users act as intermediate relays in return for transmission opportunities. Thus, primary and secondary users schedule cooperative transmission based on their mutual needs. We explore the validity and effectiveness of this model in the case of real-time applications. We also apply this model to form routing paths where secondary users relay primary packets over multiple hops in exchange for transmission opportunities. We devise cooperation algorithms based on this model for both cases and discuss our findings from simulation results.

7.1.2.1 Cooperation Algorithm in Real-time Applications

We have first analyzed the relay based collaboration model for real-time applications. Due to the time constraints in real-time packet delivery, the cooperation overhead becomes a serious issue in this model. The negotiation phase for cooperation may impose higher delay to later packets which may hurt the system performance. We have also identified that secondary transmission may cause overwhelming interference to primary transmission if not properly analyzed. When a primary user is in agreement with a secondary user, it allows the secondary user to transmit. By allowing secondary transmission, the interference relationship among users is changed. As a result, the ongoing transmission of other primary users might experience interference from the secondary transmission. Both these issues are carefully handled in our analysis. We have included the impact of transmission deadlines, negotiation overhead, and secondary interference in a user's cooperative transmission decision.

We have formulated the cooperative relay selection in real-time applications as a Markov decision process. Each state in the MDP represents the queue status of the network and each action in the MDP represents a transmission decision. Based on the state transition and the selected action the reward of primary and secondary user is defined. For primary users, we define the reward as the probability of successfully delivering a packet while for secondary users we define the reward as the number of bits transmitted for each unit transmission power spent in relaying. Based on our MDP analysis, we have presented an interference aware cooperation algorithm. In this algorithm, users try to reduce the overhead by prolonging the cooperative transmission period without going through the negotiation period. A secondary user in its offer negotiates the transmission power to reduce power consumption in relaying within the operating range. On the other hand, a primary user accepts the offer that provides best transmission time in comparison to direct transmission. Once a cooperation is set up, the cooperating users continuously monitors the change in queue size and the packet delivery rate. If the status change exceeds a certain threshold, both users terminate the cooperation and return to negotiation period. Otherwise, the users continue cooperative transmission on the negotiated terms. Thus, relay based collaboration model enhances the performance of real-time applications.

Our analysis reveals that the distance between a primary user and a secondary user plays a significant role on the success of relay based collaboration model in real-time applications. Specifically, we found that a secondary user can only cooperate with the primary users located within a certain distance from it. To further understand the effectiveness of the collaboration model and study the performance of the proposed cooperation algorithm, we have focused on three features. The first performance metric we look into is the packet reception rate. The simulation result shows that the proposed cooperation algorithm improves packet reception rate and transmission opportunities of primary and secondary users respectively than the algorithm proposed in [117]. This is because our proposed algorithm takes into consideration the interference caused from secondary transmission, and a secondary user adjusts its transmission power in relaying primary packets accordingly. The second evaluation metric we consider here is the PU overhead which denotes the frequency of negotiation periods in scheduled transmissions. The simulation results show that our proposed algorithm significantly reduces the frequency of negotiation period compared to [117]. Unlike [117], our algorithm avoids frequent negotiation by continuing an existing collaboration until the change in packet reception rate with respect to change in queue decreases. This tradeoff also reduces the power cost of secondary users in relaying primary packets which is confirmed in the cost benefit analysis. The cost benefit analysis refers to the amount of power consumption in relaying to transmit one secondary packet.

7.1.2.2 Cooperation Algorithm in Multi-hop Routing

We have extended our analysis from single hop to multiple hops in relay based collaboration model. In this model, the routing path of a primary source-destination pair is established over multiple secondary users where each secondary user relays the packets of cooperating primary users to the next one in exchange for transmission opportunities. We identified that such multi-hop relay based cooperative routing faces couple of new challenges. First, unlike single hop communication, the success in a multi-hop communication also depends on the sharing among secondary users. Second, the multi-hop cooperation needs to ensure convergence of the routing path and its stability.

We have formulated the multi-hop relay selection problem as an overlapping coalition formation game where each coalition represents the routing path of a primary source-destination pair. Secondary users may participate in one or more routing paths depending on the opportunities and thus may overlap in more than one coalition. The primary users share their bandwidth with the secondary users participating in their routing paths. We have defined the reward of primary and secondary users as the primary throughput in terms of data rate and path delay, and secondary opportunities in terms of energy consumption respectively.

We have presented a cooperation based routing algorithm. In this algorithm, a primary user initiates the search of cooperative routing path to its immediate neighbors. Consequently, the receiving secondary users forward to their neighbors if they do not have any direct path to the final destination. While a secondary user receives a routing proposal, it adds its own demand and returns to the source. Finally the source primary user accepts the new path or continues with the existing path. The decision of searching for routing path or continuing with the existing one is determined based on some carefully tuned control parameters that ensure quick convergence of the algorithm and stability of the routing paths.

The proposed cooperative routing algorithm is evaluated by varying different parameters and simulation results are compared with the algorithm in [79]. The simulation results show that the proposed algorithm increases data rate of primary users and transmission opportunities of secondary users. We also observe that the length of the routing path remains almost same whereas the number of overlapping secondary nodes increases with the increase of number of primary users in the network. This implies that each routing path has a maximum length after which it is not profitable for both primary and secondary users. On the other hand, the path length increases with increasing number of secondary users. This is because more secondary users create more opportunity for cooperative routing paths. We also vary two algorithm parameters. First, we change the weight factor that controls the tradeoff between data rate profit and delay profit of a primary user. As the primary profits incline towards data rate, the number of overlapping secondary users and path length increases. The second parameter controls the convergence rate of the algorithm. As we set smaller value, the routing paths take more time to converge. This is because for a smaller value, users intend to explore more opportunities for better routing paths. These findings reveal that the selection of parameters' values is very important for the success of the proposed cooperation algorithm.

7.1.3 Contribution on Auction based Collaboration Model

In the auction based collaboration model, primary users lease their unused spectrum (which would have been unutilized otherwise) to secondary users for monetary profits. In this dissertation, we investigate online dynamic secondary spectrum markets, design truthful mechanisms, and present our findings from the simulation of online auctions.

7.1.3.1 Online Spectrum Auctions

We have identified several major challenges to adopt auction based collaboration model in online dynamic spectrum markets. The first challenge in spectrum auctions is to ensure maximum spectrum utilization i.e. the algorithm should be able to allocate the same unit to multiple bidders as long as they are not interfering each other. The second challenge we need to address is to make online decision on spectrum allocation and pricing. The mechanism must also adhere to the desired properties such as truthfulness, individual rationality, and budget balance.

We have addressed these problems considering two cases. In the first case, we have considered that distribution information is known to the auctioneer. A bidder with transmission deadline will not value an item the same when it has an opportunity to win at later periods of its lifetime. In the distribution aware mechanism, the auctioneer uses the distribution information to calculate the amount a bidder is willing to pay at different periods of its lifetime. We have denoted that amount as a bidder's priority and used this amount to rank that bidder to consider for spectrum allocation. We have approached the calculation in three steps. In the first step, we have calculated the bidders' priority values of the dynamic setting when all bidders have the same valuation of a spectrum unit. Next, we have relaxed that assumption where bidders have different valuations. Finally, we have calculated the dynamic auction setting where sellers also have different valuations. Based on these priority values, we design two online (both single and double) auction mechanisms that are proved to be truthful, individually rational, and budget balanced.

In the second case, we have considered that the distribution information is not known to the auctioneer. We have presented spectrum allocation and pricing algorithm for the online double auction setting. We have applied bid monotonic spectrum allocation to set the order of bidders considered for spectrum. To determine the spectrum price for a winning bidder, we have calculated the critical price at each period of its lifetime and the final price is set to the minimum of those critical values. At each period, the mechanism executes three steps. In the first step, candidate bidders are selected according to the spectrum availability, interference relationship among bidders, and their bids. In the second step, debts for the current period is calculated. We have calculated the debt considering the winners who has won before the lifetime expires and the price they could have paid in the current period. In the final step, we select the winners from the candidate list in a way so that the debts in the second step can be compensated equally by the neighboring users without violating any of the auction properties.

7.1.3.2 Performance Evaluation

We have run simulation with varying distribution parameters to verify the accuracy of the priority functions for both online single and double auction settings. For both settings, the results show that the priority function is a strictly non-decreasing function with concave envelope with respect to value. The results also show that the priority of a bidder increases with increase in the number of arrival of bidders and decrease in number of supplies given everything remains same. We have thus established our observation about the bidders' willingness to pay through simulation for both distribution aware online single and double auctions.

We have also performed numeric simulations to test the performance of the proposed distribution aware (both single and double) and distribution free double auction algorithms based on four different metrics — 1) bidder satisfaction rate denoting the percentage of bidders that win spectrum units, 2) spectrum utilization rate denoting the percentage of spectrum units sold to bidders, 3) average value of a winner denoting the average valuation of winning bidders, and 4) average price of a winner denoting the price a winner pays for spectrum. We have compared their performances with Topaz [30] and offline algorithms. Users' density is also varied to enforce tests with spectrum reusability. The simulation results show that the proposed online single and double algorithms have better bidder satisfaction rate and spectrum utilization than Topaz [30]. The auction efficiency is measured in terms of the total valuation of winning bidders and the auction revenue is measured in terms of winners' payments. Again, our proposed algorithms achieve higher efficiency and higher revenue than Topaz [30] while ensuring truthfulness, individual rationality, and budget balance.

7.2 Future Work

While we have addressed some of the challenges towards the development of efficient spectrum sharing algorithms under different collaboration models, there are still some open research problems needed to be solved. We present a list of topics that will direct our future research.

7.2.1 Unified Solutions against Combined SSDF and PUE Attacks

In the sensing based collaboration model, we have discussed the SSDF attack and presented an effective solution to this problem. In this problem, we assumed that all secondary users are within the interference range of the single primary user. Each secondary user applies energy detection technique (based on received signal strength) and sends a binary report (yes/no) to the BS. However, there might be more than one primary user in the area and based on their location and transmission power, the received signal strength may vary from one secondary user to another. As a result, even honest secondary users reach wrong conclusion about the channel status following energy detection technique. Our proposed reputation based clustering algorithm may incorrectly identify some honest secondary users as attackers because of their unintentional false reporting. This will increase error rate and false alarm rate. Therefore, the secondary users should submit their received signal strength with location information to the BS instead of binary reports only. Additionally, a malicious secondary user may emulate the signal of a primary user to fool the detection method of an honest secondary user. This behavior is known as 'primary emulation attack' or PUE attack in short [5]. In this attack, a malicious secondary user emulates a primary signal during the sensing period. All honest users detect the signal, and falsely report the primary user's presence. The BS decides that the channel is busy and stops any secondary transmission. The malicious secondary users can exploit that opportunity and exclusively use the channel by themselves. The malicious users can form groups to further manipulate the system. Therefore, the future research should be directed on developing a unified solution [112] that prevents both SSDF and PUE attacks.

7.2.2 Pervasive Communications in Cooperative Cognitive Radio Networks

We have analyzed the relay based collaboration model to support real-time traffic. We have extended our analysis from single to multiple hops and presented a cooperation based routing algorithm. While the research broadens our understanding on relay based collaboration model, there are still some unresolved issues. In the existing research, the implicit assumption is that the secondary users always relay over the same spectrum as the corresponding primary users transmit. This requirement limits the spectrum sharing opportunities in real scenarios where the spectrum is already crowded. Instead, a secondary user may explore all available spectrum bands to relay packets of primary users. This pervasive mode of communication opens more sharing opportunity among users operating over different spectrum bands. Interoperability among users with different technologies and different spectrum bands will be a significant advancement towards the connectivity requirement of future networks.

7.2.3 Trust and Security issues in Cooperative Cognitive Radio Networks

In relay based collaboration model, the secondary user either amplifies the primary signal and relays it (amplify and forward) or decodes the signal, reconstructs it, and then relays it (decode and forward). The latter method offers more resistance to multi-path fading than the former method. In both cases the primary users are trusting secondary users with their packet information. This way of communication may open opportunities to the malicious secondary users [137]. With this unrestricted access to primary contents, a secondary user may manipulate the contents with malicious intent. The secondary users can also extract confidential information and use it to devise different spoofing and relay attacks. Since primary and secondary users may not belong to the same network, it is important to study the trust and security issues in mutual communication. Ensuring the integrity and confidentiality of the contents of primary users in a multi-hop cooperation framework is an important research direction.

7.2.4 Multi-unit Online Spectrum Auctions

Based on the auction based collaboration model, we have developed the online spectrum allocation mechanisms. One of the limitations of the proposed mechanisms is that the bidders can bid for single unit of spectrum only. This assumption may not be practical in real scenarios since bidders may have different bandwidth requirements. However, the proposed mechanisms cannot be directly extensible to multi-unit cases because of the following reason. A secondary user with multi-unit demand may manipulate the auction mechanism by setting a lower value for later units. Thus, a secondary user may indirectly influence the pricing of its spectrum. This opportunity for manipulation can be prevented by forcing a bidder to have the same value for each unit irrespective of its total demand. While this might work to prevent manipulation, it is unfair to the honest bidders and the auction efficiency and revenue turnout will be low. Therefore, the future research should focus on designing manipulation free online auction mechanisms supporting multi-unit demands from bidders.

The bidders' demands for spectrum may also be diverse in terms of duration. In our present work, secondary users' demand of spectrum is for one period only. Similar to multi-unit demand, a bidder may ask for spectrum for longer durations. Supporting users with spectrum demand of different durations in an online auction setting is also a challenging problem. For example, after receiving all bids for the current period, a user may be allocated spectrum for continuous usage. But the scenario may change in the next period due to arrival of new bidders, and assigning spectrum to the new user may earn more revenue than continuing with the previous bidder. In that case, the mechanism has to preempt the previously allocated user, and the mechanism cannot charge the user for partial usage [30]. Thus, it is important to accommodate such user demand online while ensuring high spectrum utilization, auction efficiency, and revenue. Following our current result and related research work, the future online spectrum auctions will address the diversity in user's demand in terms of spectrum units and durations.

7.2.5 Combinatorial Spectrum Auctions

A combinatorial auction is one where bidders submit multiple bid tuples instead for a single one. Each tuple may request a different number of spectrum units for different durations and a user may set different maximum amount he is willing to pay for each unit. We have considered an auction setting where bidders' submit a single bid request, and available spectrum are quantified in units. However, users' requirements are usually expressed in terms of minimum bandwidth and may have different preferences. For example, a bidder may want to pay more for spectrum with better propagation characteristics. However, it might also provoke the users to hide their actual demand and manipulate the auction mechanism to pay a lesser amount.

We also need to develop a bidding language to express users' demand and sellers' supply to the auctioneer efficiently and effectively. The transformation of complex supply and demand into understandable format and devising a combinatorial auction mechanism will be an important direction in future research. Also, the common assumption is that if a bidder does not get its required demand its utility remains zero. But this is not the case since its packet will be lost and this loss needs to be included in the analysis. This makes the design of combinatorial auction mechanism much more challenging. Ensuring auction properties like individual rationality and truthfulness in a combinatorial auction mechanism will constitute the future research.

7.2.6 Preventing Bidder Collusion in Spectrum Auctions

In any auction, malicious bidders may want to manipulate the outcome by changing their bids collaboratively. This form of unauthorized negotiation among bidders is known as ‘bidder collusion’. Traditional long term leasing spectrum auctions have already suffered the negative impact of bidder collusion [92]. Newer model of spectrum auctions may experience similar negative impact in terms of auction revenue and spectrum utilization. This vulnerability threatens the opportunity of small businesses against the big corporate. Only recently few studies like [144] addressed the problem and presented an auction mechanism that discourage bidders from lying about their true valuation. However, this study only considers bidders with single unit demand. Therefore, it is important to understand bidder collusion in the context of dynamic secondary market. The auction mechanism must be able to identify any such attempt of bidder collusion and take necessary actions to maintain fairness and truthfulness.

7.2.7 Spectrum Auction Infrastructure

Auction based collaboration model provides an effective means for spectrum sharing. We have successfully analyzed the properties of the auction mechanism in online settings. Different variations of spectrum auctions have been proposed by the researchers focusing on auction revenue, fairness, and truthful reporting. As the allocation algorithms mature the future research should direct to build an infrastructure for spectrum auctions. FCC has recently put forward a three tiered architecture plan for spectrum auction [26]. The researchers need to resolve lots of infrastructural and maintenance issues regarding this plan that have not been considered in literature. For example, we need to standardize the bidding protocol for the secondary users. The researchers need to develop how the FCC will maintain the available spectrum information and how it will share it across various locations. On one hand it is difficult to adopt a centralized mechanism to fit the diversity of bidders and sellers; on the other hand, decentralized mechanism would be very difficult to maintain and keep a synchronized database. Therefore, we need to consider all different tradeoffs in infrastructure planning.

Finally, while these approaches individually may improve spectrum utilization, it will be interesting to see how these approaches coexist and complement each other in future networks. This will also open the possibility of applying these sharing techniques altogether in practice. We will study and analyze the performance of these sharing techniques in the future research.

BIBLIOGRAPHY

BIBLIOGRAPHY

[1] G. Chouinard A. N. Mody. Ieee 802.22 wireless regional area networks. *IEEE 802.22-10/0073r03*, June 2010.

[2] H. Adam, C. Bettstetter, and S. M. Senouci. Multi-hop-aware cooperative relaying. In *Vehicular Technology Conference, 2009. VTC Spring 2009. IEEE 69th*, pages 1–5, April 2009.

[3] I. F. Akyildiz, Won-Yeol Lee, and Kaushik R. Chowdhury. Crahns: Cognitive radio ad hoc networks. *Ad Hoc Networks*, 7(5):810 – 836, 2009.

[4] Ian F. Akyildiz, Brandon F. Lo, and Ravikumar Balakrishnan. Cooperative spectrum sensing in cognitive radio networks: A survey. *Phys. Commun.*, 4(1):40–62, March 2011.

[5] A. Alahmadi, M. Abdelhakim, J. Ren, and T. Li. Defense against primary user emulation attacks in cognitive radio networks using advanced encryption standard. *IEEE Transactions on Information Forensics and Security*, 9(5):772–781, May 2014.

[6] Mohammed Altamaimi. Spectrum sharing: Quantifying the benefits of different enforcement scenarios, 2014.

[7] P. Anand, A.S. Rawat, Hao Chen, and P.K. Varshney. Collaborative spectrum sensing in the presence of byzantine attacks in cognitive radio networks. In *Communication Systems and Networks (COMSNETS), 2010 Second International Conference on*, pages 1–9, 2010.

[8] A. Anandkumar, N. Michael, and A.K. Tang. Opportunistic Spectrum Access with Multiple Users: Learning Under Competition. In *Proc. of IEEE INFOCOM*, San Deigo, USA, March 2010.

[9] D.D. Ariananda, M. K. Lakshmanan, and H. Nikookar. A survey on spectrum sensing techniques for cognitive radio. In *Cognitive Radio and Advanced Spectrum Management, 2009. CogART 2009. Second International Workshop on*, pages 74–79, May 2009.

[10] Mahmoud Ashour, Amr A. El-Sherif, Tamer A. ElBatt, and Amr Mohamed. Cognitive radio networks with probabilistic relaying: Stable throughput and delay tradeoffs. *CoRR*, abs/1404.6112, 2014.

[11] D. Gunawardena B. Radunovic, A. Proutiere and Peter Key. Exploiting channel diversity in white spaces. Technical Report MSR-TR-2011-53, Microsoft Research, April 2011.

[12] A. Banaei and C.N. Georghiades. Throughput analysis of a randomized sensing scheme in cell-based ad-hoc cognitive networks. In *Communications, 2009. ICC '09. IEEE International Conference on*, pages 1–6, June 2009.

[13] S. Banerjee and D.O. Wu. Final report from the nsf workshop on future directions in wireless networking. Technical report, National Science Foundation, November 2013.

[14] D. Bertsekas and R. Gallager. *Data Networks*. Prentice-Hall, 1987.

[15] Kaigui Bian and Jung-Min "Jerry" Park. Security vulnerabilities in ieee 802.22. In *Proceedings of the 4th Annual International Conference on Wireless Internet*, WICON '08, pages 9:1–9:9, ICST, Brussels, Belgium, Belgium, 2008. ICST (Institute for Computer Sciences, Social-Informatics and Telecommunications Engineering).

[16] Chandra Chekuri and Sanjeev Khanna. A ptas for the multiple knapsack problem. In *Proceedings of the Eleventh Annual ACM-SIAM Symposium on Discrete Algorithms*, SODA '00, pages 213–222, 2000.

[17] Dawei Chen, Sixing Yin, Qian Zhang, Mingyan Liu, and Shufang Li. Mining spectrum usage data: a large-scale spectrum measurement study. In *Proceedings of the 15th annual international conference on Mobile computing and networking*, MobiCom '09, pages 13–24, New York, NY, USA, 2009. ACM.

[18] Ruiliang Chen, Jung-Min Park, and Kaigui Bian. Robust distributed spectrum sensing in cognitive radio networks. In *INFOCOM 2008. The 27th Conference on Computer Communications. IEEE*, 2008.

[19] Y. Chen and H.-S. Oh. A survey of measurement-based spectrum occupancy modeling for cognitive radios. *Communications Surveys Tutorials, IEEE*, PP(99):1–1, 2014.

[20] Yanjiao Chen, Peng Lin, and Qian Zhang. Lotus: Location-aware online truthful double auction for dynamic spectrum access. In *Dynamic Spectrum Access Networks (DYSPAN), 2014 IEEE International Symposium on*, pages 510–518, April 2014.

[21] Yanjiao Chen, Jin Zhang, Kaishun Wu, and Qian Zhang. Tames: A truthful auction mechanism for heterogeneous spectrum allocation. In *INFOCOM, 2013 Proceedings IEEE*, pages 180–184, 2013.

[22] Zhili Chen, He Huang, Yu e Sun, and Liusheng Huang. True-mcsa: A framework for truthful double multi-channel spectrum auctions. *Wireless Communications, IEEE Transactions on*, 12(8):3838–3850, 2013.

[23] Zhong Chen and Xian-Da Zhang. Cooperative spectrum sharing based on amplify and forward relaying in cognitive radio networks. *Wireless Personal Communications*, 67(3):585–598, 2012.

[24] Octav Chipara, Chenyang Lu, Thomas C. Bailey, and Gruia-Catalin Roman. Reliable clinical monitoring using wireless sensor networks: experiences in a step-down hospital unit. In *Proceedings of the 8th ACM Conference on Embedded Networked Sensor Systems*, SenSys '10, pages 155–168, New York, NY, USA, 2010. ACM.

[25] Cisco visual networking index: Forecast and methodology, 2015-2020. http://www.cisco.com/c/en/us/solutions/collateral/service-provider/visual-networking -index-vni/mobile-white-paper-c11-520862.pdf, May 2015.

[26] 3.5 ghz band/ citizens broadband radio service. https://www.fcc.gov/rulemaking/12-354, April 2015.

[27] T.C. Clancy and N. Goergen. Security in cognitive radio networks: Threats and mitigation. In *Cognitive Radio Oriented Wireless Networks and Communications, 2008. CrownCom 2008. 3rd International Conference on*, pages 1–8, 2008.

[28] https://en.wikipedia.org/wiki/Cooperative_diversity.

[29] Carlos Cordeiro, Kiran Challapali, Dagnachew Birru, and Sai Shankar N. Ieee 802.22: An introduction to the first wireless standard based on cognitive radios. *Journal of Communications*, 1(1), 2006.

[30] L. Deek, Xia Zhou, K. Almeroth, and Haitao Zheng. To preempt or not: Tackling bid and time-based cheating in online spectrum auctions. In *INFOCOM, 2011 Proceedings IEEE*, pages 2219–2227, April 2011.

[31] Wei Dong, S. Rallapalli, Lili Qiu, K.K. Ramakrishnan, and Yin Zhang. Double auctions for dynamic spectrum allocation. In *INFOCOM, 2014 Proceedings IEEE*, pages 709–717, April 2014.

[32] Lingjie Duan, A.W. Min, Jianwei Huang, and K.G. Shin. Attack prevention for collaborative spectrum sensing in cognitive radio networks. *Selected Areas in Communications, IEEE Journal on*, 30(9):1658–1665, 2012.

[33] Tran Trung Duy and Hyung Yun Kong. Secondary spectrum access in cognitive radio networks using rateless codes over rayleigh fading channels. *Wireless Personal Communications*, 77(2):963–978, 2013.

[34] Adel M. Elmahdy, Amr El-Keyi, Tamer A. ElBatt, and Karim G. Seddik. On the stable throughput of cooperative cognitive radio networks with finite relaying buffer. *CoRR*, abs/1410.2419, 2014.

[35] F. Farmani, M.A. Jannat-Abad, and R. Berangi. Detection of ssdf attack using svdd algorithm in cognitive radio networks. In *Computational Intelligence, Communication Systems and Networks (CICSyN), 2011 Third International Conference on*, pages 201–204, 2011.

[36] Fcc spectrum licensing. https://www.fcc.gov/general/accessing-spectrum.

[37] FCC. TV broadcaster relocation fund workshop. http://www.fcc.gov/events/tv-broadcaster-relocation-fund-workshop, June 2012.

[38] Federal communication commission (FCC), unlicensed operation in the tv broadcast bands; additional spectrum for unlicensed devices below 900 mhz and in the 3 ghz band, FCC 04-186 and FCC 02-380. http://hraunfoss.fcc.gov/edocs_public/attachmatch/DA-11-131A1.txt, January 2011.

[39] Fcc initiatives. https://www.fcc.gov/about-fcc/fcc-initiatives.

[40] Xiaojun Feng, Yanjiao Chen, Jin Zhang, Qian Zhang, and Bo Li. Tahes: A truthful double auction mechanism for heterogeneous spectrums. *Wireless Communications, IEEE Transactions on*, 11(11):4038–4047, November 2012.

[41] Sorabh Gandhi, Chiranjeeb Buragohain, Lili Cao, Haitao Zheng, and Subhash Suri. Towards real-time dynamic spectrum auctions. *Computer Networks*, 52(4):879 – 897, 2008. Cognitive Wireless Networks.

[42] G. Ganesan and Ye Li. Cooperative spectrum sensing in cognitive radio networks. In *First IEEE International Symposium on New Frontiers in Dynamic Spectrum Access Networks, 2005. DySPAN 2005.*, pages 137–143, Nov 2005.

[43] Maksym Girnyk. Cooperative communication for multi-user cognitive radio networks, 2012. QC 20120612.

[44] Andrea Goldsmith. *Wireless Communications*. Cambridge University Press, New York, NY, USA, 2005.

[45] Mohammad T. Hajiaghayi. Online auctions with re-usable goods. In *Proceedings of the 6th ACM Conference on Electronic Commerce*, EC '05, pages 165–174, New York, NY, USA, 2005. ACM.

[46] Song Han, Xiuming Zhu, A.K. Mok, Deji Chen, and M. Nixon. Reliable and real-time communication in industrial wireless mesh networks. In *Real-Time and Embedded Technology and Applications Symposium (RTAS), 2011 17th IEEE*, pages 3 –12, april 2011.

[47] Yang Han, A. Pandharipande, and See Ho Ting. Cooperative decode-and-forward relaying for secondary spectrum access. *Wireless Communications, IEEE Transactions on*, 8(10):4945–4950, October 2009.

[48] Xiaolei Hao, Man Hon Cheung, V.W.S. Wong, and V.C.M. Leung. A stackelberg game for cooperative transmission and random access in cognitive radio networks. In *Personal Indoor and Mobile Radio Communications (PIMRC), 2011 IEEE 22nd International Symposium on*, pages 411 –416, sept. 2011.

[49] I-Hong Hou and P.R. Kumar. Scheduling heterogeneous real-time traffic over fading wireless channels. In *INFOCOM, 2010 Proceedings IEEE*, pages 1–9, 2010.

[50] D. Hu and S. Mao. Cooperative relay in cognitive radio networks: Decode-and-forward or amplify-and-forward? In *Global Telecommunications Conference (GLOBECOM 2010), 2010 IEEE*, pages 1–5, Dec 2010.

[51] H. Huang, X. Li, Y. Sun, H. Xu, and L. Huang. Pps: Privacy-preserving strategyproof social-efficient spectrum auction mechanisms. *Parallel and Distributed Systems, IEEE Transactions on*, 26(5):1393–1404, May 2015.

[52] C. S. Hyder, ABM Alim Al Islam, and Li Xiao. Enhancing reliability of real-time traffic via cooperative scheduling in cognitive radio networks. In *IWQoS*, June 15 -16 2015.

[53] Chowdhury Hyder, Li Xiao, and Max Ellison. Exploiting cooperation for delay optimization in cognitive networks. In *The 9th IEEE International Conference on Mobile Ad hoc and Sensor Systems*, MASS'12, pages 362–370. IEEE, 2012.

[54] Chowdhury S Hyder, Brendan Grebur, Li Xiao, and Martyn Ellison. Arc: Adaptive reputation based clustering against spectrum sensing data falsification attacks. *Mobile Computing, IEEE Transactions on*, 13(8):1707–1719, 2014.

[55] Chowdhury Sayeed Hyder, Brendan Grebur, and Li Xiao. Defense against spectrum sensing data falsification attacks in cognitive radio networks. In *Security and privacy in communication networks*, pages 154–171. Springer Berlin Heidelberg, 2011.

[56] C.S. Hyder and Li Xiao. Dbla: Distributed block learning algorithm for channel selection in cognitive radio networks. In *World of Wireless, Mobile and Multimedia Networks (WoWMoM), 2012 IEEE International Symposium on a*, pages 1–6, June 2012.

[57] Ahmed S. Ibrahim, Ahmed K. Sadek, Weifeng Su, and K. J. Ray Liu. Cooperative communications with relay-selection: when to cooperate and whom to cooperate with? *IEEE Transactions on Wireless Communications*, 7(7):2814–2827, 2008.

[58] Fcc adopts incentive auction. https://www.fcc.gov/about-fcc/fcc-initiatives/incentive-auctions, March 2016.

[59] A. Iyer, C. Rosenberg, and A. Karnik. What is the right model for wireless channel interference? *Wireless Communications, IEEE Transactions on*, 8(5):2662–2671, May 2009.

[60] Thomas D Jeitschko. Equilibrium price paths in sequential auctions with stochastic supply. *Economics Letters*, 64(1):67 – 72, 1999.

[61] J. Jia, J. Zhang, and Q. Zhang. Cooperative relay for cognitive radio networks. In *INFOCOM 2009, IEEE*, pages 2304 –2312, april 2009.

[62] Juncheng Jia, Jin Zhang, and Qian Zhang. Relay-assisted routing in cognitive radio networks. In *Communications, 2009. ICC '09. IEEE International Conference on*, pages 1 –5, june 2009.

[63] Tao Jing, Fan Zhang, Liran Ma, Wei Li, Xuhao Chen, and Yan Huo. Truthful online reverse auction with flexible preemption for access permission transaction in macro-femtocell networks. In Kui Ren, Xue Liu, Weifa Liang, Ming Xu, Xiaohua Jia, and Kai Xing, editors, *Wireless Algorithms, Systems, and Applications*, volume 7992 of *Lecture Notes in Computer Science*, pages 512–523. Springer Berlin Heidelberg, 2013.

[64] Tao Jing, Shixiang Zhu, Hongjuan Li, Xiuzhen Cheng, and Yan Huo. Cooperative relay selection in cognitive radio networks. In *INFOCOM, 2013 Proceedings IEEE*, pages 175–179, 2013.

[65] P. Kaligineedi, M. Khabbazian, and V.K. Bhargava. Malicious user detection in a cognitive radio cooperative sensing system. *Wireless Communications, IEEE Transactions on*, 9(8):2488–2497, 2010.

[66] Leonard Kaufman and Peter J. Rousseeuw. *Finding Groups in Data: An Introduction to Cluster Analysis*. Wiley-Interscience, 9th edition, March 1990.

[67] K. Khalil, M. Karaca, O. Ercetin, and E. Ekici. Optimal scheduling in cooperate-to-join cognitive radio networks. In *INFOCOM, 2011 Proceedings IEEE*, pages 3002–3010, 2011.

[68] A. E. Khandani, J. Abounadi, E. Modiano, and L. Zheng. Cooperative routing in static wireless networks. *IEEE Transactions on Communications*, 55(11):2185–2192, Nov 2007.

[69] Insook Kim and Dongwoo Kim. Incentive-based time sharing with cooperative secondary users in multicast primary networks. In *Signal Processing, Communications and Computing (ICSPCC), 2011 IEEE International Conference on*, pages 1 –6, sept. 2011.

[70] S. Kompella, Gam D. Nguyen, J.E. Wieselthier, and Anthony Ephremides. Stable throughput tradeoffs in cognitive shared channels with cooperative relaying. In *INFOCOM, 2011 Proceedings IEEE*, pages 1961–1969, April 2011.

[71] Z. Kong, Y. K. Kwok, and J. Wang. Auction-based scheduling in non-cooperative multiuser ofdm systems. In *Vehicular Technology Conference, 2009. VTC Spring 2009. IEEE 69th*, pages 1–4, April 2009.

[72] Vijay Krishna. *Auction Theory*. Academic press/Elsevier, 2009.

[73] K.L. Eddie Law and Wing-Chung Hung. Channel control for multi-radio multi-channel wireless mesh networks. In *Proceedings of the 3Nd ACM Workshop on Performance Monitoring and Measurement of Heterogeneous Wireless and Wired Networks*, PM2HW2N '08, pages 157–164, New York, NY, USA, 2008. ACM.

[74] M. Levorato, O. Simeone, U. Mitra, and M. Zorzi. Cooperation and coordination in cognitive networks with packet retransmission. In *Information Theory Workshop, 2009. ITW 2009. IEEE*, pages 495 –499, oct. 2009.

[75] Yonatan Levy and Uri Yechiali. Utilization of idle time in an m/g/1 queueing system. *Management Science*, 22(2):202–211, 1975.

[76] Dapeng Li, Youyun Xu, Xinbing Wang, and M. Guizani. Coalitional game theoretic approach for secondary spectrum access in cooperative cognitive radio networks. *Wireless Communications, IEEE Transactions on*, 10(3):844–856, 2011.

[77] H. Li. Multi-agent q-learning of channel selection in multi-user cognitive radio systems: A two by two case. In *Systems, Man and Cybernetics, 2009. SMC 2009. IEEE International Conference on*, pages 1893 –1898, 11-14 2009.

[78] Husheng Li and Zhu Han. Catching attackers for collaborative spectrum sensing in cognitive radio systems: An abnormality detection approach. In *New Frontiers in Dynamic Spectrum, 2010 IEEE Symposium on*, pages 1–12, 2010.

[79] Wei Li, Xiuzhen Cheng, Tao Jing, and Xiaoshuang Xing. Cooperative multi-hop relaying via network formation games in cognitive radio networks. In *INFOCOM, 2013 Proceedings IEEE*, pages 971–979, 2013.

[80] Zhongliang Liang, Shan Feng, Dongmei Zhao, and Xuemin Shen. Delay performance analysis for supporting real-time traffic in a cognitive radio sensor network. *Wireless Communications, IEEE Transactions on*, 10(1):325–335, 2011.

[81] Peng Lin, Juncheng Jia, Qian Zhang, and M. Hamdi. Dynamic spectrum sharing with multiple primary and secondary users. In *Communications (ICC), 2010 IEEE International Conference on*, pages 1 –5, may 2010.

[82] Chin-Jung Liu, Pei Huang, Li Xiao, and A.-H. Esfahanian. Interference identification and resource management in ofdma femtocell networks. In *Networking Conference, 2014 IFIP*, pages 1–9, June 2014.

[83] Hua Liu, B. Krishnamachari, and Qing Zhao. Cooperation and learning in multiuser opportunistic spectrum access. In *Communications Workshops, 2008. ICC Workshops '08. IEEE International Conference on*, pages 487 –492, 19-23 2008.

[84] Siyang Liu, Quan Liu, Jun Gao, and Jianxin Guan. Attacker-exclusion scheme for cooperative spectrum sensing against ssdf attacks based on accumulated suspicious level. In *Cyber Technology in Automation, Control, and Intelligent Systems (CYBER), 2011 IEEE International Conference on*, pages 239–243, 2011.

[85] Song Liu, Yingying Chen, W. Trappe, and L.J. Greenstein. Aldo: An anomaly detection framework for dynamic spectrum access networks. In *INFOCOM 2009, IEEE*, pages 675–683, 2009.

[86] R. Manna, R. H. Y. Louie, Y. Li, and B. Vucetic. Cooperative amplify-and-forward relaying in cognitive radio networks. In *2010 Proceedings of the Fifth International Conference on Cognitive Radio Oriented Wireless Networks and Communications*, pages 1–5, June 2010.

[87] E. Matskani, N. Chatzidiamantis, L. Georgiadis, I. Koutsopoulos, and L. Tassiulas. The mutual benefits of primary-secondary user cooperation in wireless cognitive networks. In *Modeling and Optimization in Mobile, Ad Hoc, and Wireless Networks (WiOpt), 2014 12th International Symposium on*, pages 279–286, May 2014.

[88] R.Preston McAfee. A dominant strategy double auction. *Journal of Economic Theory*, 56(2):434 – 450, 1992.

[89] Mark A. Mchenry. Spectrum occupancy measurements chicago, illinois. *Spectrum Reports*, pages 1–58, 2005.

[90] National broadband plan. https://www.fcc.gov/general/national-broadband-plan, March 2010.

[91] Cognitive radio technology, a study for ofcom. http://stakeholders.ofcom.org.uk/binaries/research/technology-research/cograd_main.pdf, February 2007.

[92] Simon Parsons, Juan A. Rodriguez-Aguilar, and Mark Klein. Auctions and bidding: A guide for computer scientists. *ACM Comput. Surv.*, 43(2):10:1–10:59, February 2011.

[93] Tao Qin, Han Yu, Cyril Leung, Zhiqi Shen, and Chunyan Miao. Towards a trust aware cognitive radio architecture. *SIGMOBILE Mob. Comput. Commun. Rev.*, 13(2):86–95, September 2009.

[94] Yasir Saleem and Mubashir Husain Rehmani. Primary radio user activity models for cognitive radio networks: A survey. *Journal of Network and Computer Applications*, 43:1 – 16, 2014.

[95] Yasir Saleem, Farrukh Salim, and Mubashir Husain Rehmani. Routing and channel selection from cognitive radio network's perspective: A survey. *Computers and Electrical Engineering*, 42:117 – 134, 2015.

[96] Shamik Sengupta and Mainak Chatterjee. Designing auction mechanisms for dynamic spectrum access. *Mobile Networks and Applications*, 13(5):498–515, 2008.

[97] Shamik Sengupta and Mainak Chatterjee. An economic framework for dynamic spectrum access and service pricing. *IEEE/ACM Transactions on Networking (TON)*, 17(4):1200–1213, 2009.

[98] Ahmed El Shafie, Tamer Khattab, Amr El-Keyi, and H. Vincent Poor. Energy-efficient cooperative cognitive relaying protocols for full-duplex cognitive radio users and delay-aware primary users. *CoRR*, abs/1406.2255, 2014.

[99] Stephen J. Shellhammer. Spectrum sensing in ieee 802.22, 2008.

[100] S. Shetty, Min Song, Chunsheng Xin, and E.K. Park. A learning-based multiuser opportunistic spectrum access approach in unslotted primary networks. In *INFOCOM 2009, IEEE*, pages 2966 –2970, 19-25 2009.

[101] Yanbin Shi, Jian Guo, and Yuanfang Jian. *Emerging Intelligent Computing Technology and Applications: 8th International Conference, ICIC 2012, Huangshan, China, July 25-29, 2012. Proceedings*, chapter Spectrum Sensing Algorithms in the Cognitive Radio Network, pages 132–138. Springer Berlin Heidelberg, Berlin, Heidelberg, 2012.

[102] Jonathon Shlens. Notes on kullback-leibler divergence and likelihood theory, 2007.

[103] O. Simeone, I. Stanojev, S. Savazzi, Y. Bar-Ness, U. Spagnolini, and R. Pickholtz. Spectrum leasing to cooperating secondary ad hoc networks. *Selected Areas in Communications, IEEE Journal on*, 26(1):203 –213, jan. 2008.

[104] B. Sklar. Rayleigh fading channels in mobile digital communication systems .i. characterization. *Communications Magazine, IEEE*, 35(7):90–100, Jul 1997.

[105] S. Sodagari, A. Attar, V. C M Leung, and S.G. Bilen. Denial of service attacks in cognitive radio networks through channel eviction triggering. In *Global Telecommunications Conference (GLOBECOM 2010), 2010 IEEE*, pages 1–5, 2010.

[106] C. Sorrells, P. Potier, Lijun Qian, and Xiangfang Li. Anomalous spectrum usage attack detection in cognitive radio wireless networks. In *Technologies for Homeland Security (HST), 2011 IEEE International Conference on*, pages 384–389, 2011.

[107] https://www.fcc.gov/general/cellular-service.

[108] General survey of radio frequency bands (30mhz to 3ghz). http://www.sharedspectrum.com/wp-content/uploads/2010_0923-General-Band-Survey-30MHz-to-3GHz.pdf, September 2009.

[109] P. Steenkiste, D. Sicker, G. Minden, and D. RayChaudhuri. Final report from the nsf workshop on future directions in cognitive radio network research. Technical report, National Science Foundation, March 2009.

[110] Carl R. Stevenson, Gerald Chouinard, Zhongding Lei, Wendong Hu, Stephen J. Shellhammer, and Winston Caldwell. Ieee 802.22: The first cognitive radio wireless regional area network standard. *Comm. Mag.*, 47(1):130–138, January 2009.

[111] Weifeng Su, J.D. Matyjas, and S. Batalama. Active cooperation between primary users and cognitive radio users in cognitive ad-hoc networks. In *Acoustics Speech and Signal Processing (ICASSP), 2010 IEEE International Conference on*, pages 3174 –3177, march 2010.

[112] Victor Sucasas, Saud Althunibat, Ayman Radwan, Hugo Marques, Jonathan Rodriguez, Seiamak Vahid, Rahim Tafazolli, and Fabrizio Granelli. Lightweight security against combined ie and ssdf attacks in cooperative spectrum sensing for cognitive radio networks. *Security and Communication Networks*, 8(18):3978–3994, 2015. sec.1315.

[113] Jun Sun, E. Modiano, and Lizhong Zheng. Wireless channel allocation using an auction algorithm. *IEEE Journal on Selected Areas in Communications*, 24(5):1085–1096, May 2006.

[114] Qihang Sun, Qian Wang, Kui Ren, and Xiaohua Jia. Fair pricing in the sky: Truthful frequency allocation with dynamic spectrum supply. In *Network Protocols (ICNP), 2014 IEEE 22nd International Conference on*, pages 245–256, Oct 2014.

[115] Yinglei Teng, Yong Zhang, Chao Dai, Fan Yang, and Mei Song. Dynamic spectrum sharing through double auction mechanism in cognitive radio networks. In *Wireless Communications and Networking Conference (WCNC), 2011 IEEE*, pages 90 –95, march 2011.

[116] Vaclav Valenta, Roman Marsalek, Genevieve Baudoin, Martine Villegas, Martha Suarez, and Fabien Robert. Survey on spectrum utilization in europe: Measurements, analyses and observations. In *The Proceedings of the 5th International ICST Conference on Cognitive Radio Oriented Wireless Networks and Communications (CROWNCOM)*, pages 1–5, June 2010.

[117] Liping Wang and Viktoria Fodor. Cooperate or not: The secondary user's dilemma in hierarchical spectrum sharing networks. In *Communications (ICC), 2013 IEEE International Conference on*, pages 2650–2655. IEEE, 2013.

[118] S. Wang, P. Xu, X. Xu, S. Tang, X. Li, and X. Liu. Toda: Truthful online double auction for spectrum allocation in wireless networks. In *New Frontiers in Dynamic Spectrum, 2010 IEEE Symposium on*, pages 1–10, April 2010.

[119] Tianyu Wang, Lingyang Song, Zhu Han, and W. Saad. Overlapping coalitional games for collaborative sensing in cognitive radio networks. In *Wireless Communications and Networking Conference (WCNC), 2013 IEEE*, pages 4118–4123, 2013.

[120] Wenkai Wang, Husheng Li, Yan Sun, and Zhu Han. Catchit: Detect malicious nodes in collaborative spectrum sensing. In *Global Telecommunications Conference, 2009. GLOBECOM 2009. IEEE*, pages 1–6, 2009.

[121] Wenkai Wang, Husheng Li, Y.L. Sun, and Zhu Han. Attack-proof collaborative spectrum sensing in cognitive radio networks. In *Information Sciences and Systems, 2009. CISS 2009. 43rd Annual Conference on*, pages 130–134, 2009.

[122] Ieee 802.22 working group on wireless regional area networks. http://www.ieee802.org/22/.

[123] Guangen Wu, Pinyi Ren, and Chao Zhang. A waiting-time auction based dynamic spectrum allocation algorithm in cognitive radio networks. In *Global Telecommunications Conference (GLOBECOM 2011), 2011 IEEE*, pages 1–5, 2011.

[124] Yao Xiao and Leonard J. Cimini. Impact of overhead on spectral efficiency of cooperative relaying. *Wireless Communications, IEEE Transactions on*, 12(5):2228–2239, May 2013.

[125] Ping Xu and Mo Li. Tofu: Semi-truthful online frequency allocation mechanism for wireless networks. *Networking, IEEE/ACM Transactions on*, 19(2):433–446, April 2011.

[126] Ping Xu, ShiGuang Wang, and Xiang-Yang Li. Salsa: Strategyproof online spectrum admissions for wireless networks. *IEEE Trans. Comput.*, 59(12):1691–1702, December 2010.

[127] Dongyue Xue and E. Ekici. Cross-layer scheduling for cooperative multi-hop cognitive radio networks. *Selected Areas in Communications, IEEE Journal on*, 31(3):534–543, 2013.

[128] Dejun Yang, Xi Fang, and Guoliang Xue. Truthful auction for cooperative communications. In *Proceedings of the Twelfth ACM International Symposium on Mobile Ad Hoc Networking and Computing*, MobiHoc '11, pages 9:1–9:10, New York, NY, USA, 2011. ACM.

[129] Dejun Yang, Xiang Zhang, and Guoliang Xue. Promise: A framework for truthful and profit maximizing spectrum double auctions. In *INFOCOM, 2014 Proceedings IEEE*, pages 109–117, April 2014.

[130] Youwen Yi, Jin Zhang, Qian Zhang, and Tao Jiang. Spectrum leasing to multiple cooperating secondary cellular networks. In *Communications (ICC), 2011 IEEE International Conference on*, pages 1 –5, june 2011.

[131] Youwen Yi, Jin Zhang, Qian Zhang, Tao Jiang, and Jietao Zhang. Cooperative communication-aware spectrum leasing in cognitive radio networks. In *New Frontiers in Dynamic Spectrum, 2010 IEEE Symposium on*, pages 1–11, 2010.

[132] F.R. Yu, H. Tang, Minyi Huang, Zhiqiang Li, and P.C. Mason. Defense against spectrum sensing data falsification attacks in mobile ad hoc networks with cognitive radios. In *Military Communications Conference, 2009. MILCOM 2009. IEEE*, pages 1–7, 2009.

[133] T. Yucek and H. Arslan. A survey of spectrum sensing algorithms for cognitive radio applications. *IEEE Communications Surveys Tutorials*, 11(1):116–130, First 2009.

[134] Yi Zeng and T.M. Chen. Measurement-based real-time traffic model classification. In *Communications, 2004 IEEE International Conference on*, volume 4, pages 1857–1861 Vol.4, 2004.

[135] Shun-Cheng Zhan and Shi-Chung Chang. Design of truthful double auction for dynamic spectrum sharing. In *Dynamic Spectrum Access Networks (DYSPAN), 2014 IEEE International Symposium on*, pages 439–448, April 2014.

[136] Jin Zhang and Qian Zhang. Stackelberg game for utility-based cooperative cognitiveradio networks. In *Proceedings of the tenth ACM international symposium on Mobile ad hoc networking and computing*, MobiHoc '09, pages 23–32, New York, NY, USA, 2009. ACM.

[137] Ning Zhang and Jon W. Mark. *Security-aware Cooperation in Cognitive Radio Networks*. Springer Briefs in Computer Science. Springer, 2014.

[138] Yang Zhang, Chonho Lee, D. Niyato, and Ping Wang. Auction approaches for resource allocation in wireless systems: A survey. *Communications Surveys Tutorials, IEEE*, 15(3):1020–1041, 2013.

[139] Zengfeng Zhang, Lingyang Song, Zhu Han, W. Saad, and Zhaohua Lu. Overlapping coalition formation games for cooperative interference management in small cell networks. In *Wireless Communications and Networking Conference (WCNC), 2013 IEEE*, pages 643–648, 2013.

[140] B. Zhao and S. Shimamoto. Time division based multi-radio multi-channel mac protocol for wireless mesh networks. In *Telecommunications (ConTEL), Proceedings of the 2011 11th International Conference on*, pages 293–300, June 2011.

[141] Lei Zhong, Qianyi Huang, Fan Wu, and Guihai Chen. Trade: A truthful online combinatorial auction for spectrum allocation in cognitive radio networks. *Wireless Communications and Mobile Computing*, 2013.

[142] Xia Zhou, Sorabh Gandhi, Subhash Suri, and Haitao Zheng. ebay in the sky: Strategy-proof wireless spectrum auctions. In *Proceedings of the 14th ACM International Conference on Mobile Computing and Networking*, MobiCom '08, pages 2–13, New York, NY, USA, 2008. ACM.

[143] Xia Zhou and H. Zheng. Trust: A general framework for truthful double spectrum auctions. In *INFOCOM 2009, IEEE*, pages 999–1007, 2009.

[144] Xia Zhou and Haitao Zheng. Breaking bidder collusion in large-scale spectrum auctions. In *Proceedings of the Eleventh ACM International Symposium on Mobile Ad Hoc Networking and Computing*, MobiHoc '10, pages 121–130, New York, NY, USA, 2010. ACM.